Flow Diagnostics and Optimal Design of Vertical Axis Wind Turbines for Urban Environments

Martin Emilov Zahariev

MSc by Research in Renewable Energy

Director of Research: Dr. Taimoor Asim

2016

University of Huddersfield

School of Computing and Engineering

Copyright Statement

i. The author of this thesis (including any appendices and/or schedules to this thesis) owns any copyright in it (the "Copyright") and he has given The University of Huddersfield the right to use such copyright for any administrative, promotional, educational and/or teaching purposes.

ii. Copies of this thesis, either in full or in extracts, may be made only in accordance with the regulations of the University Library. Details of these regulations may be obtained from the Librarian. This page must form part of any such copies made.

iii. The ownership of any patents, designs, trademarks and any and all other intellectual property rights except for the Copyright (the "Intellectual Property Rights") and any reproductions of copyright works, for example graphs and tables ("Reproductions"), which may be described in this thesis, may not be owned by the author and may be owned by third parties. Such Intellectual Property Rights and Reproductions cannot and must not be made available for use without the prior written permission of the owner(s) of the relevant Intellectual Property Rights and/or Reproductions

Acknowledgements

I would like to express my sincere gratitude to my supervisors Dr. Taimoor Asim and Prof. Rakesh Mishra for their support in the planning of the structure of the research work, and especially with the analysis of the results and their presentation in the thesis.

I would also like to express my thanks to my family for their continuous support throughout my studies at the University of Huddersfield.

Last but not the least, I would like to express my thanks to University of Huddersfield for giving me access to the software and the excellent facilities that were required for the successful completion of my Master's degree.

Martin Emilov Zahariev

Abstract

The gap between the supply and the demand of electricity is rapidly increasing throughout the world, due to the decommissioning of old coal-fired power plants, and the stringent regulations on carbon emissions. Power suppliers need renewable energy generating technologies which are both environment friendly and sustainable in a long term. The requirement of renewable technologies is resulting in an increased financing of the research and development in the solar and wind energy sectors. This increase in the research and development in these renewable sectors can be observed all across the developed world and in particular, the European Union, as a result of its commitment to its Renewable Energy Directive. In the United Kingdom, the wind energy sector has predominantly grown in the recent years, with the construction of multiple wind farms, both on-shore and off-shore. This is resulting in significant advancement in the designs of large wind turbines. However, the abundantly available wind energy in the urban areas is still an energy source to be explored.

The current research study is aimed at exploring the design and analysis methodologies of small-to-medium sized wind turbines for urban applications, as the published research in this area is severely limited. A drag based Vertical Axis Wind Turbine (VAWT) has been considered in the present study as these types of VAWTs are more suitable for urban environments. Such VAWTs operate at lower wind speeds, have multidirectional structure, simpler construction, lower manufacturing and maintenance costs, robust design, long lasting operational life, smaller size, low level of noise and vibrations, and possess the ability to self-start and be packed closer together. Improvements to the standard drag based VAWT designs are required to make the best use of their inherent design benefits, which coupled with a more refined and effective design can lead to a wide spread use of drag based VAWTs in urban centres, increasing renewable energy production. Detailed investigates on the effects of various innovative geometrical features on the performance of the VAWT have been carried out. This has been achieved through the use of advanced Computational Fluid Dynamics (CFD) based techniques.

The first aspect of the study is to carry out a detailed flow diagnostics of a standard drag based VAWT (the baseline model). Various innovative geometrical features have then been integrated with the baseline model to analyse their effects on the performance of the model. For this purpose, three dimensional models of the VAWT have been numerically analysed for the flow of dry and clean air in urban environments. Furthermore, sliding mesh technique has been employed to rotate the rotor of the VAWT. An in-depth qualitative and quantitative analysis of the global and local flow related parameters has been carried out, while instantaneous torque variations have been monitored throughout the rotation of the VAWT. The second aspect of the study is to critically analyse the start-up process (accelerating rotor) in order to determine the entire operating range of a helical VAWT design. Advanced CFD based technique, known as dynamic mesh, has been employed for this purpose. The advantage of dynamic mesh over sliding mesh is that sliding mesh assumes a constant operating point of the VAWT, while dynamic mesh generates the complete performance map of the VAWT; from the start-up to the constant operating point. Hence, the use of dynamic mesh technique is essential in understanding the transient accelerating behaviour of the VAWT. The third aspect of the current study is to develop an innovative in-house built CFD package for aerodynamic design analysis of VAWTs. The developed package is based on existing open source CFD solvers. Predictions from the developed package have been validated against a well-known and widely used commercial CFD software (ANSYS). The developed package has been shown to predict the complex flow structures in the vicinity of the VAWT, and its performance parameters, with reasonable accuracy, and hence can be used as an inexpensive tool for CFD based design analysis of VAWTs for small-to-medium sized enterprises (SMEs).

Contents

Flow Diagnostics and Optimal Design of Vertical Axis Wind Turbines for Urban Environments
By Martin Zahariev, School of Computing and Engineering, University of Huddersfield, UK (2016)

V

Flow Diagnostics and Optimal Design of Vertical Axis Wind Turbines for Urban Environments
By Martin Zahariev, School of Computing and Engineering, University of Huddersfield, UK (2016)

VI

List of Figures

Flow Diagnostics and Optimal Design of Vertical Axis Wind Turbines for Urban Environments
By Martin Zahariev, School of Computing and Engineering, University of Huddersfield, UK (2016)

VII

Flow Diagnostics and Optimal Design of Vertical Axis Wind Turbines for Urban Environments
By Martin Zahariev, School of Computing and Engineering, University of Huddersfield, UK (2016)

IX

List of Tables

Flow Diagnostics and Optimal Design of Vertical Axis Wind Turbines for Urban Environments
By Martin Zahariev, School of Computing and Engineering, University of Huddersfield, UK (2016)

X

Nomenclature

F	Force	[N]
T	Torque	[Nm]
M	Moment	[Nm]
L	Lift Force	[N]
D	Drag Force	[N]
C	Chord Length	[m]
V	Free Stream Velocity (wind velocity)	[m/s]
Cd	Drag Coefficient	[N/A]
Cl	Lift Coefficient	[N/A]
Cm	Moment Coefficient	[N/A]
Ct	Torque Coefficient	[N/A]
Cp	Power Coefficient	[N/A]
Ma	Mach Number	[N/A]
Re	Reynolds Number	[N/A]
Uc	Speed of Sound	[m/s]
Vs	Speed of Object	[m/s]
N	Number of Blades	[N/A]
H	Height of the Rotor	[m]
R	Radius of the Rotor	[m]
e	Overlap Distance	[m]
Pt	Turbine Power (Output Power)	[W]
Pw	Wind Power (Input Power)	[W]
x	Linear Distance	[m]
ν	Linear Speed	[m/s]
t	Time	[s]
TSS	Time Step Size	[s]
A	Area (swept area)	[m^2]
b	Interference factor	[N/A]
$\dot{m}$	Mass flow rate	[kg/s]
$\dot{P}$	Power Flux	[W/m^2]

Greek Symbols

α	Angel of Attack	[°]
λ	Tip Speed Ratio (TSR)	[N/A]
ω	Angular Velocity	[rad/s]
η	Efficiency	[%]
ρ	Air Density	[kg/m^3]
τ	Torque	[Nm]
μ	Dynamic Viscosity	[Pa.s]

Acronyms

WT	Wind Turbine
VAWT	Vertical Axis Wind Turbine
HAWT	Horizontal Axis Wind Turbine
DC	Direct Current
AC	Alternating Current
EU	European Union
USA	United States of America
USSR	Union of Soviet Socialist Republics
NACA	National Advisory Committee for Aeronautics
TSR	Tip Speed Ratio
TSS	Time Step Size
SMWT	Small and Medium Wind Turbine
LWT	Large Wind Turbine
FiT	Feed-in-Tariff
RO	Renewable Obligation
CFD	Computational Fluid Dynamics
FEA	Finite Element Analysis
2D	2 dimensional
3D	3 dimensional
SST	Shear Stress Transport
CC	Curvature Correction
RNG	Re-Normalisation Group

Flow Diagnostics and Optimal Design of Vertical Axis Wind Turbines for Urban Environments
By Martin Zahariev, School of Computing and Engineering, University of Huddersfield, UK (2016)

XII

Chapter 1
Introduction

This chapter provides an overview of current wind power technologies and their associated benefits. From this review, a number of key questions are raised which correspond to recent trends observed in the micro wind energy community and in particular the suitability of current technologies to operate effectively within the urban environment. The research topic has been introduced, with the details of different types of wind turbines, and their advantages and operational characteristics. Motivation to carry out this research and the main aims of this study are the highlight of this chapter.

Flow Diagnostics and Optimal Design of Vertical Axis Wind Turbines for Urban Environments
By Martin Zahariev, School of Computing and Engineering, University of Huddersfield, UK (2016)

1

1.1   Wind Energy

Wind energy originates from the solar energy. The wind flow is caused by the uneven heating of the earth's surface by the sun. The uneven heating of earth's surfaces causes the hot air to rise, and the cold air to fall, creating air movement. The wind energy can be harnessed and converted to a more useful form of energy, such as mechanical or electrical [1]. The modes of harnessing and converting the wind energy into useful form of energy are discussed in the next section.

1.2   Harnessing Wind Energy

Wind energy can be harnessed using various types of mechanical artefacts. One of the earliest ways to harness the wind energy was to drive sail boats across the Mediterranean Sea. The wind machines (both old-fashioned wind mills and modern wind turbines) are devices that convert wind's kinetic energy into mechanical energy. In the old-fashioned wind mills, the mechanical energy had been directly used via systems of shafts and pulleys to drive the grinding wheels. These wind mills are as old as the human civilization itself, and were first used in Ancient Persia. The design of the first wind mill was of a vertical axis type i.e. the shaft of the wind mill is perpendicular to the ground (vertical), and was based on the concept of utilizing the drag force experienced by the mill. A schematic illustration of this type of wind machines can be seen in figure 1.1 [2].
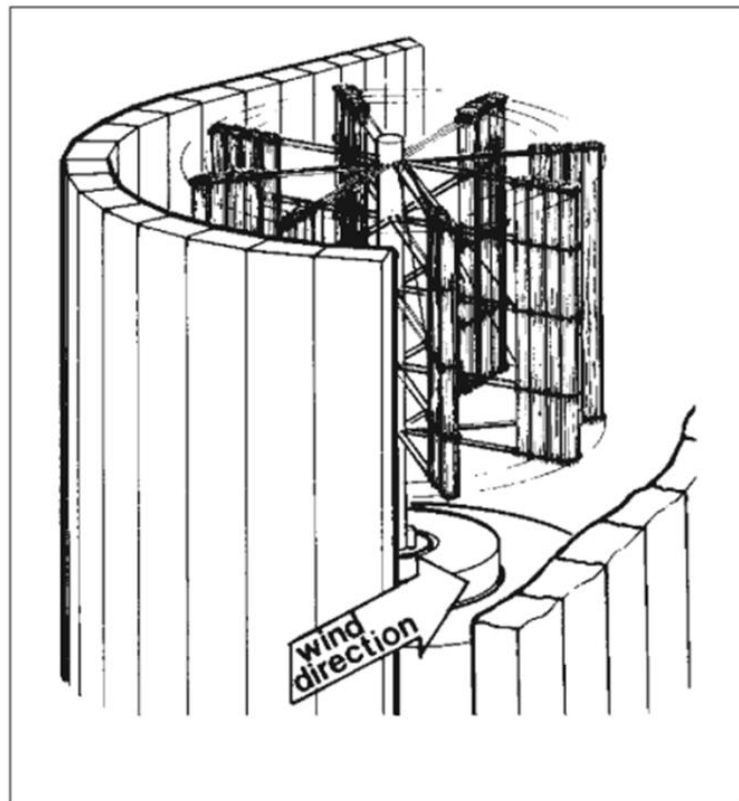
Figure 1.1: Simple Wind Device used in Ancient Persia [2]

Later on, these wind mills were used worldwide to grind various crops into flour. The design of these wind mills have changed throughout the centuries, for example, the European wind mills were of the horizontal axis type, yet the application was still the same. In modern wind turbines, the extracted mechanical energy is further converted, via the use of an electrical generator, into electrical energy. The generator can be DC or AC depending on the application. The wind turbines of today are being constantly redesigned with the goal of maximizing their output and efficiency, since they are seen by many as a viable answer to ever increasing energy requirements.

Flow Diagnostics and Optimal Design of Vertical Axis Wind Turbines for Urban Environments
By Martin Zahariev, School of Computing and Engineering, University of Huddersfield, UK (2016)

2

The first use of a wind machine to generate electricity, and lay the foundations of the modern wind turbines, has been recorded in 1887 in Glasgow by James Blyth. He was experimenting with several different designs of wind turbines and eventually developed a drag based vertical axis wind turbine, which he used to power his holiday home for 25 years [3]. An illustration of Blyth's vertical axis wind turbine is shown in figure 1.2.

Figure 1.2: Blyth's Wind Turbine [4]

1.3 Types of Wind Turbines

The two main wind turbine designs are the Horizontal Axis Wind Turbine (HAWT) and the Vertical Axis Wind Turbine (VAWT). The names HAWT and VAWT represent the rotation of the turbines perpendicular and parallel to the ground respectively (with their shafts being horizontal and vertical respectively). VAWTs are further divided into two types i.e. lift based and drag based VAWTs. As the current study focuses on the design and performance analysis of VAWTs, the following sections discuss the types and operational characteristics of such turbines in detail.

1.3.1 Lift based Vertical Axis Wind Turbines

After the first VAWT was being developed (James Blyth design), during the 1920s, another design of a vertical axis wind turbine was developed by a Frenchman named George Darrieus. This design is commonly known as Darrieus VAWT. It is also known as eggbeater windmill because of the way the two (or more) blades are attached to the vertical axis, resembling an egg [3]. Figure 1.3 shows a small windfarm made of several 2 blade Darrieus VAWTs.

Flow Diagnostics and Optimal Design of Vertical Axis Wind Turbines for Urban Environments
By Martin Zahariev, School of Computing and Engineering, University of Huddersfield, UK (2016)

3
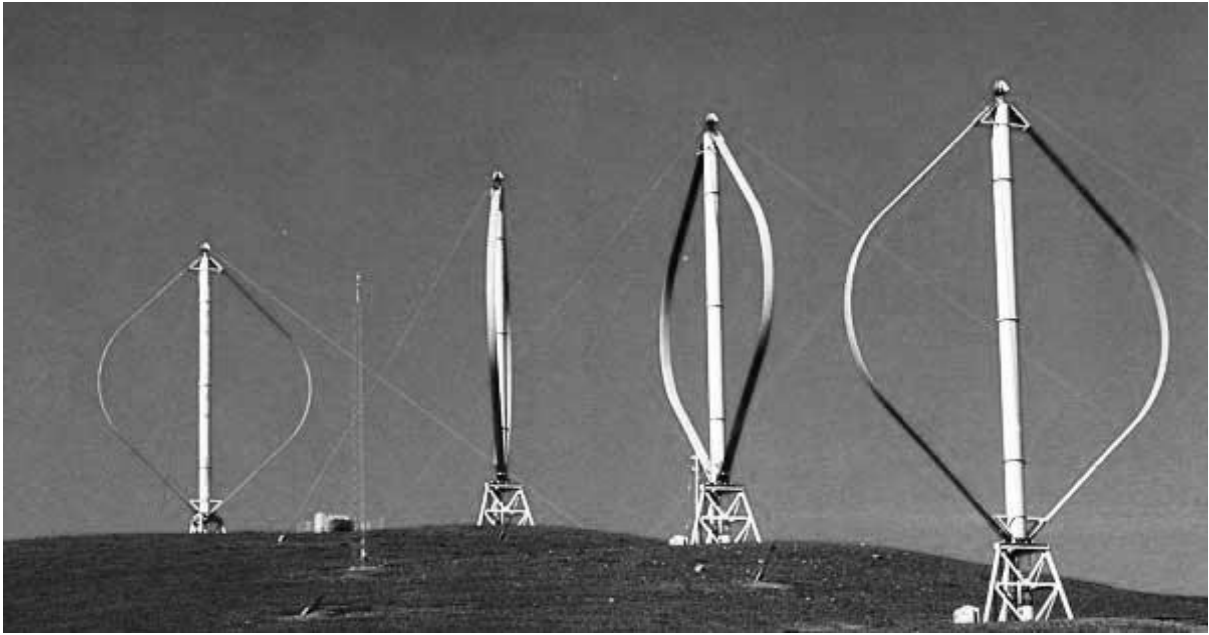
Figure 1.3: Darrieus VAWT design [5]

An H-Rotor design of the lift based VAWT was developed, which is the most efficient design of VAWTs. Further development on the H-Rotor is the helically twisted shape H-Rotor that has higher efficiency and more stable torque output. In figure 1.4, illustrations of the 3 different lift based VAWT designs are shown.

| (a) | (b) | (c) |
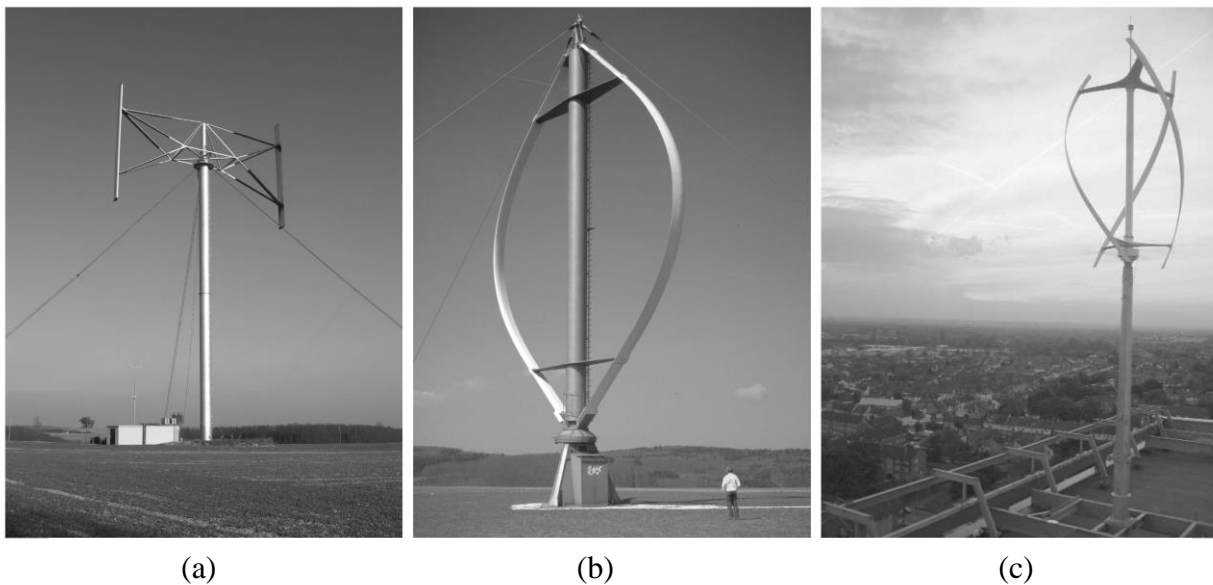
Figure 1.4: (a) H-Rotor design (b) Eggbeater design (c) Helical H-Rotor design [6]

The number of blades (solidity) is an important performance parameter of VAWTs (see figure 1.5). It is generally defined as:

$$\text{Solidity} = \frac{\text{No. of blades x chord length}}{\text{Diameter}} \tag{1.1}$$

Flow Diagnostics and Optimal Design of Vertical Axis Wind Turbines for Urban Environments
By Martin Zahariev, School of Computing and Engineering, University of Huddersfield, UK (2016)

4
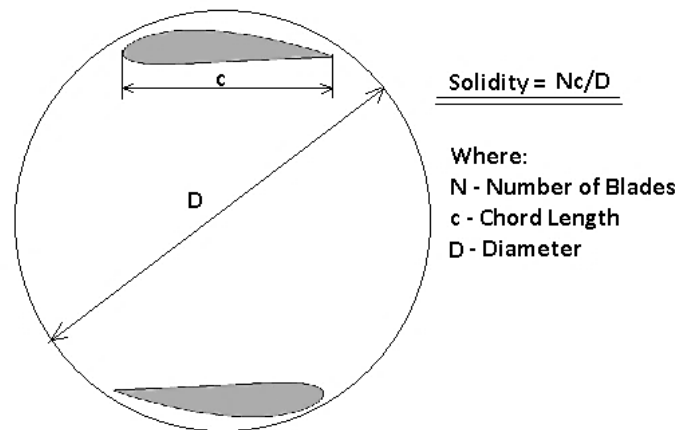
Figure 1.5: Solidity definition

It can be observed that both too low or too high solidity results in lower efficiency, therefore, depending on a particular VAWT design, there exists an optimal solidity ratio that gives best performance, which is usually around 0.2 - 0.3. If a given VAWT has different height of the rotor compared to the height of the blade (in V-Shaped VAWTs), the height term has to be included in equation 1.1 for calculating the solidity. In figure 1.6, the effects of solidity on the coefficient of power (Cp) of the VAWT are shown at different Tip Speed Ratios (TSRs).
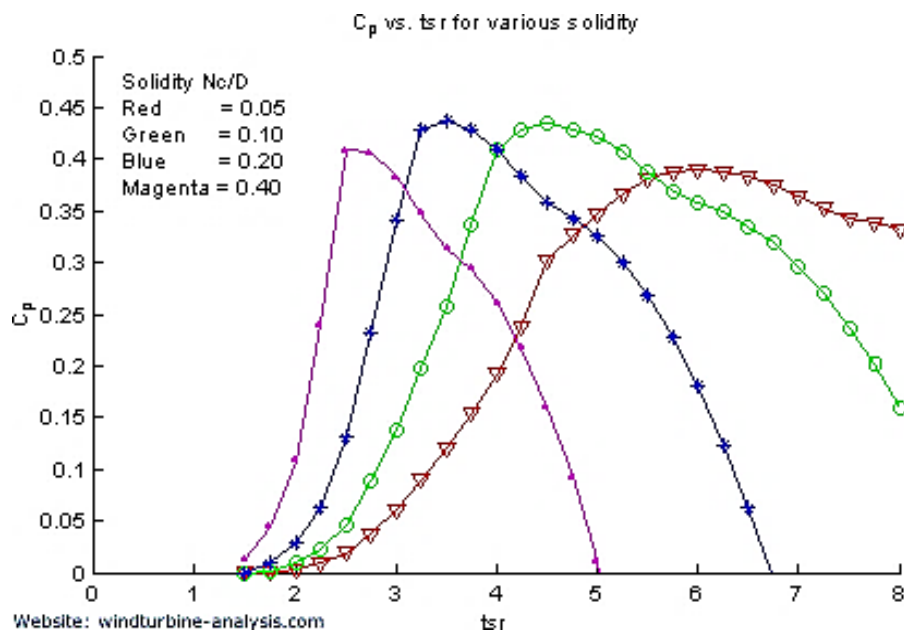
Figure 1.6: Solidity effect on a lift based VAWT [7]

In general, the blades of lift based VAWTs are non-adjustable, therefore, they require less control mechanisms. This design simplicity of the lift based VAWTs, although highly beneficial in terms of manufacturing and operational costs, has its toll on the efficiency [8]. Regardless of the fact that lift based VAWTs are less efficient than HAWTs, they have other advantages, such as simpler designs, smaller size, lower cost of manufacturing and installation, lower maintenance costs etc. They also have yet another major benefit - the way they disturb the surrounding air can be highly beneficial to other turbines in the same wind farm, if positioned properly. In figure 1.7, a detailed depiction of this is presented, showing the interaction of a VAWT with the wake of another VAWT. Hence, more VAWTs can be installed in the same area as compared to the HAWTs [9].

Flow Diagnostics and Optimal Design of Vertical Axis Wind Turbines for Urban Environments
By Martin Zahariev, School of Computing and Engineering, University of Huddersfield, UK (2016)

5
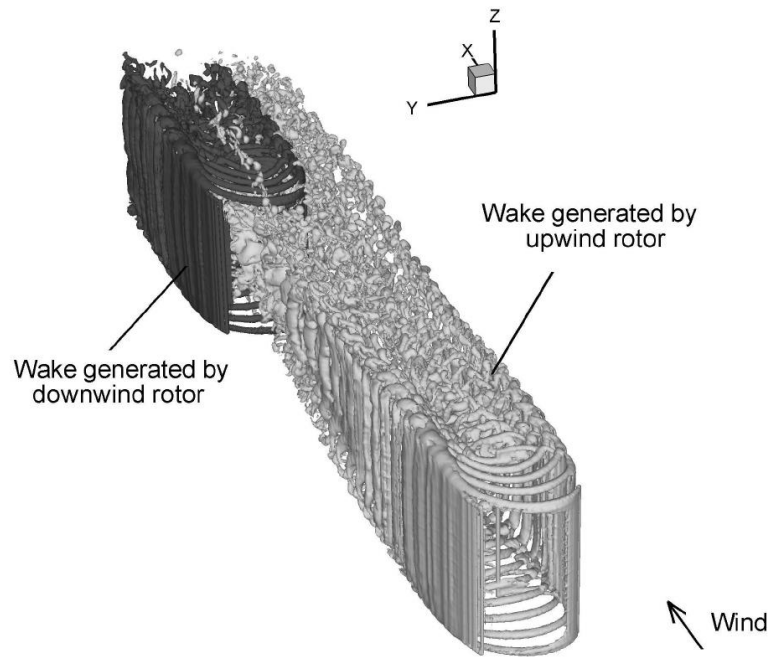
Figure 1.7: Crossover Stream [6]

The velocity of air deflected tangentially by the upwind VAWT is higher than the incident wind velocity. This is beneficial to the power extraction of the downwind VAWT, increasing the overall efficiency of the entire wind farm.

1.3.2 Drag based Vertical Axis Wind Turbines

Another variation of the VAWT design is the Savonius type, or the drag based VAWT, named after Finnish engineer Sigurd Johannes Savonius [3]. It is the only drag based wind turbine design, and is the one considered for design modifications and performance analysis in the present study. They operate at a much lower TSR. As these VAWTs operate under the principle of drag force exertion, the rotational speed of the turbine can rarely go above the wind speed, making the Savonius type VAWTs operating at lower speeds, yet yielding high torque. Figure 1.8 depicts different types of Savonius VAWTs.
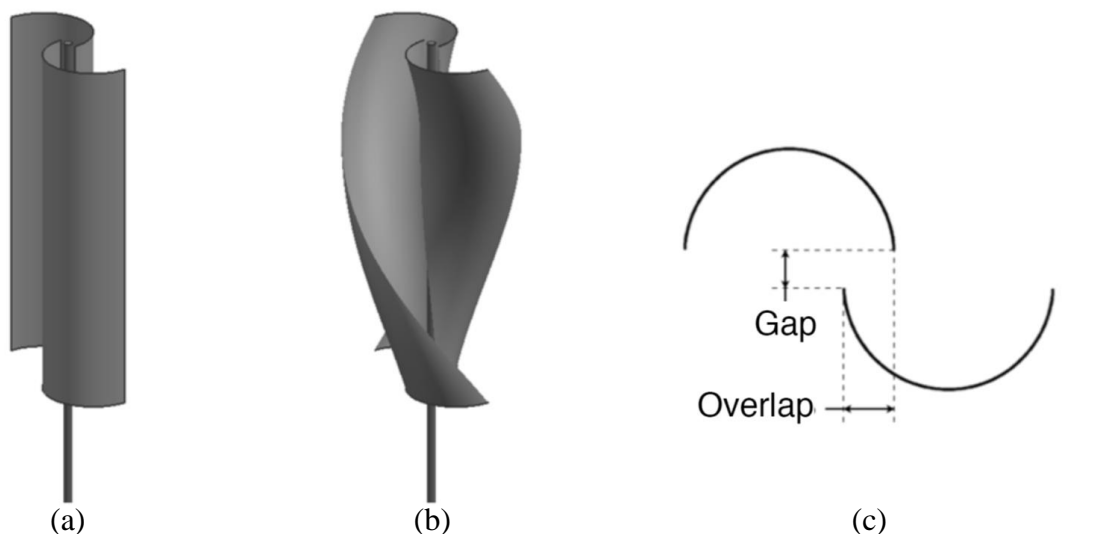
Figure 1.8: (a) Savonius VAWT (b) Helical Savonius VAWT (c) Gap and Overlap definition [10]

Flow Diagnostics and Optimal Design of Vertical Axis Wind Turbines for Urban Environments
By Martin Zahariev, School of Computing and Engineering, University of Huddersfield, UK (2016)

6

In figure 1.8, the overlap ratio is defined as follows:

$$\text{Overlap Ratio (S)} = \frac{e}{C} \tag{1.1}$$

It can be seen in figure 1.9 that the overlap allows the air leaving the advancing blade to strike the retreating blade, and by doing so, increasing the driving force.
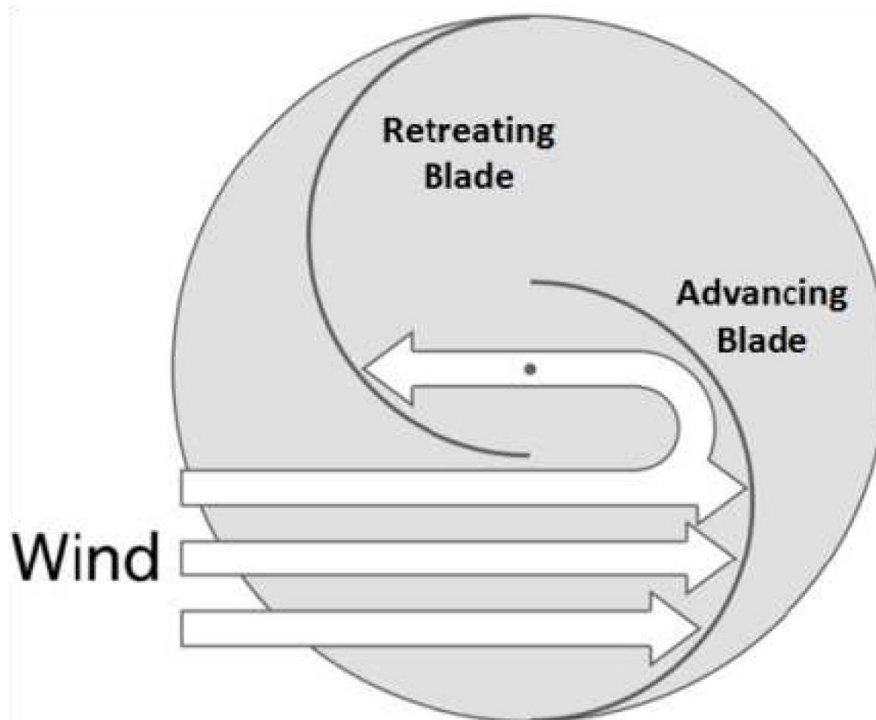
Figure 1.9: Savonius Rotor Operation [11]

Another important design parameter of a Savonius type VAWT is the aspect ratio, which is the ratio between the height of the rotor and the chord length of the blade. It plays an important role in the aerodynamic performance of the rotor [12], and can be defined as:

$$\text{Aspect Ratio (AR)} = \frac{H}{C} \tag{1.2}$$

The Drag based VAWTs are less efficient than the lift based VAWTs, but they have other benefits that, in some cases, outweighs the lack of efficiency. They have simpler design, rotate at lower speeds, the gearbox and bearings are under less stress making them more reliable, long lasting and requires less maintenance. They can also self-start, operate at wide range of wind conditions, and are quieter due to their higher torque generation and lower rotational speed, making them more suitable for urban environments. They are not only used to generate electricity, but also to drive water pump and other mechanical equipment.

Innovative blade profiles for the Savonius rotors have been developed to obtain better efficiency. Some of the newly developed profiles are shown in figure 1.10.

Flow Diagnostics and Optimal Design of Vertical Axis Wind Turbines for Urban Environments
By Martin Zahariev, School of Computing and Engineering, University of Huddersfield, UK (2016)

7

(a)   (b)   (c)   (d)
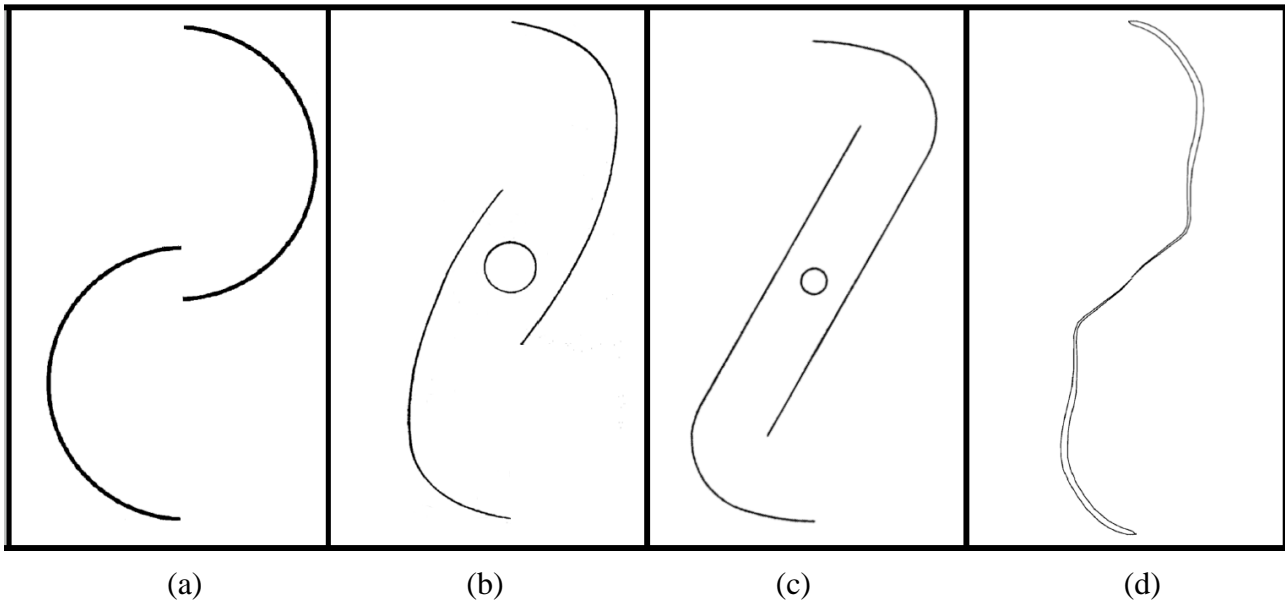
Figure 1.10: (a) Savonius (b) Standard Benesh (c) Improved Benesh (d) Rahai Profiles [10]

As the blades can be quite big and heavy, depending on the aspect ratio, a methodology of stabilizing the structure is required. There are several ways of achieving this, as shown in figure 1.11, where the central shaft with the weight rings, the frame structure and the end plates methods of stabilizing the structure have been shown.

(a)   (b)   (c)
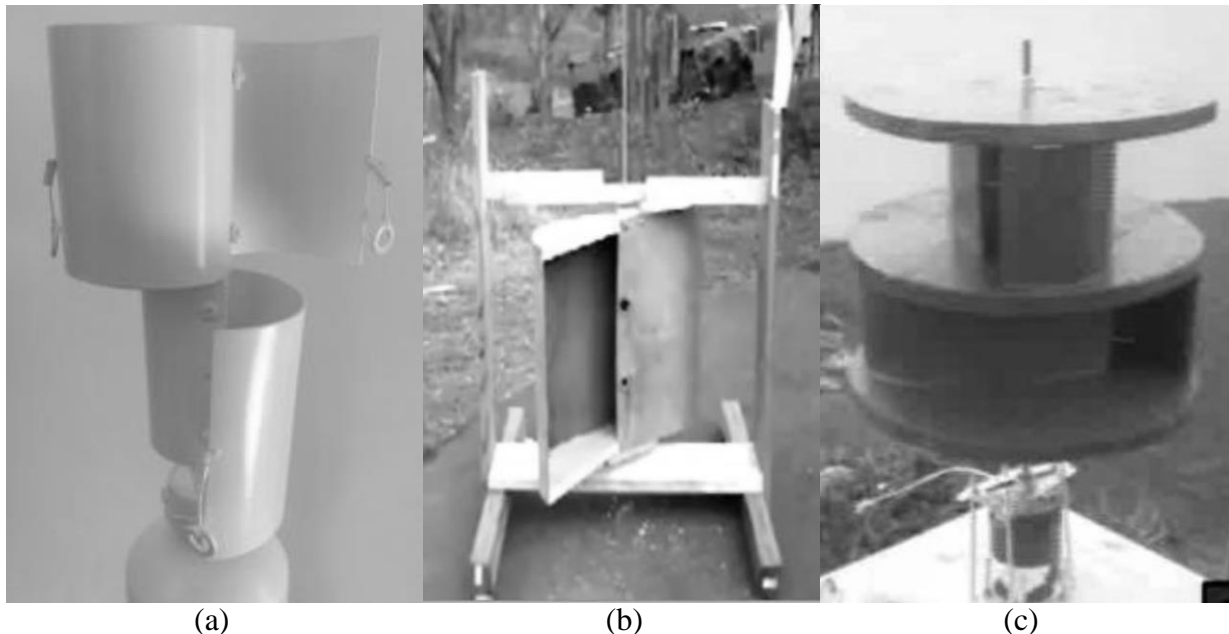
Figure 1.11: (a) Central shaft and weight rings (b) Frame structure (c) Flat discs (end plates) [13]

As the drag based VAWTs are operating at lower rotational speeds, the gearbox has to have higher speed ratio to increase the speed of the shaft to the generator. Drag based VAWTs are usually made for the small wind turbine market, therefore, there are conventional electrical generators that can be vertically installed, reducing the complexity of the design [14].

Flow Diagnostics and Optimal Design of Vertical Axis Wind Turbines for Urban Environments
By Martin Zahariev, School of Computing and Engineering, University of Huddersfield, UK (2016)

8

1.4   Operational Parameters of Wind Turbines

The method of energy extraction in wind turbines is mainly defined by the way the blades interact with the incident air flow. As mentioned earlier, VAWTs can be drag based, lift based or a combination of both. Improvements in the blade design usually results in higher efficiency. There are other design and performance parameters that influence the efficiency and performance characteristics of a wind turbine. Even though there are major differences between the different types of wind turbines, their performance can be characterized in a similar way, taking under account the number of blades (solidity), overall geometry (aspect ratio, overlap ratio etc.), and other process parameters, such as Tip Speed Ratio (TSR), Angular velocity (ω) and Free Stream Velocity (V). The primary goal of this characterization is to determine the Torque (T) and Power (Pt) outputs, and the Coefficient of Power (Cp), which is also known as Efficiency, at these conditions.

The overall wind turbine performance can be expressed as the variations in Cp against the TSR. TSR (λ) can be defined as:

$$\lambda = \frac{\omega \times R}{V} \tag{1.3}$$

where R is the radius of the rotor. The power output and the coefficient of power can be expressed as:

$$Pt = T \times \omega \tag{1.4}$$

and:

$$Cp = \frac{Pt}{\frac{1}{2}\rho A V^3} \tag{1.5}$$

where A is the swept area of the VAWT, which can be calculated as:

$$A_{VAWT} = 2Rh \tag{1.6}$$

h being the height of the VAWT. The power output of a VAWT is affected by the torque generated by it, which in-turn can be expressed as a function of the coefficient of moment/torque (Cm) as:

$$Cm = \frac{T}{\frac{1}{2}\rho A R \times V^2} \tag{1.7}$$

It is noteworthy that Cp is limited to a maximum value of 59.3%, in accordance with the Betz Law that proves this limit [15]. In figure 1.12, the Cp versus TSR relationship has been shown for the most common types of wind turbines.

Flow Diagnostics and Optimal Design of Vertical Axis Wind Turbines for Urban Environments
By Martin Zahariev, School of Computing and Engineering, University of Huddersfield, UK (2016)

9
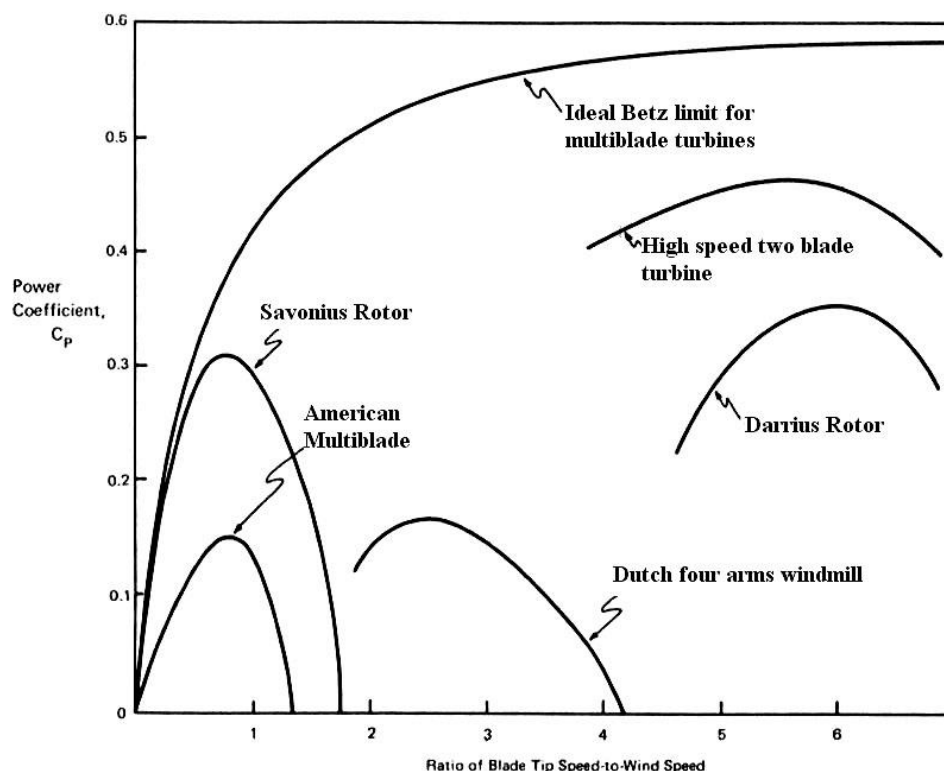
Figure 1.12: Performance Curves of Various Types of Turbines [15]

1.5   General Market Information of Wind Turbines

HAWTs are considered better than VAWTs solely on their higher efficiency. This has ensured that they are the most dominant design of wind turbines, with more than 90% of the market share of wind turbines [14]. The major focus of the wind turbine industry in the recent past has been the capacity of the wind turbines. High capacity (higher output) wind turbines are usually grouped in wind farms, which makes it easier to accommodate them into the electrical grid. This is yet another reason why HAWTs dominate the market of wind turbines, as their designs can be very large with a power output that is quite high. In the recent years, the focus of the industry has slightly shifted towards wind turbines suitable for urban environments (such as VAWTs). The primary goal is towards increasing the efficiency and reliability of VAWTs. This means that as HAWT designs are still more efficient than VAWTs, there has been on-going research and development of VAWTs to increase their efficiency [16]. A lot of Companies worldwide are manufacturing not only HAWTs and VAWTs, but also Hybrid systems where the wind power can be combined with solar, water and other types of renewable energy systems to create much more efficient products [17].

The UK market of small and medium wind turbines (SMWTs) is quite large, with 23,597 SMWTs deployed in the UK between 2005 and 2012. The UK manufacturers of SMWTs have also exported 24,939 SMWTs in the same time period. The total capacity of these turbines is 102.48 MW, and the market size in 2012 was £105.65 million [18]. The SMWTs market is expected to grow quite significantly in the coming years as the government is subsidizing the customers through the Feed-in Tariff (FiT) scheme and the Renewable Obligation (RO) scheme. Some limitations and regulations to these schemes are changing, due to major changes in legislation driven by the EU, aimed at the large wind turbine market, however, the UK government is keeping the option to choose between FiT and RO schemes for projects between 50kW and 5MW. Therefore, the market for SMWTs is still less regulated compared to the market for large wind turbines, which has been projected to increase to £157 million from 2013 onwards [18].

Flow Diagnostics and Optimal Design of Vertical Axis Wind Turbines for Urban Environments
By Martin Zahariev, School of Computing and Engineering, University of Huddersfield, UK (2016)

10

It can be seen in table 1.1 that for the small and medium wind turbines market, the average FiT is quite high (from £0.27 to £0.19); while for the large wind turbines market, it is much lower (£0.05 - £0.09). Hence, there is incentive to invest in SMWT market, as capital cost is low and FiT is high, even though payback time is longer.

Table 1.1: wind turbines Capital Cost, Feed-In-Tariff and Payback Periods [19]

Turbine size	Capital cost per turbine	Feed-in-Tariff generation rate (current, £/kWh)	Simple payback period
Building-mounted micro (2.5kW)	£10,000	£0.27	May not payback within lifetime
Micro (6kWh)	£20,000- £28,000	£0.27	May not payback within lifetime
Small (20-50kW)	£50,000 - £125,000	£0.24	8-15 years
Medium (100kW-850kW)	£250,000 - £1.8 million	£0.09 - £0.19	7-9 years
Large (1MW–2.5 MW)	£2 million - £3.3million	£0.05 - £0.09	Less than 1 year – 5 years

In figure 1.13, it can be seen that the SMWTs market is predominantly dominated by the HAWT designs, yet at-least 2-3% market share is held by the VAWT designs, trending to increase in the near future.
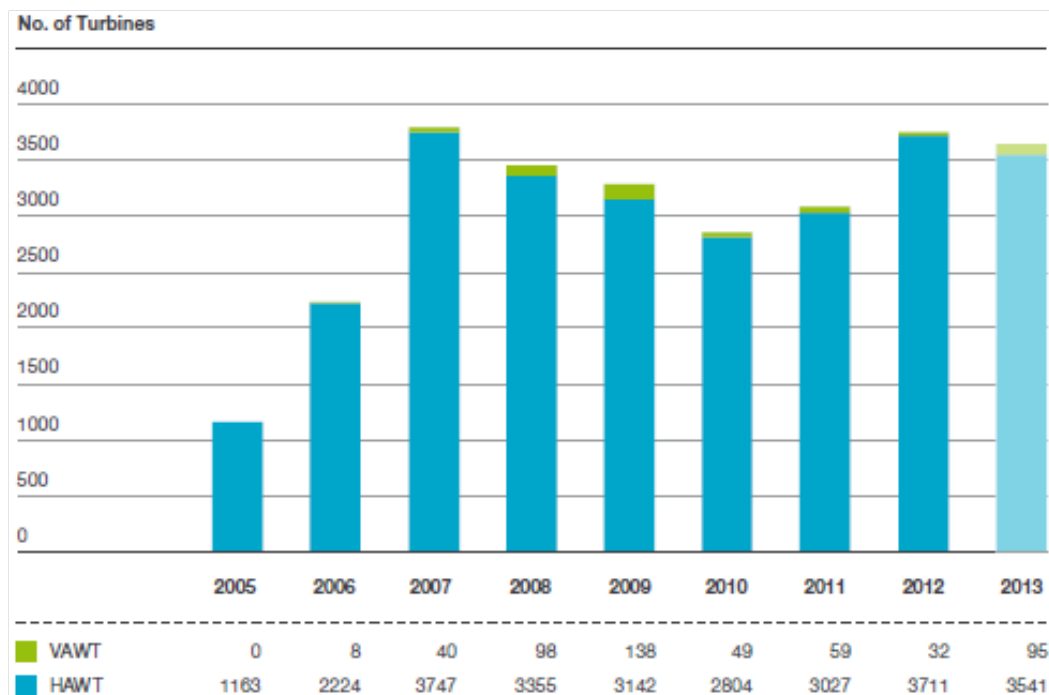
Figure 1.13: VAWT vs. HAWT market in the UK [18]

1.6 Future Developments

Other than the common wind turbine designs discussed earlier, there are also proposed concept designs that are in various stages of development, and have various different alleged advantages. They are to be further researched and developed in the upcoming years. Some of the most notable of these concept designs are discussed here.

Flow Diagnostics and Optimal Design of Vertical Axis Wind Turbines for Urban Environments
By Martin Zahariev, School of Computing and Engineering, University of Huddersfield, UK (2016)

11

1.6.1 High Altitude Wind Turbines

The advantage of this type of wind turbine is to harness the high altitude winds' energy, as the high altitude winds are one of the largest unused sources of renewable energy in the world. There is around 100 times more energy in the high altitude winds, which are more uniform than the ones close to the ground, making them more reliable. The high altitude wind turbine designs currently utilize horizontal axis technology, but the same principle can be used for vertical ones as well. The high altitude winds' energy can be harnessed by installing a wind turbine on a very tall tower. Buoyant Airborne Turbine (BAT) technology has been developed and driven by Altaeros Energies. It comprises of a ground station, tethers (guide cables), Buoyant Shell (balloon like construction) and a conventional HAWT inside the buoyant shell. This technology to lift and hold the turbine has been derived from the communication industry, which has used similar principles to lift and hold monitoring equipment high in the atmosphere [20]. In figure 1.14, wind power density has been plotted against the height of the tower to show the benefits of the BAT design over existing wind turbines.
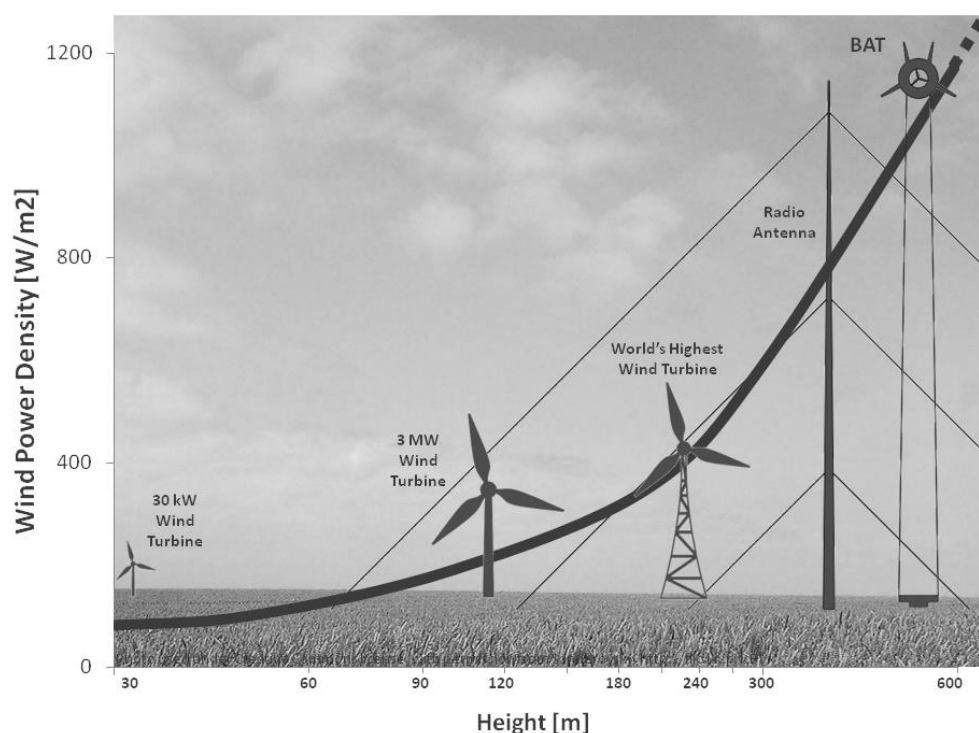
Figure 1.14: Wind power density versus height for various wind turbines [20]

1.6.2 Direct Drive Technology

Another recent development in the wind turbine designs is the direct drive technology. It uses modern control electronics mounted on a specially designed electrical generator, allowing the rotor's slowly rotating shaft to be directly connected to the generator, removing the need of a gearbox. This in-turn reduces the size of the nacelle, the number of bearings required, the amount of lubrication needed, and the control electronics associated with the gearbox are no longer needed. The primary advantage of this technology is that it has fewer rotating components, which increases the service life and the reliability of such turbines. Currently, companies (General Electric (GE) and Enercon) are developing and installing direct drive HAWTs. The designs are of large multi-megawatt type. The US Department of Energy (DOE) is giving quite a sizable funding to develop direct drive wind turbines [21]. In figure 1.15, a breakdown of the components of a GE 10MW direct drive wind turbine has been shown.

Flow Diagnostics and Optimal Design of Vertical Axis Wind Turbines for Urban Environments
By Martin Zahariev, School of Computing and Engineering, University of Huddersfield, UK (2016)

12
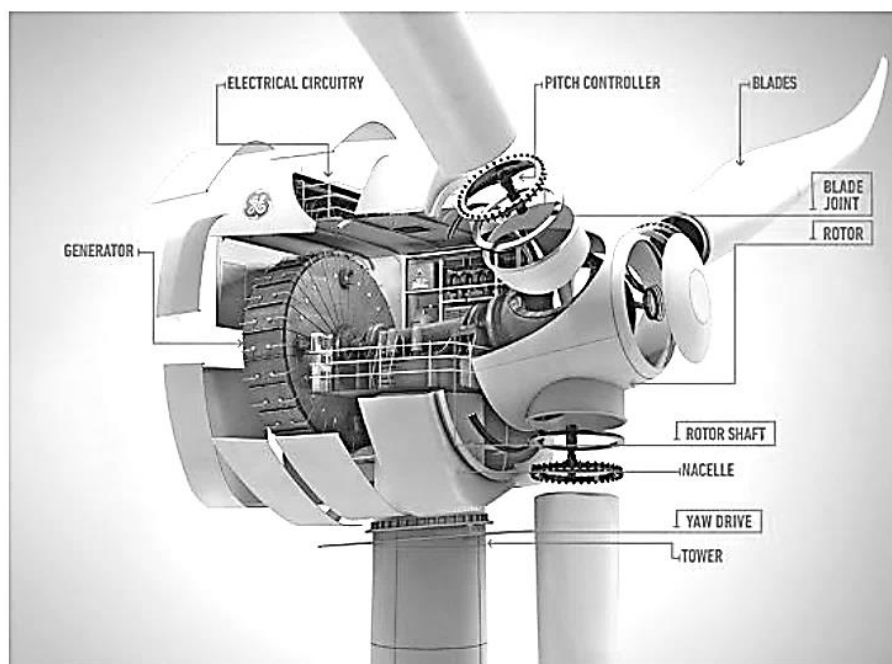
Figure 1.15: GE 10MW Direct Drive Design [21]

1.6.3 Jet-Flow based Wind Turbine

The jet engine inspired HAWT designs are aimed at increasing the efficiency of the wind turbines. This innovative design has been developed by a company named FloDesign. The design is based on aerospace technology known as Mixed Ejector. The US Department of Energy has funded 8.3 million US dollars to the company to continue the research and develop a prototype [22]. The jet based wind turbine is undergoing extensive testing in Massachusetts, USA. The turbine consists of a multi-blade stator and rotor, and it is designed to suck the air in, providing much higher rotational speed. The turbine casing is designed as a mixed ejector, which is basically a pump with no moving parts that allows the air to be evacuated from the turbine faster, thus creating suction effect [23].

1.6.4 V-Shape Offshore Lift-Based VAWTs

Lift based VAWTs can have efficiency similar to the HAWTs theoretically. In the offshore market, large lift based VAWTs are being developed i.e. V-Shaped lift based offshore VAWT [24]. The long V-shaped blades are of a complex airfoil design, but as the geometry has no curves, they are much easier to manufacture. The advantages of the V-shape design are that it can be mounted on both fixed and floating platforms, and the blades do not rotate against gravity, like in the HAWT designs. Therefore, they can be made much larger, and are easier to maintain. The suggested design to be built starts from 10MW, hence, the total power output of these turbines can be much higher than HAWTs. A concept design has been developed in a feasibility study made in the UK, under the brand name NOVA. It includes private companies such as Wind Power Limited, QinetiQ and various academic institutions like Cranfield University, Strathclyde University and Sheffield University. The design is to be further developed and commercialized, with the long term goal of installing a 1GW capacity of V-shaped wind turbines by 2020 [25]. In figure 1.16, the V-shaped offshore concept design has been shown along with its mounting arrangement.

Flow Diagnostics and Optimal Design of Vertical Axis Wind Turbines for Urban Environments
By Martin Zahariev, School of Computing and Engineering, University of Huddersfield, UK (2016)

13

Figure 1.16: V-Shaped VAWT 10MW concept design [25]

1.6.5 Shielded drag based VAWT design

The shielded drag based VAWT designs incorporate wind shields to adjust the angle at which the air strikes the rotor, increasing the overall efficiency of the design. The design consists of a stator and a rotor. The rotor blades are designed in a way to utilize both lift and drag forces exerted on them. One of such designs has been developed by Wind Power Systems, which is available in the market. It has been tested and certified to have Cp of 35%, which compared to traditional VAWTs is 40% higher, making the shielded concept design superior in terms of efficiency [26]. Figure 1.17 depicts the different components of this VAWT design.
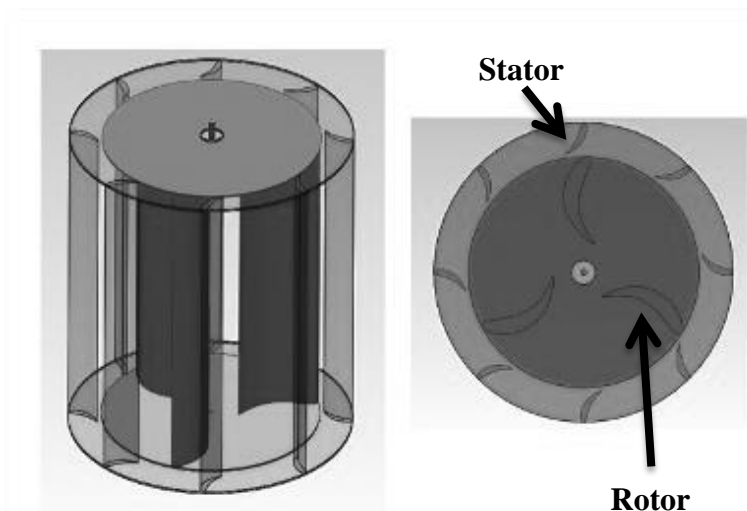
Figure 1.17: Shielded VAWT design [26]

A specially designed low-radar signature version of this VAWT design by Wind Power Systems has already been sold to the US military to power up remote military ground installations. The military stand-alone version of the design is shown in figure 1.18.

Flow Diagnostics and Optimal Design of Vertical Axis Wind Turbines for Urban Environments
By Martin Zahariev, School of Computing and Engineering, University of Huddersfield, UK (2016)

14

Figure 1.18: Wind Power Systems, LLC, PA-VAWTs Military Designs [26]

Other variations of the shielded design are also being developed by Trubina Energy AG, Germany [27].

1.6.6 Helical VAWTs

Another recent development in both lift based and drag based VAWTs is the helically (spirally) twisted blade design. This allows for a more uniform torque generation, and reduces vibrations and noise. The turbine is more stable operationally and the efficiency is higher [28]. An example of a helically twisted lift based VAWT is the QR5 model made by Quiterevolution; a London based company developing such designs for urban environments. Even though the design has a slightly higher efficiency than H-Rotor designs, significant reduction in noise and vibration levels is the primary advantage of such designs. The company has sold around 100 turbines in the last three years, which accounts for 40% of VAWT's market share [22]. One of the biggest companies in the market of SMWTs worldwide is UGE (Urban Green Energy); a New York based company that is also developing helically twisted VAWT designs, which have been shipped to more than 70 countries so far [29].

Drag based VAWTs using helical twists are also gaining popularity. A US-based company Helix Wind Corporation is currently developing a Savonius-like design with helical twists and ribbon blades. The price of lift based VAWT is around $15,000, while for a helical drag-based VAWT is $8,000 [30]. Helix Wind Corporation has recently been bought by Sauer Energy Inc., which is developing even bigger configurations of the drag-based helically twisted VAWT designs. At the moment, they offer 4.5kW helical designs [31].

1.6.7 Lift and Drag based Combined VAWTs

A concept model that has been developed and used since the early 80s, is regaining popularity in the market, as the demand for wind turbines that can operate in varying wind conditions is increasing. The combined (hybrid) designs are more efficient and reliable, but their manufacturing is complex [10]. These hybrid designs can vary in size significantly, and are primarily developed for SMWT market. They are capable of self-starting, and have wider operational range i.e. from 3 to 12m/s wind speed. The novel hybrid designs prototypes are undergoing developmental stages. WindUp and ISB are aiming to develop combined VAWTs of 1kW to 200kW output [32].

Flow Diagnostics and Optimal Design of Vertical Axis Wind Turbines for Urban Environments
By Martin Zahariev, School of Computing and Engineering, University of Huddersfield, UK (2016)

15

1.7 Motivation

From the general review carried out in this chapter, a number of key areas have been identified for further investigation. These key areas are concerned with the design and diagnostics of Vertical Axis Wind Turbines (VAWTs). VAWTs provide uni-directionality and hence are well suited to urban flow conditions, and variations in flow direction. Hence, a modelling technique is required to analyse the VAWT which can take into account these effects. Sliding mesh technique in CFD has been shown to have the ability to consider the complex blade interactions of the VAWT and hence has been used in this study. Furthermore, it has been shown that CFD can be used as an effective tool to predict the performance output of a VAWT with reasonable accuracy.

Optimal designing of vertical axis wind turbines is very important as far as commercial viability of such machines is concerned. The optimal design of a drag based VAWT is based on the introduction of various innovative design modifications to the conventional drag based VAWT design (the baseline model). These design modifications include internal guide vanes, tapering of the blades and helical twisting of the blades. The best design has then been analysed to cover its complete performance spectrum i.e. the start-up process, when the VAWT is accelerating, using Dynamic Mesh technique, along with the steady operational range by using Sliding Mesh technique.

With the ever increasing cost of commercial CFD software, it has been noticed and strongly felt that there is a need to develop much cheaper solution to this, while exhibiting the same level of robustness and accuracy that commercial CFD software provide. Hence, an in-house built design analysis tool/package has been developed considering the small-to-medium sized enterprises (SMEs). The developed package is based on available open source CFD solvers, which are very difficult to use (and limited support available), for turbomachinery in general (and VAWTs in specific) market. The developed design package offers the perfect solution to exorbitant commercial CFD software, yet depicts the same level of robustness and accuracy.

1.8 Research Aims

The specific research aims formulated for this research study are described in this section, whereas the objectives for this study will be discussed after carrying out an extensive literature review in the next chapter. Based on the motivation of this study, the research aims have been broken down into the following:

1. Flow diagnostics and optimisation of drag based concept VAWT designs for the complete performance spectrum

2. Development of an in-house built CFD package for aerodynamic design analysis of drag based VAWTs

The aforementioned research aims cover a wide range of operation of the VAWTs and hence can be considered satisfactory for this study. Detailed literature review is presented in the next chapter which focuses on the aforementioned research aims in order to find knowledge gaps in the existing literature.

Flow Diagnostics and Optimal Design of Vertical Axis Wind Turbines for Urban Environments
By Martin Zahariev, School of Computing and Engineering, University of Huddersfield, UK (2016)

16

1.9   Thesis Organisation

Based on the discussions presented in the previous sections, this thesis presents the body of work, which has been carried out for the current research study.

Chapter 1 provides an overview of wind turbines, with a focus on VAWTs. The operational parameters of drag based VAWTs have been discussed, along-with market analysis of wind turbines. From this overview, the motivation for carrying out this research is described, which identifies key areas to be reviewed in Chapter 2.

Chapter 2 consists of a detailed literature review of the relevant published work in the development of drag based VAWTs in chronological order, emphasising on the development of various geometrical features, improving the overall efficiency. The literature review also covers the developments of the methods for practical and computer based testing of the performance of VAWTs. The scope of the research has also been summarised in this chapter, which also leads to the specific research objectives being formulated for the current research study.

Chapter 3: This chapter shows the governing principles of the numerical modelling (CFD) and explains the creation of the geometry, methods of meshing, selection of turbulence models, boundary conditions and various solver settings used. This chapter also discusses the two techniques that have been used to conduct the numerical analysis (Sliding Mesh and Dynamic Mesh techniques) and the convergence criteria required for the numerical analysis.

Chapter 4: This chapter shows the mesh independence study, the time step independence study and the benchmark tests required to validate the numerical model. The performance analysis of the baseline models is also presented in this chapter. The effects of internal guide vanes, tapering and helical twists in the blades, on the performance of the VAWT, are critically analysed and presented in a structured manner, indicating the optimal VAWT design. The optimal design has then been analysed for its complete performance spectrum i.e. inclusion of the start-up process (accelerating VAWT) by using Dynamic Mesh technique.

Chapter 5 comprises of the development of an in-house built CFD package for aerodynamic design analysis of VAWTs. The in-house built CFD package has been used to conduct critical flow field and performance analysis of the optimal VAWT design from Chapter 4, and the results have been compared against commercial CFD software.

Chapter 6 concludes the study and clearly states the major conclusions and findings of the research work. The chapter also presents the attainment of objectives, shows novel contributions, explains the limitations of the work, and give future recommendations.

In the next chapter a detailed literature review of the development of drag based VAWTs has been presented in a chronological order.

Flow Diagnostics and Optimal Design of Vertical Axis Wind Turbines for Urban Environments
By Martin Zahariev, School of Computing and Engineering, University of Huddersfield, UK (2016)

17

Chapter 2
Literature Review

This chapter provides a critical review on the published literature in the area of wind turbines in general, and VAWTs in specific. The reviewed literature has been mainly focused on the introduction and optimization of various geometrical features to VAWTs, and the methods of analysing their performance, and conducting flow diagnostics. Scope of the research has also been presented A list of specific research objectives has been formulated.

Flow Diagnostics and Optimal Design of Vertical Axis Wind Turbines for Urban Environments
By Martin Zahariev, School of Computing and Engineering, University of Huddersfield, UK (2016)

18

2.1 Review of the development and analysis of drag based VAWTs

One of the first detailed researches into Savonius drag based VAWT designs have been made by Von G. Bach [33] in 1931. The investigations were conducted with the goal to determine the efficiency, and the practical applications of such a device. The research has been conducted experimentally, using the basic form of a wind tunnel. Within it, various different blade profiles and rotor configurations have been tested, alongwith the standard Savonius profile. In figure 2.1, several different VAWT profiles and configurations are presented.
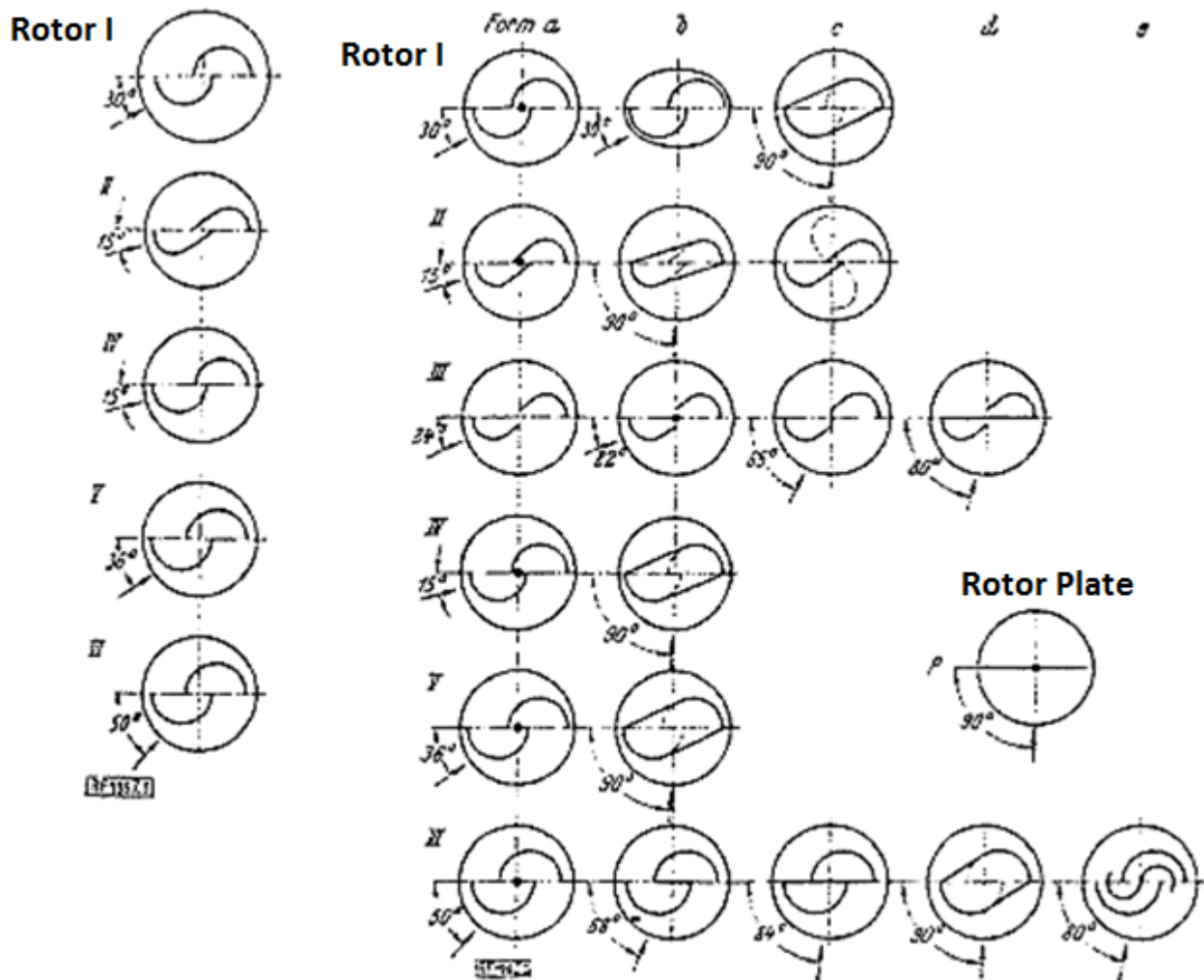
Figure 2.1: Blade Profiles and Rotor Configurations [33]

The measurement instruments used to determine the performance of the rotors were a dynamometer, attached to one of the shafts to determine the torque, and a pitot tube inserted into the wooded frame to determine the wind velocity. Within the wind tunnel, the rotors with different blade profiles have been suspended on two shafts in a wooden frame positioned in front of the wind tunnel. In figure 2.2, the experimental setup has been shown.

Flow Diagnostics and Optimal Design of Vertical Axis Wind Turbines for Urban Environments
By Martin Zahariev, School of Computing and Engineering, University of Huddersfield, UK (2016)

19
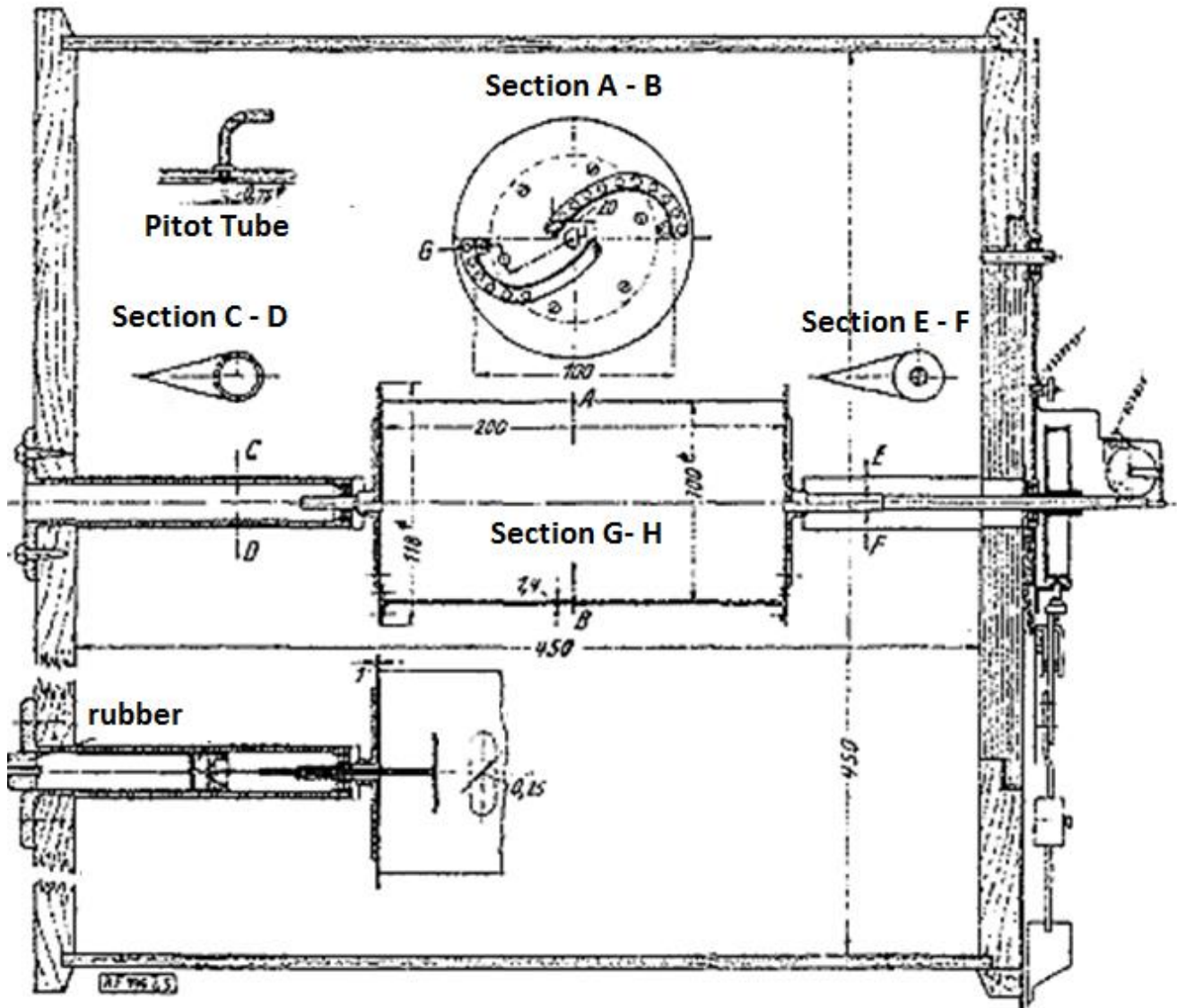
Figure 2.2: Wooden frame structure holding the Rotor [33]

An innovative technique, at that time, was used to visualise the flow field in the vicinity of the VAWT models. This technique was the use of silk threads in order to generate a picture of the flow field distribution, which in-turn provides better understanding of the flow propagation, and helps improving the design. With all the limitations of the technology at that time, an improved blade profile had been measured to reach efficiencies of 25 to 28%, which is high compared to even today's standards. Blade twisting, tapering and aspect ratio variations were not included in the investigations. Although some basic changes to the overlap ratio had been tested, the gap ratio was kept at zero. Other limitations and inaccuracies of this research were the lack of precise measuring equipment.

In 1930s, research into drag based VAWTs wasn't very intensive, with the exception of several researches carried out in Japan (English translation not available). After World War 2, the research mainly focused on using wind turbines for applications other than generating energy, such as water pump, fans etc. [34]. After the oil crisis in 1973, when the interest into wind turbines for energy generation was renewed, significant research and development into wind turbines of all types was carried out [34].

Flow Diagnostics and Optimal Design of Vertical Axis Wind Turbines for Urban Environments
By Martin Zahariev, School of Computing and Engineering, University of Huddersfield, UK (2016)

20

In the late 70s, a very detailed research into drag based Savonius type VAWTs has been carried out, which took several years to complete, and it is one of the most influential researches into Savonius type VAWTs. The Loughborough Report (a.k.a. wind tunnel test on a Savonius rotor) was made by A. J. Alexander and B. P. Holownia. The complete report was published in the Journal of Industrial Aerodynamics in 1978. The research covered various Savonius rotor configurations, including variations in the aspect ratio, overlap ratio and gap ratio. The research also included the effects of adding several geometrical features, including end extensions, end plates, addition of third blade, and flow shields, on the performance of the VAWTs. The experimental investigations were conducted at various wind velocities, ranging from 6 − 9m/s, in a wind tunnel with blockage ratio up to 0.3. The research study has been conducted to prove that, with the adjustments to the basic Savonius rotor design parameters and the addition of simple geometrical features, the efficiency of this type of turbines can reach upto 25%, without compromising the inherent simplicity and robustness of the design. In figure 2.3, some of the research outcomes have been presented, depicting the Cp versus TSR curve for the various designs they had tested [12].
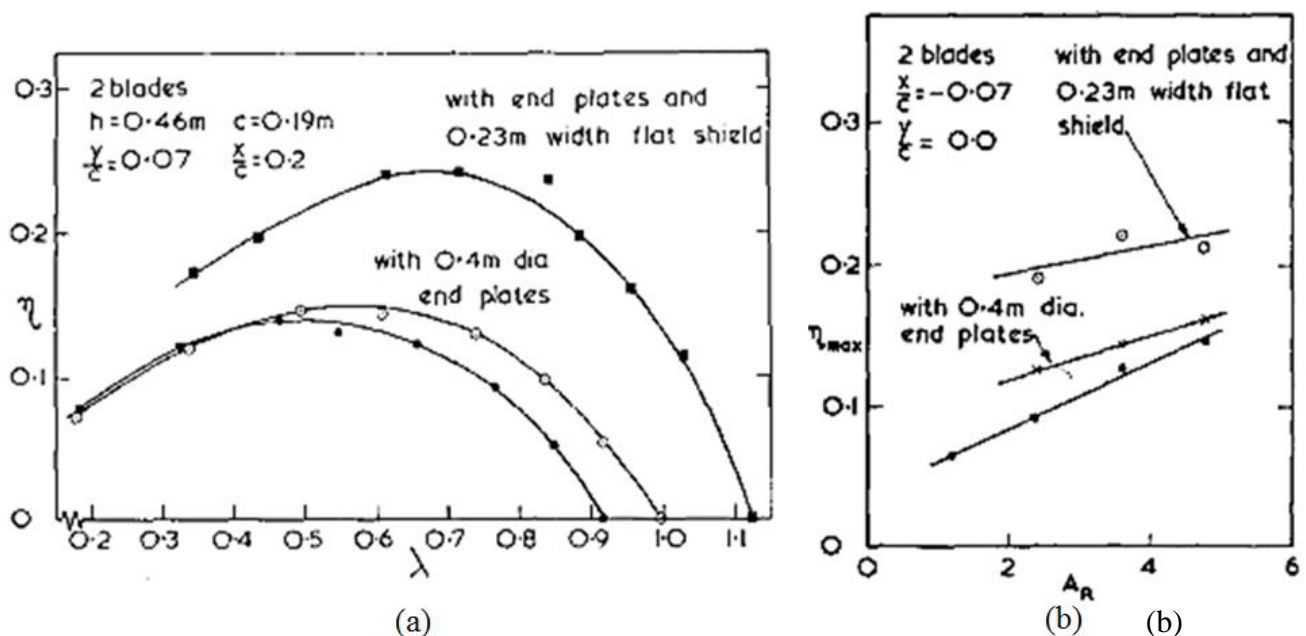
Figure 2.3: (a) Efficiency vs TSR (b) Efficiency vs Aspect Ratio [12]

As the objective of the experimental investigations was not to vary the simplicity of the Savonius design, no changes to the blade profile have been made. Therefore, the shape of the blade profile, tapering of the blade profile, and helical twist to the blades were not examined in this work [12].

In the following year (1979), another research has been published in the proceedings of the Indian Academy of Science by P. N. Shankar [35]. The study considers the Darrieus VAWTs, as they have efficiency similar to the HAWT designs. The study discovered that these VAWT designs have a major issue with self-start-up due to low-torque characteristics. The solution found to this issue was the drag based Savonius design of the VAWT. However, the research regarding Savonius VAWTs was severely limited. The study investigated different Savonius VAWT designs, including variations in the overlap ratio, number and profiles of blades. The test had been conducted at wind speeds ranging from 7.6 to 15.2m/s to simulate both the start-up and operational conditions. The results from this study are depicted in figure 2.4 [35].

Flow Diagnostics and Optimal Design of Vertical Axis Wind Turbines for Urban Environments
By Martin Zahariev, School of Computing and Engineering, University of Huddersfield, UK (2016)

21
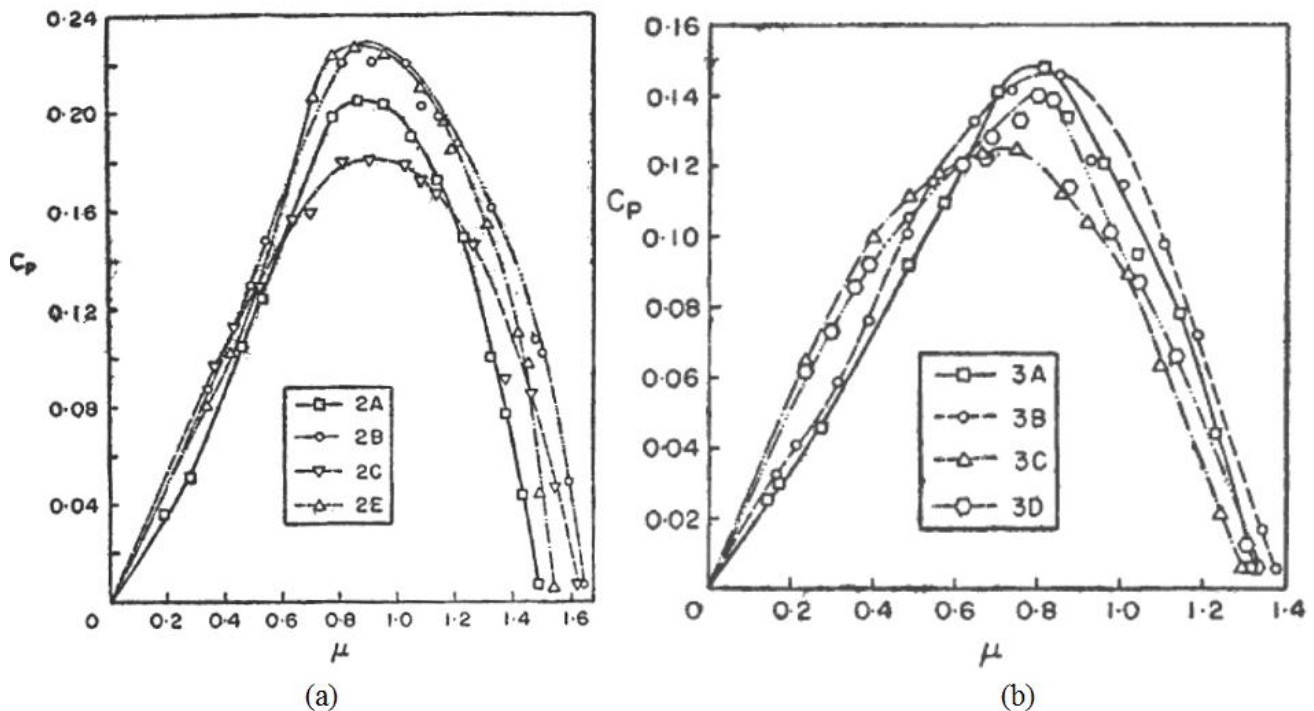
Figure 2.4: Cp vs TSR (a) 2 blades (b) 3 blades [35]

One year later, in 1980, research study for the Australian Department of Defence was carried out by Crook et al. [36]. This study focuses on the development, manufacturing and deployment of a 1kW wind-powered generator suitable for remote locations. The design was of a straight blade Darrieus type (H-Type) VAWT, with the addition of Savonius drag based rotor (with end plates) in the centre of the Darrieus design, to make the hybrid design self-starting. Several variations of both designs have been investigated prior to manufacturing, which, for the drag based VAWT, included variations in the aspect ratio, the addition of end plates and the introduction of central shaft support structure. The hybrid wind turbine was designed to work at average wind speed of 7.5m/s, allowing it to be operational at lower tower heights. The goal of this research was to save oil used in energy generation in remote scientific or military installations.

The Darrieus rotor operates at higher TSR values. At the same TSR values, the Savonius rotor consumes power rather than generating it. In order to calculate the power consumption, a mathematical linear extrapolation technique had been used. The technique is based on the local conditions and assumes linearity. It has been successfully used to calculate the power consumption of the Savonius rotor at these TSR values, and the design was modified accordingly. In figure 2.5, Cp versus TSR curves have been plotted for both the pre-modified and the modified designs. The adjusted Savonius design has lower aspect ratio and efficiency, but it was operational at higher TSR values. The power consumption of the modified Savonius design was lower at these TSR values; hence the combined design met its design criteria. The research focused on some novel features of the Savonius design, such as central shaft and how it affects the overlap ratio, but in general, it focused more on the hybrid VAWT. As a recommendation for follow-up research, the researchers pointed out the requirement for more detailed investigations into the individual design features of both VAWT designs, and how they interact with each other. A diagrammatic representation of this 1kW combined wind turbine design has been shown in figure 2.6 [36].
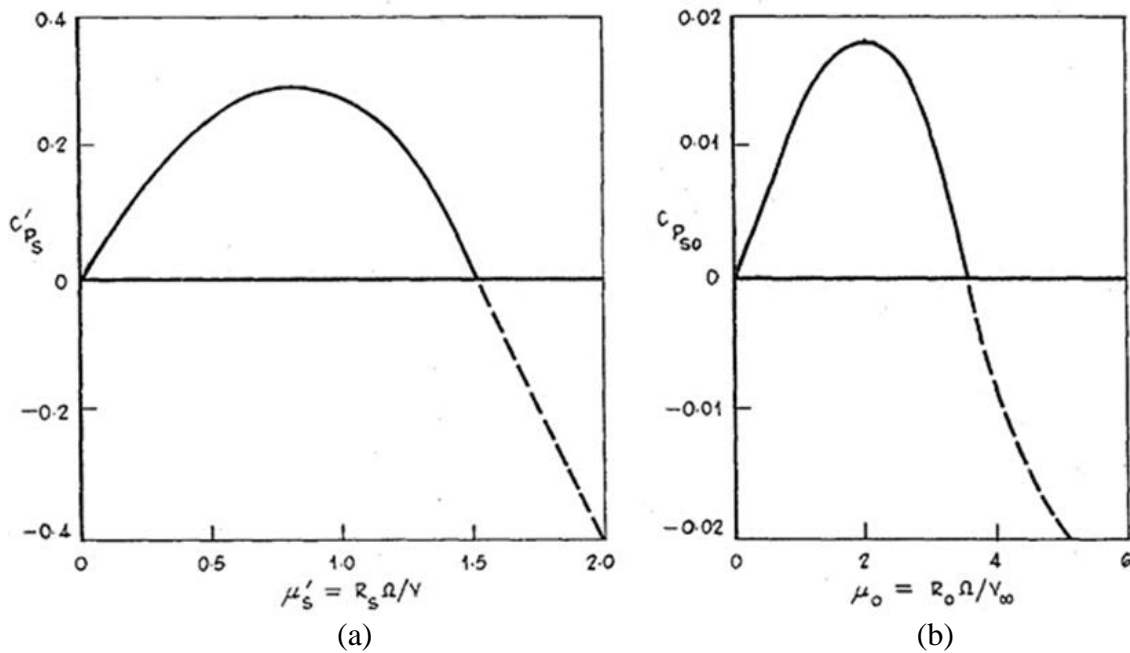
Figure 2.5: Cp vs TSR (a) Pre-modified design (b) Modified design [36]
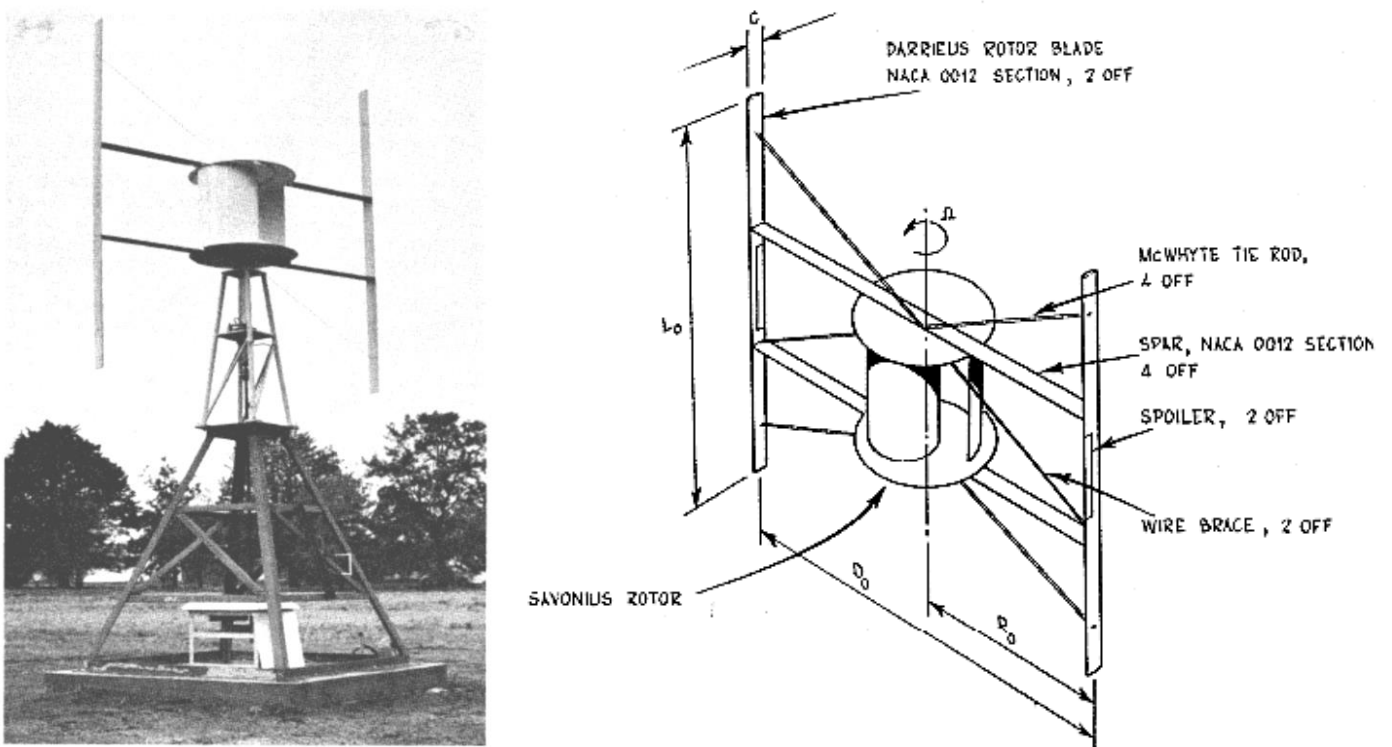
Figure 2.6: Hybrid VAWT design [36]

In 1986, a detailed research into Savonius VAWTs has been carried out by Takenori Ogawa and Haruo Yoshida [37]. The research study includes the testing of five different configurations of end plates (no end plate, circular, semi-circular, and two elliptical end plates at 45° and 60°). Moreover, three different shapes of deflecting plates (triangular, circular and flat deflecting plate) have also been tested. The primary goal was to figure out the design of the Savonius VAWT that can provide 16% efficiency, and to determine what type of different features can be added to the design to further increase the efficiency to 24% [37].

Flow Diagnostics and Optimal Design of Vertical Axis Wind Turbines for Urban Environments
By Martin Zahariev, School of Computing and Engineering, University of Huddersfield, UK (2016)

23

In 1987, a research study was carried out by Fernando [38], aimed at investigating the performance and wake aerodynamics of a Savonius VAWT. The research included wind tunnel based experiments of scaled models in order to determine the effects of changes in overlap ratio, gap ratio, aspect ratio, blade profile shape, Reynolds number and wind flow blockages shielding, on VAWT's performance. Two further models were also tested, the first model being a semi-empirical model, based on central vortex approach. The results were similar to the experimental results, but under-predicted the efficiency at lower TSR values. In figure 2.7, the Cp versus TSR curves have been shown for various models both from the experimental and semi-empirical approaches [38].
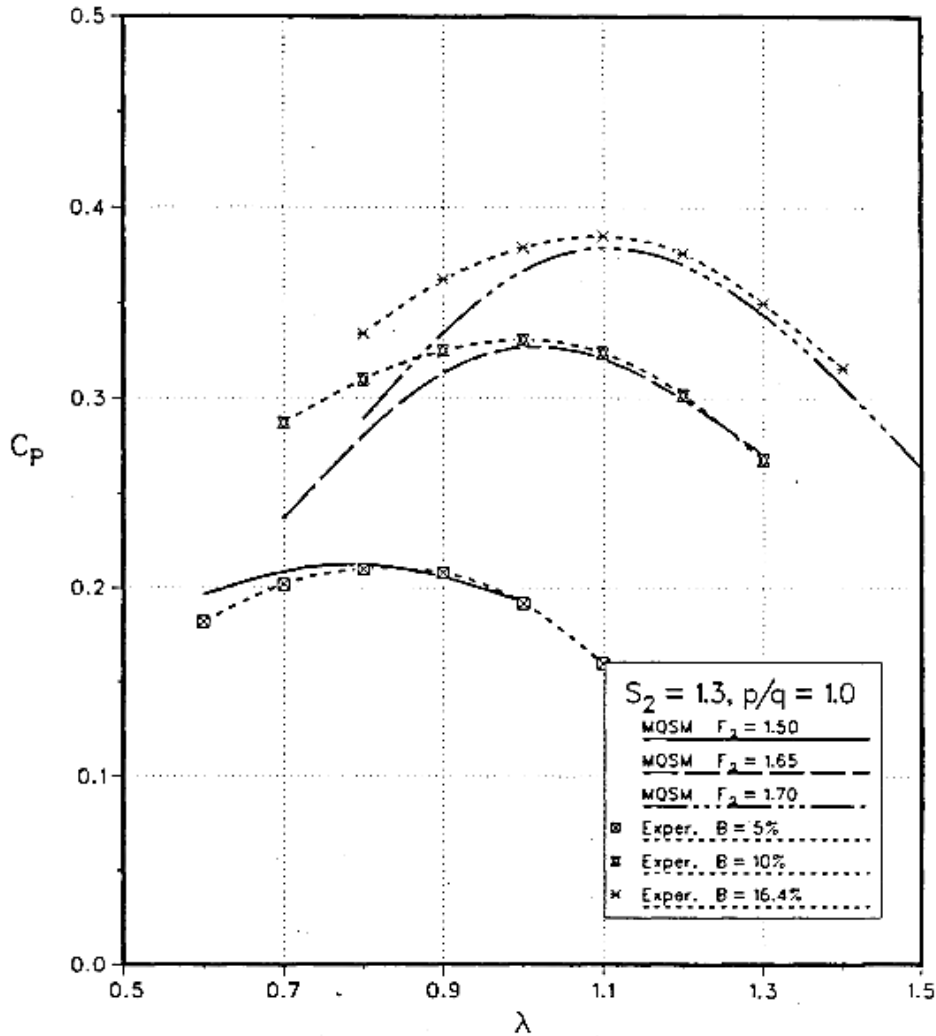
Figure 2.7: Cp vs TSR experimental and semi-empirical approaches [38]

The second method was a purely numerical method, using Navier-Stokes equations, as the problem is characterized by viscous, turbulent, separated and time dependant behaviour. The model had been simplified, and instead of FEM (Finite Element Method), a version of the BEM (Boundary Element Method), called Direct Vortex Method (DVM), had been used. The model geometry had been simplified, and 2D versions were used to reduce the computational cost. The blades were represented as thin surfaces, and the edge points were considered as control point. The results were found to be quite sensitive to $\frac{\partial \Gamma_{st}}{\partial t}$ term; therefore, a second order accuracy was achieved by using Gaussian three-point differential equation at the mid-point. The flow visualization study was compared to the computational results, as shown in figure 2.8, where it has been deduced that the numerical method captures the complex flow behaviour exhibited by the VAWT.

Flow Diagnostics and Optimal Design of Vertical Axis Wind Turbines for Urban Environments
By Martin Zahariev, School of Computing and Engineering, University of Huddersfield, UK (2016)

24
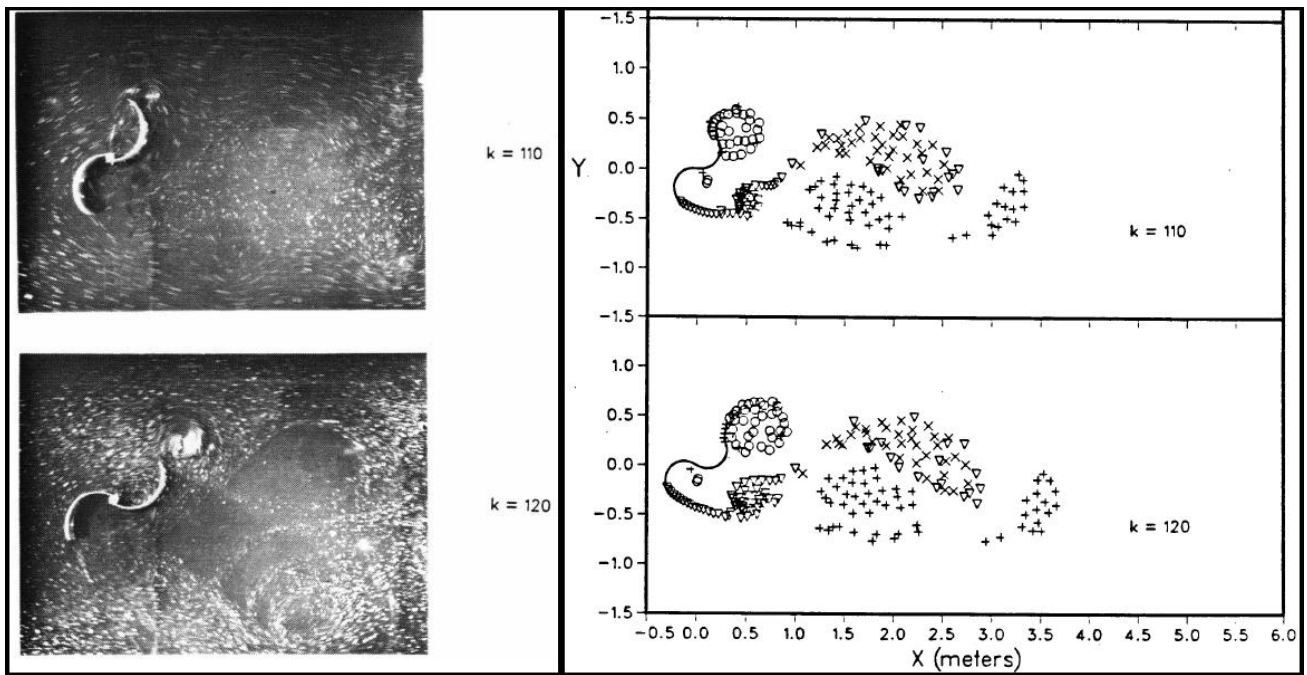
Figure 2.8: Flow visualization study and computational results [38]

The results obtained are compared to the experimental ones in figure 2.9, showing Cp versus TSR.
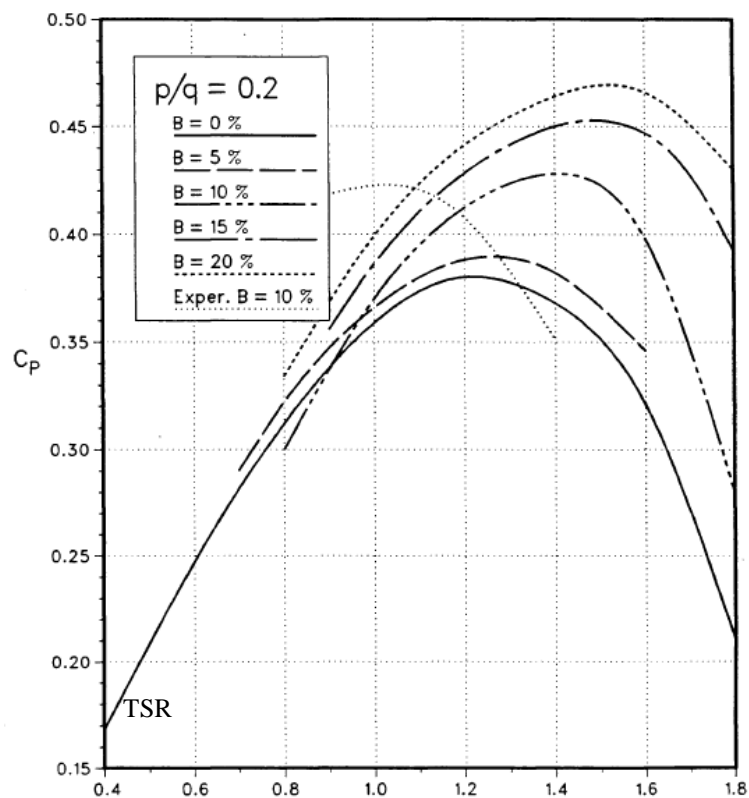
Figure 2.9: Cp vs TSR computation and experimental curves [38]

Flow Diagnostics and Optimal Design of Vertical Axis Wind Turbines for Urban Environments
By Martin Zahariev, School of Computing and Engineering, University of Huddersfield, UK (2016)

25

In early 90s, with the advancement of the computer technology, one of the first researches that solely used a computational method was carried out in Japan by Aldoss and Kotb [39]. The research study provided detailed flow information around a two blade stationary Savonius rotor, positioned perpendicularly to the incident flow. The Direct Vortex Method (DVM) was employed. The work has been carried out in order to better understand the theory behind the calculations of the initial torque of the Savonius rotor. 300 time steps (0.006s for each time step) numerical simulation was simulated, where the flow velocity distributions are shown in figure 2.10 [39]:
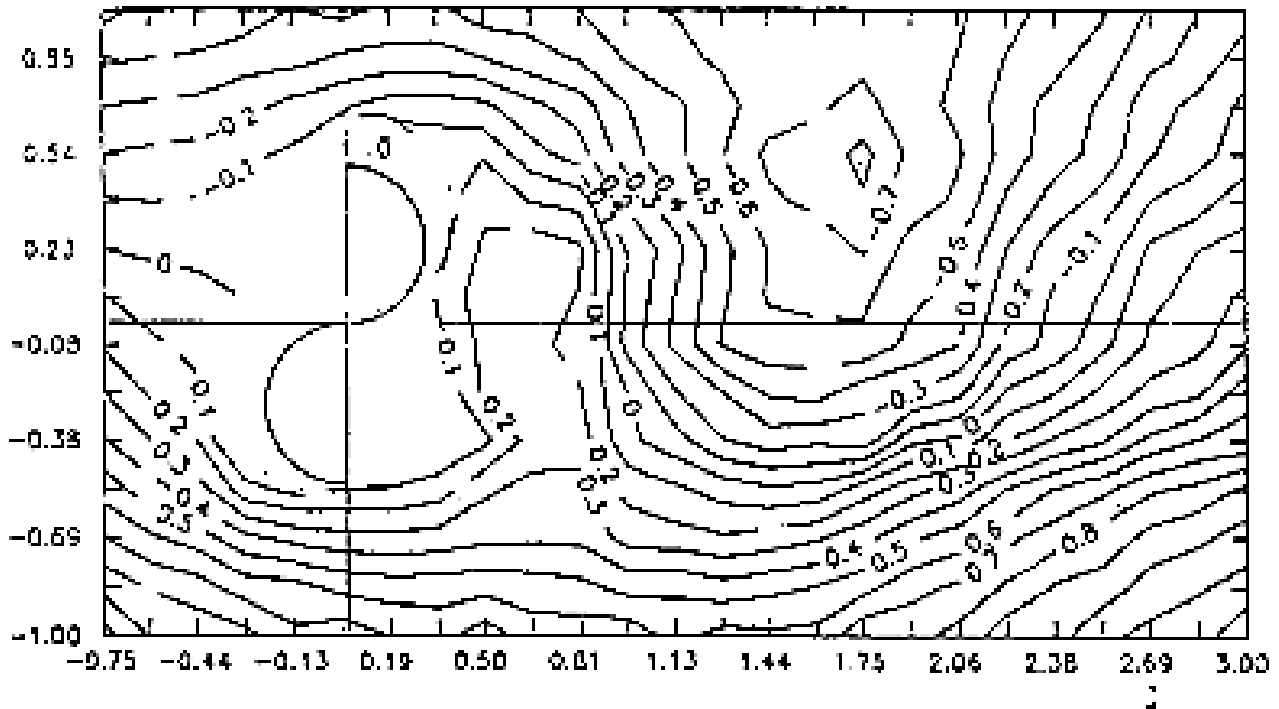
Figure 2.10: Flow velocity iso-contours [39]

The local pressure values around the blades were used to calculate the torque, and it has been found that at this position, the returning blade has negative torque, while the advancing blade has positive torque. The low initial torque characteristics observed in experiments were obtained through the use of computer simulation [39].

In 1992, a study was carried out by Fujisawa and Gotoh [40], focusing on generating the flow field accurately using experimental approaches. The research study included several flow visualisations studies, which described the instantaneous flow field in the vicinity of a Savonius rotor, with and without rotation. A detailed investigation into the effects of the flow separation has been undertaken at various TSR values, on the efficiency of the VAWT. The research study has been carried out with the use of an open circuit type wind tunnel, where the Savonius rotor has been installed with CCD camera, smoke wire, mirror, Ar laser and a smoke machine, as shown in figure 2.11 [40]. A detailed understanding of the rotational effects on the flow separation, and the overall flow region, were the main objectives of the research. It has been noticed that the flow separation at the convex side of the advancing blade is reduced by the rotation effect. It has also been observed that the attached flow is prone to separate at large rotor angles, and the rotation effect causes induced flow in the overlap regions, resisting the overlap flow, hence reducing the effects of the overlap. Another finding is that the attached flow to the convex side of the rotor grows with the TSR, and eventually becomes saturated; therefore, explaining why the turbine has higher efficiency at low TSR values [40].
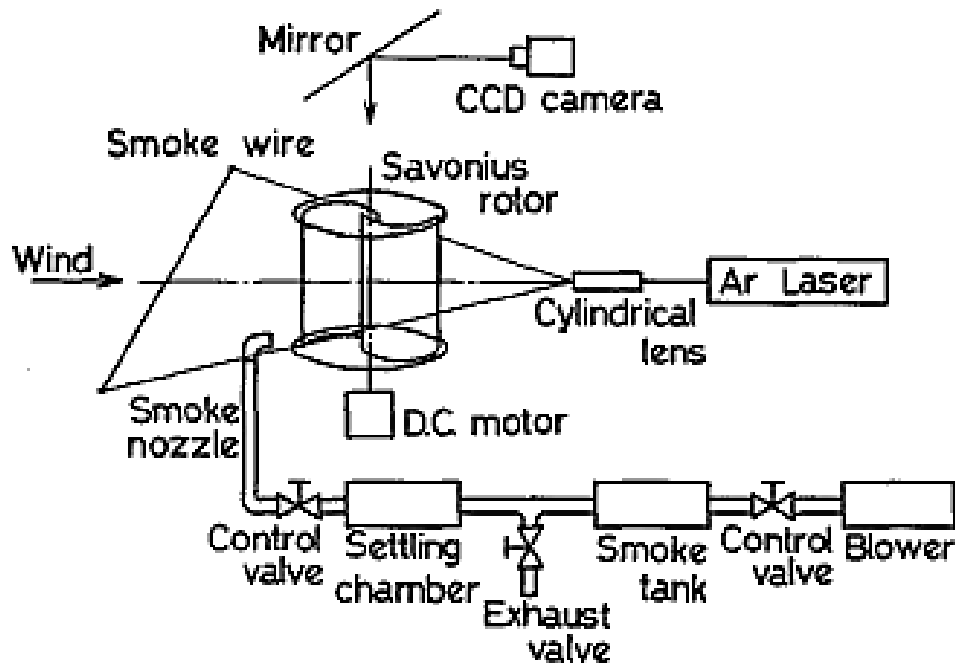
Figure 2.11: Experimental setup [40]

Even though the method is very detailed in explaining the effects of turbine's individual features to the local flow conditions, it is limited in terms of how many variations of the design had been tested. Therefore, the research study doesn't explain how changes to these individual features affect the local flow conditions, and how that can be used to increase the overall efficiency.

In mid-90s, a detailed research has been carried out, using both experimental and numerical methods, to describe the effects of the overlap, and compare the results from the two methods. The research was carried out by Fujisawa [41]. The research work investigated the local flow field, in and around Savonius rotor, at various overlap ratios. The experimental method included measurements of the phase-averaged velocity distributions, using Particle Imaging Velocimetry (PIV) with conditional sampling technique. The numerical simulations were carried out using the Direct Vortex Method. The velocity distribution at various overlap ratios have been shown in figure 2.12. The tests have been carried out in both stationary and rotational mode, and it has been found that in the stationary mode, an increase in the overlap ratio results in an increase in the torque output. Whereas, in the rotational mode, a limit to how much the overlap ratio can be increased has been found, and any further increase results in reduced efficiency. Therefore, the optimal overlap ratio has been found out. The numerical method predicted the basic patterns of the flow field at stationary position, at high rotor angles. At lower rotor angles, it failed to accurately predict the flow variations in the vicinity of the rotor, and downstream the rotor, which can be due to the 3D nature of the real flow, and the fact that the numerical method assumes flow separation at the blade tips only. The numerical method worked better for the rotational mode, where the assumptions of flow separation matched better with the real world scenarios [41].

Flow Diagnostics and Optimal Design of Vertical Axis Wind Turbines for Urban Environments
By Martin Zahariev, School of Computing and Engineering, University of Huddersfield, UK (2016)

27
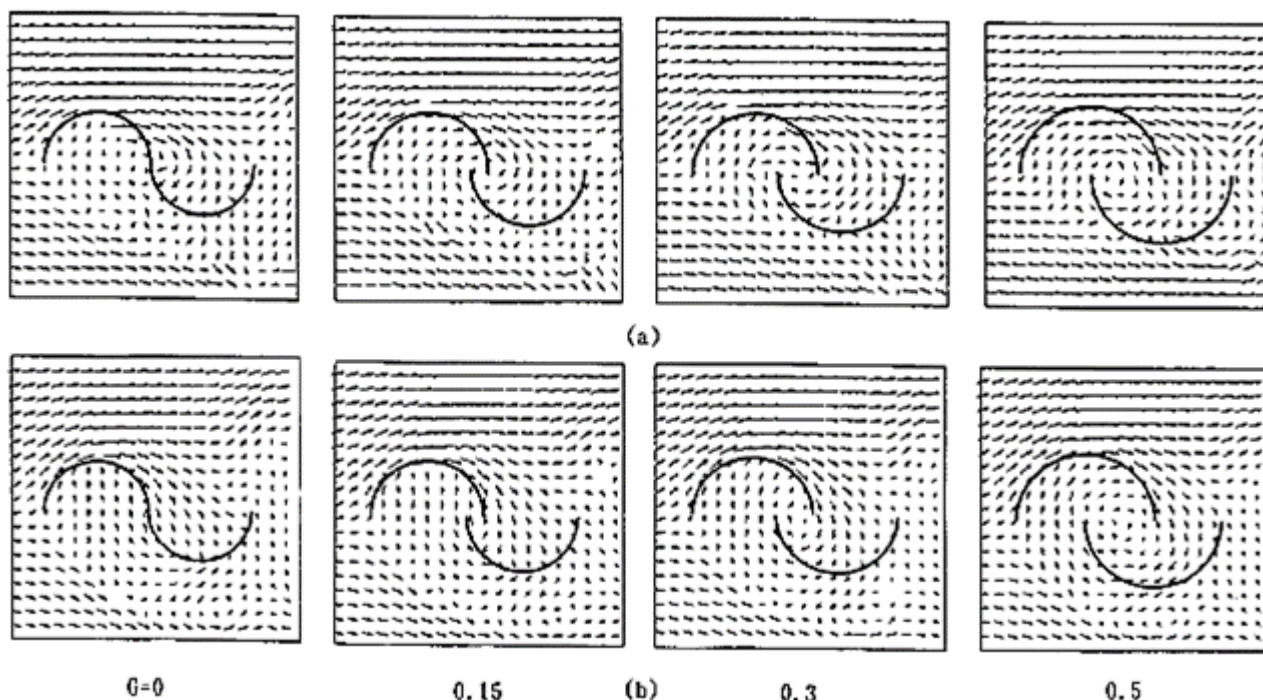
Figure 2.12: Velocity Distribution (a) Experimental (b) Numerical [41]

The numerical methods used so far were very simple (2D blade element\momentum theory (BEMT) type), and practical flow field investigation had proven that discrepancies between the experimental and numerical methods exist. These discrepancies are addressed by Dua and Selig [42] by considering a more complex 3D incompressible steady momentum integral boundary layer equation. Both laminar and turbulent models have been used to improve the accuracy of the numerical methods in predicting the effects of rotation on the blade's boundary layer. Using this method, it has been found out that the separation point on the blade is shifted due to rotation, which has beneficial effect on lift force. It has also been observed that coriolis and centrifugal forces are vital to the stall delay, and that this shifts the separation point further downstream. However, the complex transient effects have not been address in the study.

In 2000, a retrospective look into the market of wind turbines has been carried out by Ackermann and Soder [43]. The work states that during the 1990s, the installed capacity of wind turbines doubled every three years, and that the market is growing intensively. It also states that this increase is due to the expansion of HAWT's market. The work also states that the VAWTs were developed and commercially produced until the end of the 1980s, but during the 1990s, the research and development into VAWTs has almost stopped worldwide [43].

Interest in VAWT renewed, and one of the most promising designs i.e. hybrid VAWT was further investigated by Gupta, Das and Sharma [44]. The research included practical testing of a mid-sized hybrid VAWT in a wind tunnel. The Savonius turbine was placed on top of the Darrieus turbine, not forming a resistance for the incident flow to the Darrieus turbine. Their research also included various overlap changes of the Savonius turbine, and discussion on how this affects the overall efficiency. The new design reached 25% efficiency, and discussed the role of the overlap in detail. The research study rekindled the interest in VAWTs and showed how changes to certain features can affect the performance, and pointed out that further research is required to completely understand the operation of the VAWT.

Flow Diagnostics and Optimal Design of Vertical Axis Wind Turbines for Urban Environments
By Martin Zahariev, School of Computing and Engineering, University of Huddersfield, UK (2016)

28

In 2008, a research study was carried out by Nakajima et al. [45]. The study focused on using the Savonius design for hydro-applications, and investigated the effects of blade's phase difference of two-stage rotor configuration design, through the use of flow field analysis and various measurement techniques. The turbine was submerged in water and was connected to a torque transducer. Two-stage turbine designs were tested, and the flow fields had been visualized through the use of black pigment (ink) injected into water. In figure 2.13, the flow visualizations have been presented at 0°, 45°, 90° and 135° rotation for the bi-rotor configurations.
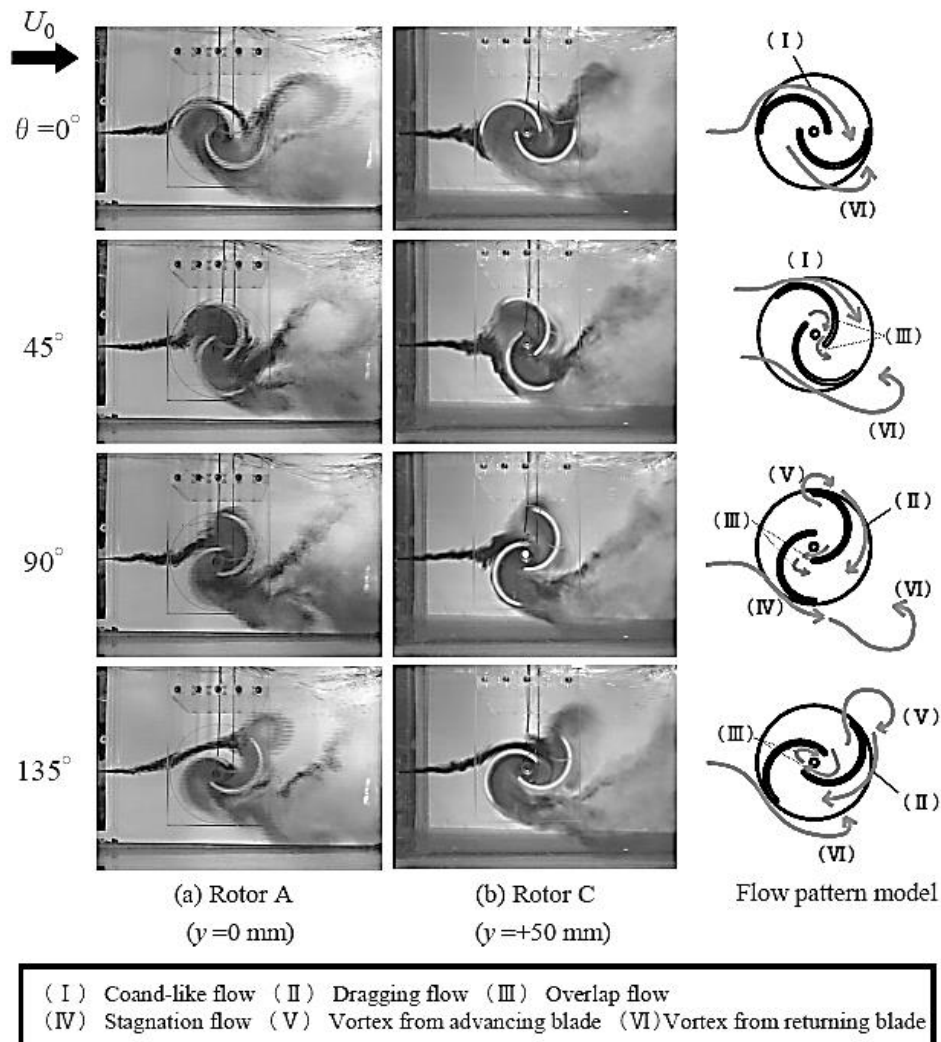
Figure 2.13: Flow Visualization [45]

The 90° blade's phase shift on a two stage Savonius rotor has been found to increase the efficiency of the turbine by approximately 10%. Torque enhancement on the advancing blade has been noticed, while pressure restoration on the returning blade increases the performance output of the turbine. A year later, in 2009, another study, considering the Savonius design for hydro-application, was carried out by Yaakob et al. [46]. The research study included application of the Savonius design for marine environment, based on the fact that it operates at lower incident flow velocities and is ideal for capturing marine currents. The work also examined the effects of the overlap ratio, ranging from 0.1 to 0.6. COSMOSfloworks CFD solver has been used in the study for 3D simulations of two-staged marine Savonius turbines, calculating the torque generated by each blade at various rotational angles. The pressure contours from the study, at 0°, 45°, 90° and 135°, are shown in figure 2.14.

Flow Diagnostics and Optimal Design of Vertical Axis Wind Turbines for Urban Environments
By Martin Zahariev, School of Computing and Engineering, University of Huddersfield, UK (2016)

29

| 0° | 45° | 90° | 135° |
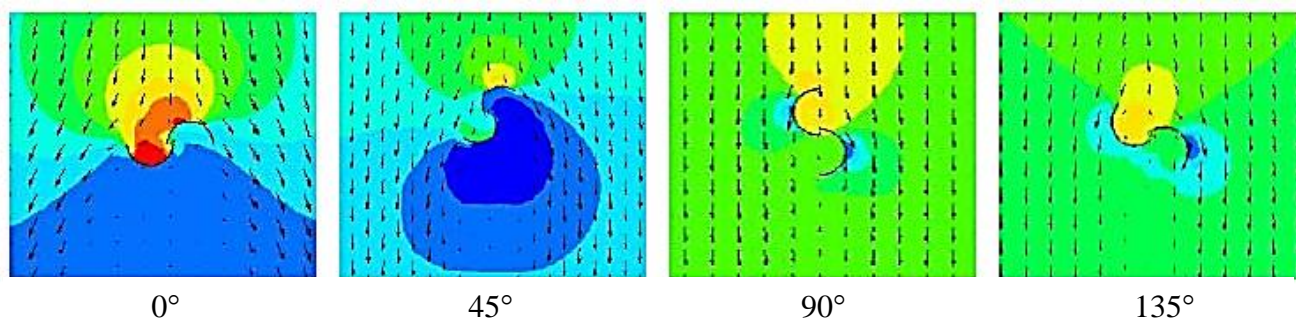
Figure 2.14: Pressure contours [46]

The work was carried out with the goal of finding efficient turbine designs to capture the low-velocity marine currents. It was found out that the optimal overlap ratio of 0.21 can be used for that application as it had sinusoidal torque characteristic. Other advanced features, such as helical twist, advanced blade profiles etc. were not tested in the study, nor was any analysis of local conditions associated with overlap, gap and aspect ratio was carried out.

In 2010, a research was carried out by Alam and Iqbal [47], focusing on combining the lift and drag based turbines for hydro-applications. The research used the two-stage Savonius marine turbine and combined it with a lift based 4 blades VAWT to test the hybrid design. The work was carried out using experimental approaches, achieving Cp values of 0.15. The tests however were limited, not considering the effects of individual features of the combined design.

Mahmoud et al. [48] carried out experimental studies on various models of the Savonius type VAWT. The work involved testing 2, 3 and 4 blade configurations, various aspect and overlap ratios, and single and double stage turbine designs. It was being observed that the 2 blades model has higher efficiency compared to 3 and 4 blades models. The two stage rotor depicted higher efficiency than single stage model. Furthermore, it was noticed that the increase in aspect ratio increases the efficiency of the turbine. The tests regarding the overlap ratio variations were limited as the design had a central shaft, which was passing through the overlap region.

With the increase of the computer power availability and solver improvements, more and more research studies were aimed to carry out numerical simulations of VAWTs using CFD based solver for design and performance analysis. One such research was carried out by Morshed [49] in 2010. The work included testing 3 blade Savonius turbine designs with no overlap, low overlap and high overlap ratios. 2D VAWT models were used to carry out steady state simulations of the turbines at various rotation angles. It was observed that the turbine with low overlap ratio gives higher efficiency compared to turbines without or with the high overlap ratios.

Mohamed et al. [50] numerically tested deflecting plates of various shapes and angles, alongwith various advanced blade profiles, with an objective to improve the efficiency of drag based VAWTs. 2D transient simulations, using Sliding Mesh technique, were carried out. Through this work, the authors managed to develop an advanced blade profile that increases the overall efficiency by 38.9%. In figure 2.15, this new high efficiency VAWT design is shown.

Flow Diagnostics and Optimal Design of Vertical Axis Wind Turbines for Urban Environments
By Martin Zahariev, School of Computing and Engineering, University of Huddersfield, UK (2016)

30
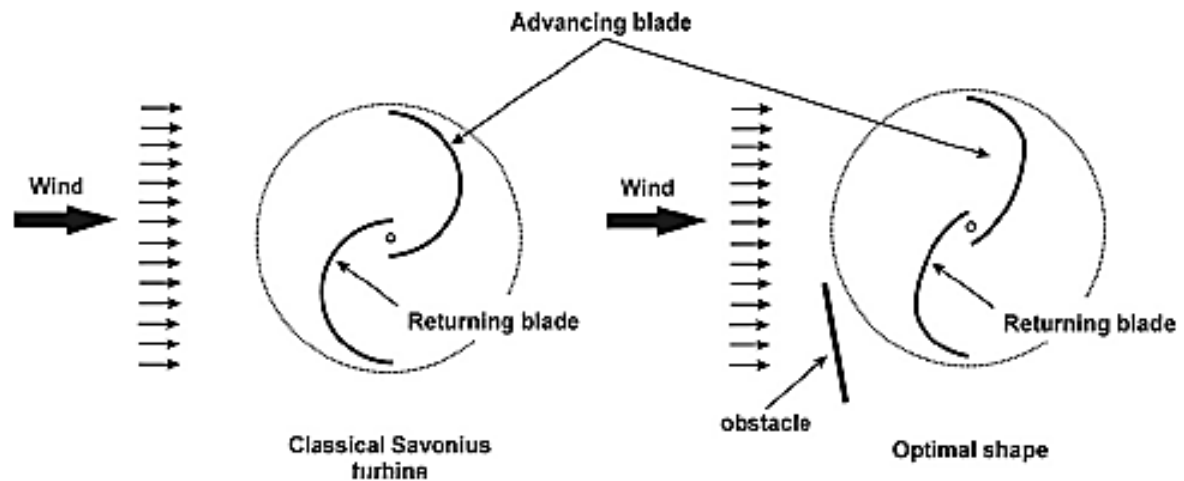
Figure 2.15: Design optimization [50]

Mohamed et al. extended the work further [51], investigating various advanced blade profiles, multiple rotors shielding arrangements, multiple deflector shields, number of blades, shield positioning and geometry. Detailed discussions on mesh independence, domain's dimensions independence, turbulence modelling, time step independence and convergence studies are reported as shown in figure 2.16.

(a)   (b)
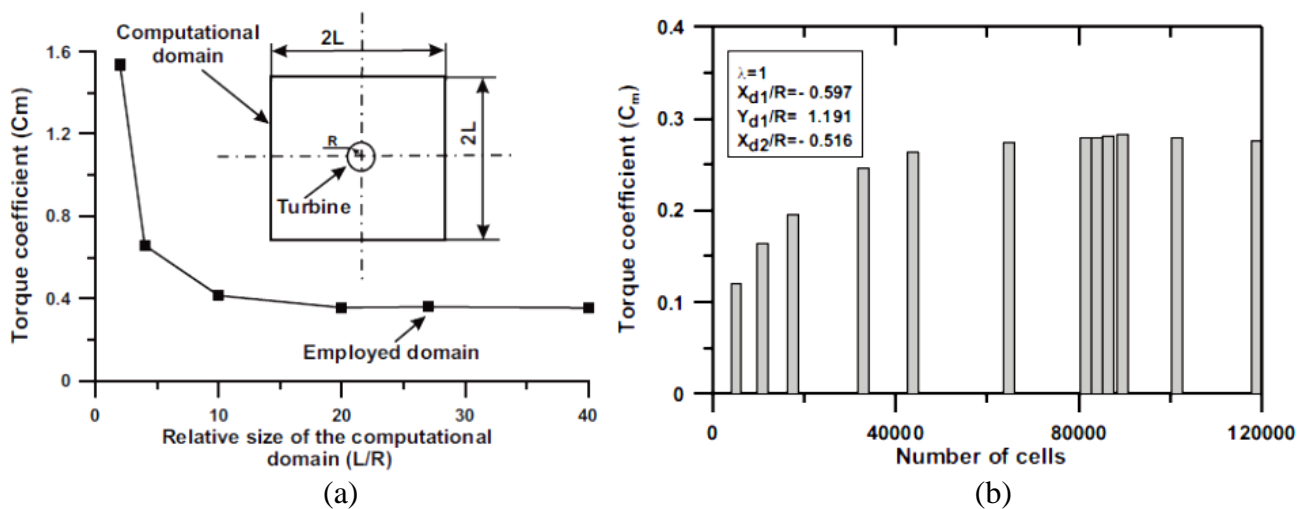
Figure 2.16: (a) Domain independence (b) Mesh independence [51]

Dobrev and Massouh [52] used Particle Image Velocimetry (PIV) to visualize the flow field in the vicinity of VAWTs. Numerical investigations, based on sliding mesh technique and Detached Eddy Simulations (DES), were also carried out. Their research study concluded that the efficiency, the wake, and the shedding vorticity can be predicted by using 3D numerical technique and DES\k-ω turbulence model, to higher accuracy than 2D numerical techniques can. The work did not test any advanced features, as it was mainly aimed at numerical modelling techniques and their accuracy.

In 2013, a research was carried out by Patel et al. [53] investigating the effects of the overlap ratio on the efficiency of the Savonius turbines. The research was carried out using numerical methods, consisting of 3D sliding mesh models of a standard Savonius VAWTs. The research study found out that the Savonius rotor is most efficient at an overlap ratio of 0.2. However, the study did not include variations of the gap and aspect ratios.

Flow Diagnostics and Optimal Design of Vertical Axis Wind Turbines for Urban Environments
By Martin Zahariev, School of Computing and Engineering, University of Huddersfield, UK (2016)

31

In 2014, a research study was carried out by Ahmed e al. [54], investigating several different configurations of the Savonius VAWTs, having different number of blades, at different overlap ratios. The research study considered 2D sliding mesh based numerical models. The primary aim of the research study was to determine the optimal configuration of a standard Savonius VAWT in terms of number of blades and overlap ratio. Al-Faruk and Sharifian [55] investigated the effects of overlap ratios, blade arc angles and the diameter of the hot air inlet, inducing the swirling effect, on the efficiency of the turbine. The hot air was injected through a hole on the bottom end plate of the turbine, causing swirling flow in the overlap region. The research was carried out to determine the optimal value for the overlap ratio and the blade arc angle for a swirling type Savonius turbine. The research found the turbine efficiency to increase by 25.5%. The research study however did not test other geometrical variations that are considered in the present study.

2.2   Scope of Research

The literature review presented in this chapter has shown that there are various geometric variables within a VAWT that significantly affects its performance output. These geometrical features include the gap, overlap ratio, blade twisting and tapering, the number of blades, the size of the VAWT etc. There is a need for a study, carried out in a systematic way that quantifies these effects and link them to the design process of a VAWT. Furthermore, it has also been observed that the numerical modelling of VAWTs is quite simplistic, often utilizing steady state approaches. Hence, a detailed investigations into the transient behavior of VAWTs is required, and that too to cover the complete performance spectrum of the turbine i.e. from start-up to steady operation of the turbine.

Another important point that has been noticed is that there is a need to develop an inexpensive CFD package for aerodynamic design analysis of VAWTs. This is because small-to-medium sized enterprises (SMEs) cannot afford to buy expensive commercial CFD software, while severely restricts their development in terms of complex flow distribution understanding in the vicinity of the VAWT. Moreover, it is utmost importance to extensively validate the predictions from the developed package against well-known and widely used commercial CFD software. The developed package should be able to predict the complex flow structures in the vicinity of the VAWT, and its performance parameters, with reasonable accuracy.

2.3   Research Objectives

Based on the research aims presented in the previous chapter, and after conducting a detailed literature review, the following objectives have been formulated which will aid the research aims and address the issues in the existing knowledge:

1.   Detailed flow diagnostics of VAWTs with internal guide vanes.
2.   Detailed flow diagnostics of VAWTs with tapered blades.
3.   Detailed flow diagnostics of VAWTs with helically twisted blades.
4.   Determination of the optimal design of VAWT.
5.   Detailed analysis of the optimal VAWT design to cover a wide range of operation i.e. from start-up to steady operation point.
6.   Development of an in-house built CFD package for aerodynamic design analysis of VAWTs.

In order to satisfactorily achieve the aforementioned research objectives, this study uses Computational Fluid Dynamics (CFD) based tools to numerically simulate the flow of air in the vicinity of drag based VAWTs. The next chapter presents the numerical modelling techniques being incorporated in this study.

Chapter 3
Numerical Modelling of Vertical Axis Wind Turbines

In order to investigate the research objectives outlined in the previous chapter, advanced CFD based techniques have been used to simulate the flow of air in the vicinity of the VAWT. This chapter presents various aspect of the numerical modelling of such turbines using commercial CFD software. Furthermore, some of the aspects related to the development of the design analysis package have also been discussed in this chapter. Discussions on the Sliding Mesh and Dynamic Mesh techniques, for steady operation and start-up of the VAWT respectively, are the highlights of this chapter.

3.1 Introduction to Computational Fluid Dynamics

Computational Fluid Dynamics (CFD) in general can be described as a tool for investigating any system involving fluid flow, heat transfer and chemical reactions. It works by simulating the laws of physics governing these problems, in a structured grid computer environment, and solving the corresponding mathematical equations in an iterative manner. The first CFD techniques to be used on a computer were developed in the 1960s, and in the later decades, the CFD techniques were available mainly to the aerospace industry. In recent years, with the increased availability of CFD software, and the increase in computational speed, the CFD techniques have been used for other applications as well. For example, internal combustion engines, gas turbines, prediction of erosion and other chemical processes, and even more recently, the automotive industry has begun to use CFD techniques in the design of efficient vehicles. The constantly increasing accuracy of the CFD, methods and the constantly reducing cost of high power computers, is an indication that the CFD methods will become more integral part of the design and development of new components, and the associated optimizations of existing designs

3.1.1 CFD Principles of Operation

There are several distinct CFD discretization methods available at present, and they are as follows: finite volume method, finite element methods, finite difference method, spectral element methods, and boundary element method. The most common method used in developing CFD solvers is the finite volume method (FVM), as it has an advantage in terms of solution speed and memory usage. It is quite beneficial for large problems, involving high Reynolds number turbulent flows, and for problems involving source term dominated flows, like combustion chambers. In the FVM methods, the governing partial differential equations are changed to a conservative form, and solved over discrete control volumes.

$$\frac{\partial}{\partial t} \iiint Q dV + \iint F dA = 0 \tag{3.1}$$

Equation 3.1 is an example of FVM equation where Q is vector of conserved variable, F is vector of fluxes, V is volume of the control volume element and A is the surface area of the control volume element. As the CFD codes are organised around numerical algorithms, aimed at solving the given problem flow field, they have 3 main common elements.

1. Pre-processing   2. Solver Settings   3. Post-processing

The pre-processing consists of defining the geometrical features of the problem, defining the flow domain in which the geometry is situated, creation of the required mesh, setting up physical modelling parameters (such as turbulence modelling), and specifying the boundary conditions. The solver settings consist of selection of the appropriate solver for the problem, specifying solution monitoring, convergence criteria, and specifying the operational conditions (such as start\end times, time steps, number of iterations etc.). The post-processing consists of examining the results by extracting useful numerical data of the finished simulation/s, usage of monitoring tools to extract quantitative data per given iteration or time step, and visualizing the flow fields to determine flow patterns.

3.1.2 Fluid Flow Numerical Modelling

The numerical modelling of a VATW is dictated by the following conservation laws:

Conservation of Mass

The mass conservation equation, or the continuity equation, can be written for an unsteady, three-dimensional, incompressible, viscous flow of air in the vicinity of a VAWT, in a conservation form, as follows:

$$\nabla . \left(\rho \vec{V} \right) = 0 \tag{3.2}$$

Conservation of Momentum

The conservation of momentum equations have been derived from Newton's second law of motion by Claude-Louis Navier and George Gabriel Stokes, and hence are often called Navier-Stokes equations. Three-dimensional Navier-Stokes equations in conservation form for VAWTs can be expressed as:

$$\frac{\partial(\rho u)}{\partial t} + \nabla . \left(\rho u \vec{V} \right) = -\frac{\partial p}{\partial x} + \frac{\partial \tau_{xx}}{\partial x} + \frac{\partial \tau_{yx}}{\partial y} + \frac{\partial \tau_{zx}}{\partial z} + \rho f_x \tag{3.3}$$

$$\frac{\partial(\rho v)}{\partial t} + \nabla . \left(\rho v \vec{V} \right) = -\frac{\partial p}{\partial y} + \frac{\partial \tau_{xy}}{\partial x} + \frac{\partial \tau_{yy}}{\partial y} + \frac{\partial \tau_{zy}}{\partial z} + \rho f_y \tag{3.4}$$

$$\frac{\partial(\rho w)}{\partial t} + \nabla . \left(\rho w \vec{V} \right) = -\frac{\partial p}{\partial z} + \frac{\partial \tau_{xz}}{\partial x} + \frac{\partial \tau_{yz}}{\partial y} + \frac{\partial \tau_{zz}}{\partial z} + \rho f_z \tag{3.5}$$

3.2   Pre-Processing

This section details the pre-processing part of the numerical modeling of VAWTs carried out in the present study. Pre-processing includes geometry creation and mesh generation. As multiple VAWT models have been considered in this research work, the geometry creation and mesh generation for only one of the 3D models is discussed here.

3.2.1 Geometry Creation

The geometrical parameters of VAWT design are based on dimensionless ratios and relationships between different features, which themselves are based on known theories. The dimensionless ratios considered here are the overlap ratio of 0.22, gap ratio of 0.07 and the aspect ratio of 5. The end plates are 20% larger in diameter that the rotor [12]. Another parameter used for the creation of the geometric model is the level of helical twist applied to the blades. Example of 0.5 revolutions of twist on the blades of the VAWT across its entire vertical length is shown here. The VAWT has vertical length (H) of 2.5m, chord length (C) of 0.5m, overlap distance (X) of 0.11m, gap distance (Y) of 0.035m, rotor diameter (Dr) of 0.88m, rotor radius (R) of 0.44m, and end plate diameter (De) of 1.1m. These dimensions have been used to create the VAWT model, where the 2D sketch of the profile has been shown in figure 3.1. The 3D CAD model extruded helically out of this 2D profile is shown in figure 3.2.

The size of the flow domain has been selected from domain's dimensions independence study reported in a previous research work by Mohamed et al. [51] (see figure 2.16). Hence, the flow domain for this research study has been created with length of 17.6m, width of 17.6m and height of 12.7m, as shown in figure 3.3.

Flow Diagnostics and Optimal Design of Vertical Axis Wind Turbines for Urban Environments
By Martin Zahariev, School of Computing and Engineering, University of Huddersfield, UK (2016)

35
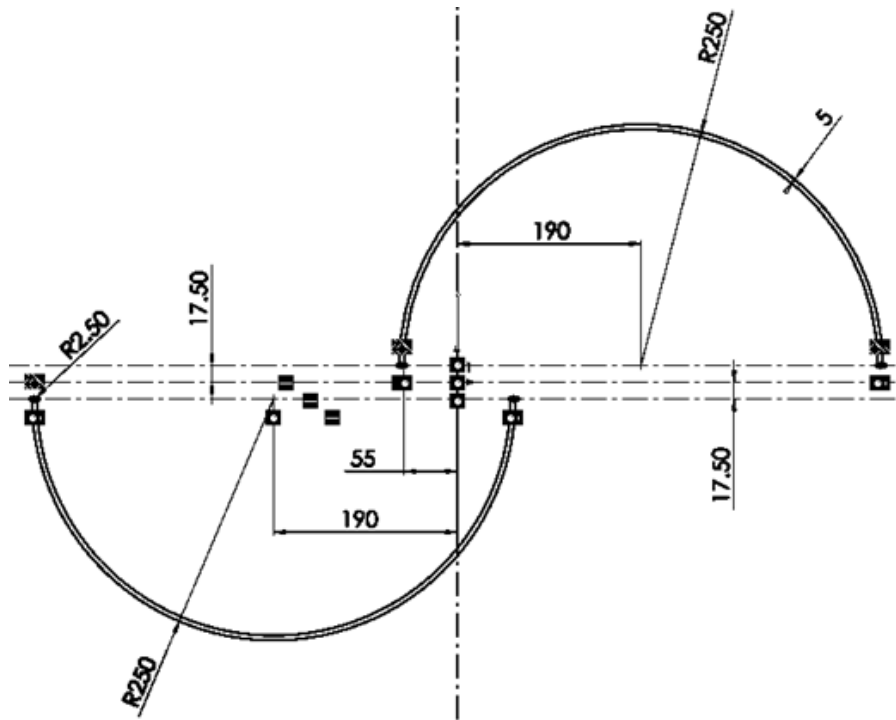
Figure 3.1: 2D profile sketch of the VAWT design
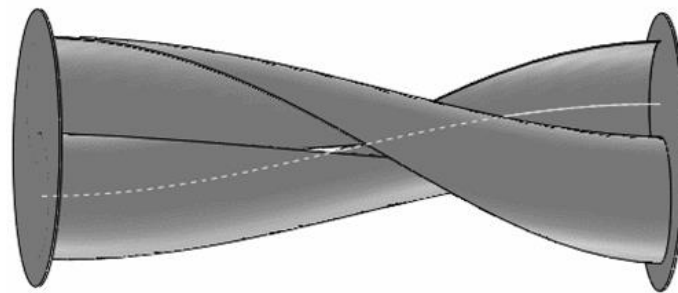
Figure 3.2: 3D model of the VAWT
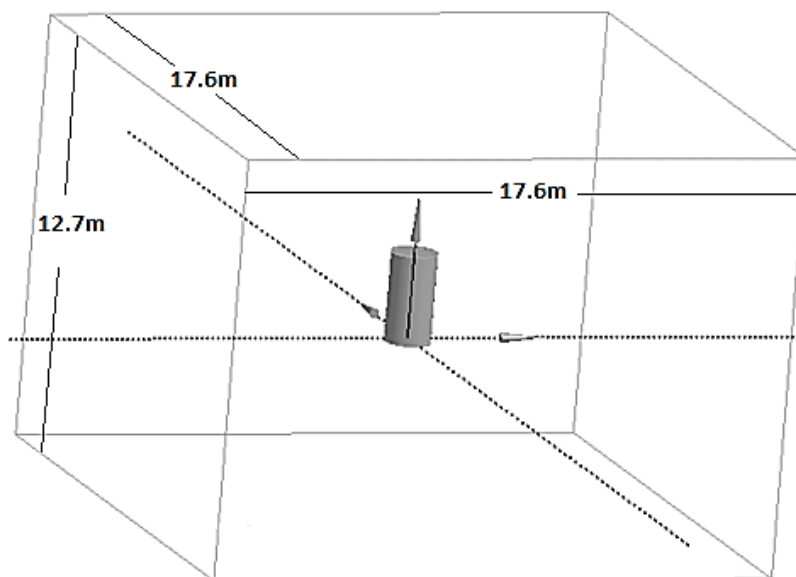
Figure 3.3: Flow domain dimensions

Flow Diagnostics and Optimal Design of Vertical Axis Wind Turbines for Urban Environments
By Martin Zahariev, School of Computing and Engineering, University of Huddersfield, UK (2016)

36

The rotating domain for sliding mesh simulations has a dimeter of 1.4m, and height of 2.7m. These dimensions have been carefully selected to ensure that there will be enough space between the VAWT and the rotational domain so that the mesh can be refined to a higher level. The shape of the rotational domain is cylindrical in shape, with flat ends for simulations in commercial CFD software, and semi-hemispherical ends for the simulations in the in-house developed design analysis package (to achieve higher levels of mesh refinement), as shown in figure 3.4.

(a)   (b)
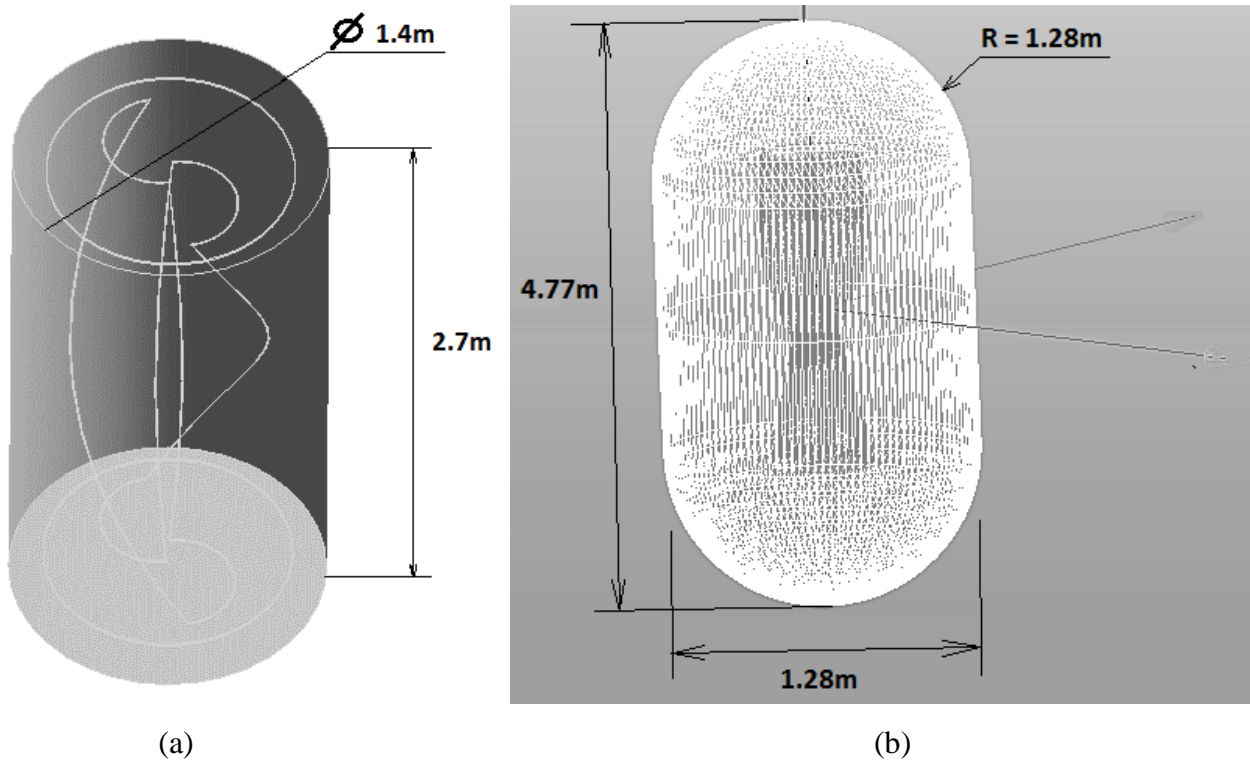
Figure 3.4: Rotational domain's shape and dimensions (a) for commercial CFD solver (b) for the in-house built CFD package

3.2.2 Meshing of the flow domain

The mesh size in the flow domain has been controlled using a global sizing function, while for the rotational domain; several mesh control functions have been used to refine the mesh. The global function used for the flow domain has a minimum element size of 15mm, a maximum element size of 400mm, and a growth rate of 1.2 to ensure smooth transition. The refinement level of the flow domain interface (between the flow domain and the rotational domain) is set to level 1 to further refine the elements on the interface. The rotational domain has been refined using body sizing function, with a minimum element size of 15mm, a maximum element size of 200mm, and a growth rate of 1.2. The mesh on the blades' surfaces have been refined using a face sizing function, with a minimum element size of 15mm, a maximum element size of 20mm, and a growth rate of 1.2. Another face sizing function has been used to further refine the blades and endplates' edges, with element size of 10mm and a growth rate of 1.2. The resulting mesh meets the quality criteria, such as skewness, element quality, aspect ratio, Jacobian ratio and orthogonal quality. The resulting mesh has a total of 2,082,425 elements, with 374,563 node points. In figure 3.5, a cross sectional view of the mesh has been shown.

Flow Diagnostics and Optimal Design of Vertical Axis Wind Turbines for Urban Environments
By Martin Zahariev, School of Computing and Engineering, University of Huddersfield, UK (2016)

37
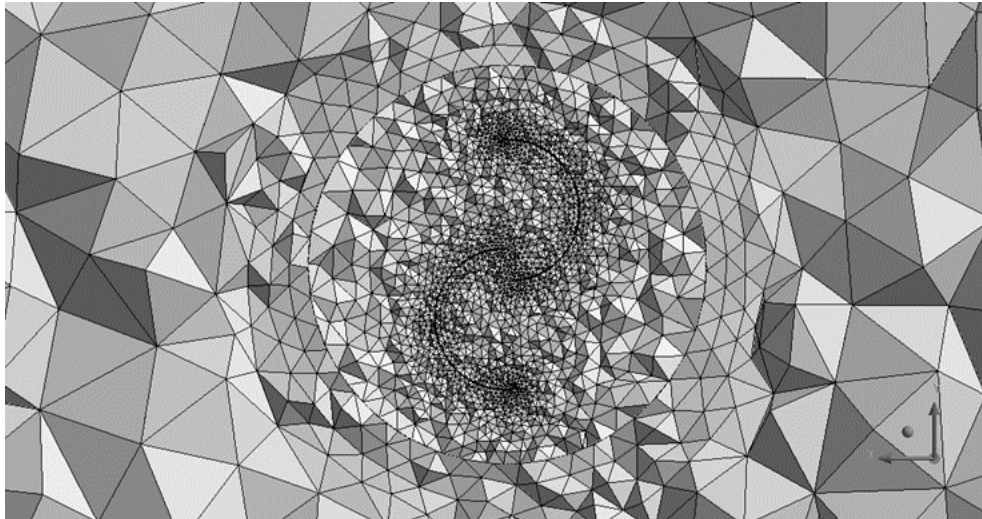
(a)
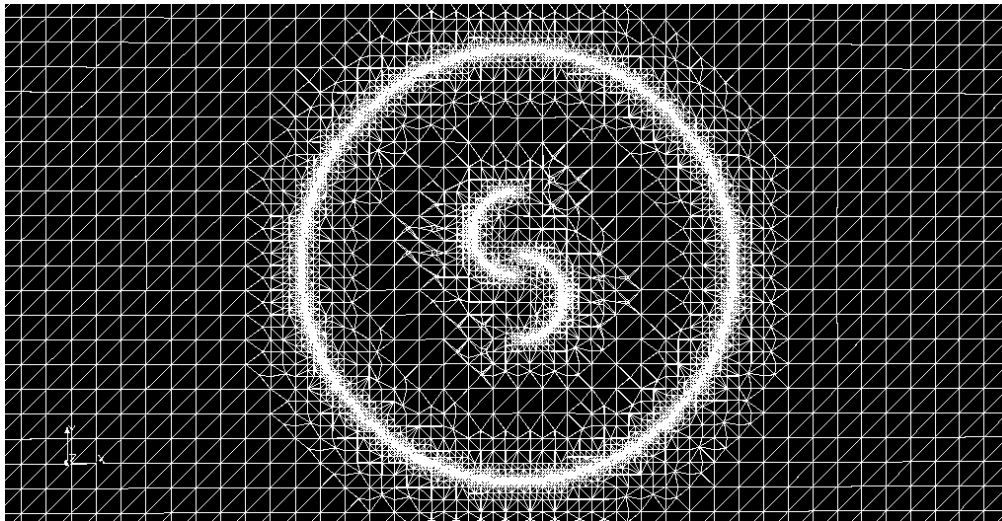
(b)

Figure 3.5: Cross section of the mesh (a) for commercial CFD solver (b) for the in-house built CFD package

3.3 Solver Settings

The required settings for the solver have been specified in this section, where the turbulence model, boundary conditions, sliding mesh/dynamic mesh application, solution methods, convergence criteria, monitors setup, and the simulation parameters have been discussed.

3.3.1 Rotation of the VAWT

Sliding mesh technique has been used in the first aspect of the present study, in order to rotate the VAWT. The sliding mesh model is the most accurate method for simulating flows in multiple moving reference frames, but also the most computationally demanding. In the sliding mesh technique, two or more cell zones are used. Each cell zone is bounded by at least one interface zone where it meets the opposing cell zone. The interface zones of adjacent cell zones are associated with one another to form a mesh interface. The two cell zones will move relative to each other along the mesh interface. During the calculation, the cell zones slide (i.e. rotate) relative to one another along the mesh interface in discrete steps. As the rotation takes place, node alignment along the mesh interface is not required. Since the flow is inherently unsteady, a time-dependent solution procedure

Flow Diagnostics and Optimal Design of Vertical Axis Wind Turbines for Urban Environments
By Martin Zahariev, School of Computing and Engineering, University of Huddersfield, UK (2016)

38

is required. The sliding mesh model allows adjacent meshes to slide relative to one another. In doing so, the mesh faces do not need to be aligned on the mesh interface. This situation requires a means of computing the flux across the two non-conformal interface zones of each mesh interface. The flow domain is divided into sub-domains, each of which may be rotating and/or translating with respect to the inertial frame. The governing equations in each sub-domain are written with respect to that sub-domain's reference frame. At the boundary between two sub-domains, the diffusion and other terms in the governing equations in one sub-domain require values for the velocities in the adjacent sub-domain. The commercial solver used in the present study enforces the continuity of the absolute velocity to provide the correct neighboring values of velocity for the sub-domain under consideration. When the relative velocity formulation is used, velocities in each sub-domain are computed relative to the motion of the sub-domain.

Sliding mesh technique assumes that the VAWT is operating at a steady rotational speed. Hence, to cover a wide range of VAWT's operation, especially its start-up process, until it reaches that steady operational point, Dynamic Mesh technique has been used in the second aspect of this study. Dynamic mesh has the ability to predict the entire performance spectrum of the VAWT. The dynamic mesh technique can be used to model flows where the shape of the domain is changing with time due to motion on the domain boundaries. The motion can be a prescribed motion or an unprescribed motion where the subsequent motion is determined based on the solution at the current time, which is the case in the present study. VAWT's angular velocities are calculated from the force balance on the VAWT. The update of the volume mesh is handled automatically at each time step based on the new positions of the boundaries.

Diffusion based smoothing method has been used for the flow and rotational domains, with a diffusion parameter of 0.1, indicating mesh smoothing in the near VAWT region. Local cell and face based re-meshing has been used in the present study. A User Defined Function (UDF) has been specified to the dynamic mesh model containing the information about the material of the VAWT. Aluminum (density of 2719kg/m^3) has been used as the material for the VAWT design. Mass and moments of inertia of the 3D VAWT model have been calculated. The values have then been used to make the Six Degree of Freedom (6DOF) UDF. As the VAWT only rotates around the Z axis in the present case, all other motions have been restricted in the UDF. Figure 3.6 shows the UDF used in the present study.

```
#include "udf.h"
DEFINE_SDOF_PROPERTIES(motion, prop, dt, time, dtime)
{
prop[SDOF_MASS]          = 104.8;
prop[SDOF_IXX]           = 279.36;
prop[SDOF_IYY]           = 279.36;
prop[SDOF_IZZ]           = 13.3;
prop[SDOF_IXY]           = 0.0;
prop[SDOF_IXZ]           = 0.0;
prop[SDOF_IYZ]           = 0.0;
prop[SDOF_ZERO_TRANS_X]  = TRUE;
prop[SDOF_ZERO_TRANS_Y]  = TRUE;
prop[SDOF_ZERO_TRANS_Z]  = TRUE;
prop[SDOF_ZERO_ROT_X]    = TRUE;
prop[SDOF_ZERO_ROT_Y]    = TRUE;
prop[SDOF_ZERO_ROT_Z]    = FALSE;
}
```

Figure 3.6: 6DOF UDF for VAWT

3.3.2 Turbulence Modelling

Turbulence has been modelled in the present study using the Realizable k-ε turbulence model. It is a two equation model that calculates turbulent kinetic energy (k) and the turbulent dissipation rate (ε) in the flow and rotational domains. This model performs well in case of flows exhibiting rapid strain, high pressure gradient, shear flows, moderate swirls, vortices, transitional flows and boundary layer separation, all of which are expected in case of a VAWT. Non-equilibrium wall functions have been used in the present study as they account for high pressure gradients, therefore increasing the accuracy [56]. The curvature correction has also been used as it introduces a term sensitive to rotation, and streamlines curvatures to the Reynolds Averaged Navier-Stokes turbulence equations. It improves the prediction accuracy for rotational components and aerodynamic forces [57].

3.3.3 Boundary Conditions

Inlet air flow velocity of 8m/s has been used as the primary boundary condition in the present study. It is the average annual wind speed in Huddersfield, UK. TSR, in case of sliding mesh simulations, has been kept constant at 0.7; however, the present study also covers a wide range of TSR values (in different sections). The outlet of the flow domain has been specified with atmospheric conditions, while the moving surfaces (blades, top and bottom endplates) have been specified with no-slip boundary conditions. Incompressible time-dependent solver has been employed for the flow of air at a constant density of 1.225kg/m^3.

3.3.4 Solution Methods

In order to accurately predict the flow field, the pressure-velocity coupling and the spatial discretisation settings have to be specified. SIMPLE pressure-velocity coupling scheme has been used as it converges faster for these types of problems. The SIMPLE algorithm calculates the pressure gradient from the pressure distribution, and obtains the velocity field approximation out of the momentum equations. Green–Gauss node based spatial discretisation gradient has been used as it preservers second-order spatial accuracy. It works by creating a precise value of a linear function at a given node out of the surrounding cells. 2nd order upwind schemes have been selected for the rest of the spatial discretisation schemes, for better accuracy.

3.3.5 Solver Execution

The solution has been initialization using the standard initialization procedure available in the commercial CFD solver. This initializes the fields and allows for the solver to be started. The same standard initialization procedure has been applied to the in-house developed package.

A time step size of 0.00411sec has been used in the present study, which corresponds to 3° rotation of the VAWT per time step at TSR of 0.7. For the other TSR values tested in the present study the time step size has been changed accordingly to keep the 3° of rotation per time step. The model has been rotated for four complete revolutions, where it has been established that the solution becomes statistically steady after the second revolution. Therefore, the data has been gathered in the third revolutions of the VAWT, as the data from the first two revolutions contains an excessive numerical diffusion.

3.4   Scope of the work

First the standard Savonius VAWT has been numerically tested at multiple TSR values (0.4 to 1) to generate the performance curve (TSR versus Cp), in order to determine the TSR value corresponding to peak efficiency of the VAWT.

Multiple models comprising of different internal guide vanes configurations (guide vane angles of 10°, 20° and 30°, and thickness of 10%, 50% and 90%) have been numerically tested at peak efficiency point. Then they have been further tested at TSR values one lower and one higher than the peak efficiency TSR value, to make sure that the modified designs are demonstrating peak efficiencies at the same TSR.

Various VAWT models having different tapered blade designs (X-shape, ◊-shape and Δ-shape) have been numerically tested at their peak efficiency points. Then they have been further tested at TSR values one lower and one higher than the peak efficiency TSR value, to make sure that the modified designs are demonstrating peak efficiencies at the same TSR.

Multiple VAWT models having different helical twists (0.25, 0.5, 1, 1.5 and 2 revolutions) have been numerically tested at their peak efficiency points. As the high level of helical twisting increases the solidity of the VAWT, it is expected that the models with higher level of twist will have peak efficiency at lower TSR values. Therefore, these models have been tested at wider TSR range. Only the best/optimal model has been tested for complete TSR range of 0.4 to 1.

The start-up process (accelerating VAWT) has been numerically analyzed using dynamic mesh technique for the best/optimal model only. This provides with the complete performance spectrum of the best/optimal VAWT design.

An in-house built CFD package has been developed for design analysis of VAWTs, based on existing open source CFD solvers. In order to verify the robustness and accuracy of the developed package, tests on the optimal VAWT design have been carried out at multiple TSR values (0.5, 0.6, 0.7, 0.8 and 0.9).

The next chapter includes the discussions on the different geometrical features of the VAWT, including the complete performance spectrum of the optimal VAWT design.

Chapter 4
Flow Diagnostics of Drag based Vertical Axis Wind Turbines

A thorough flow analysis, both qualitative and quantitative has been carried out in this chapter. Local and global flow and performance parameters have also been critically analysed. Results of spatio-temporal discretisation studies have been presented in this chapter, in order to show that the results are independent of both the mesh and the time step sizes. Benchmark study has been carried out to show that the numerical techniques used in the present study predict the flow and performance parameters of VAWTs with reasonable accuracy. Various innovative design features, such as internal guide vanes, tapered blades, and helical twists, have been generated and analysed for both the flow and performance parameters. Moreover, a complete performance spectrum of the optimal VAWT design has been generated, comprising of both its start-up process and up to its steady operational point.

4.1 Mesh Independence Study

The mesh independence study has been conducted to determine the mesh size which provides a balance between the computational cost and the accuracy of the predicted results. For this purpose, the size of the turbine, rotational domain and the stationary domain were kept the same, along-side the boundary conditions and solver settings. Four different meshes were generated, with overall number of elements per model equal to 1, 1.5, 2 and 2.5 million.

Revolution averaged coefficient of moment and coefficient of power of the VAWT has been recorded and compared for different mesh models considered here. It can be seen in table 4.1 that the difference in coefficient of moment between 1 and 1.5million mesh models is 15.76%, which decreases to 0.49% between 1.5 and 2million mesh models. The performance of the VAWT model changes significantly from 1 to 1.5million mesh elements, however, further increasing the mesh density has insignificant effect on VAWT's performance. Hence, the mesh model comprising of 1.5million elements has been chosen for further analysis in the present study.

Table 4.1: Mesh independence study

Mesh Size (#cells)	Coefficient of Moment	Coefficient of Power	Difference in coefficient of moment and power between the different meshes (%)
1,000,000	0.171	0.120	N/A
1,500,000	0.203	0.142	15.76
2,000,000	0.204	0.143	0.49
2,500,000	0.206	0.144	0.97

4.2 Time Step Independence Study

As sliding mesh technique has been primarily employed in the present study to rotate the VAWT, it is important to specify an appropriate time step size for its rotation, which predicts the complex flow features with reasonable accuracy with respect to time. For this purpose, time step size has been represented in terms of degree of rotation of the VAWT per time step. Three different time step sizes of 1°, 2°, and 3° of VAWT's rotation have been numerically analysed. Before extracting the predicted coefficient of moment of the VAWT, it has been ensured that the solution has reached a statistically steady state i.e. the solution is independent of the numerical errors, such as convergence.

Figure 4.1 on the next page depicts the instantaneous variations in the torque coefficient of the VAWT models corresponding to 1, 2 and 3 degree of rotation. It can be clearly seen that these variations are sinusoidal in nature, with the number of peaks (both positive and negative) equal to the number of rotor blades i.e. 2 in the present case. Furthermore, it can also been seen that 1 degree model under predicts the torque generated by the VAWT slightly, however, the average torque difference between all the three models are around 2% as summarized in table 4.2. Hence, the model with 3 degree rotation of the VAWT, per time step, has been chosen for further analysis in the present study.

Table 4.2: Time Step Independence averaged results for Cm

Time Step Size (Degrees)	Average Cm	Difference (%)
1	0.196	N/A
2	0.200	1.79
3	0.205	2.30
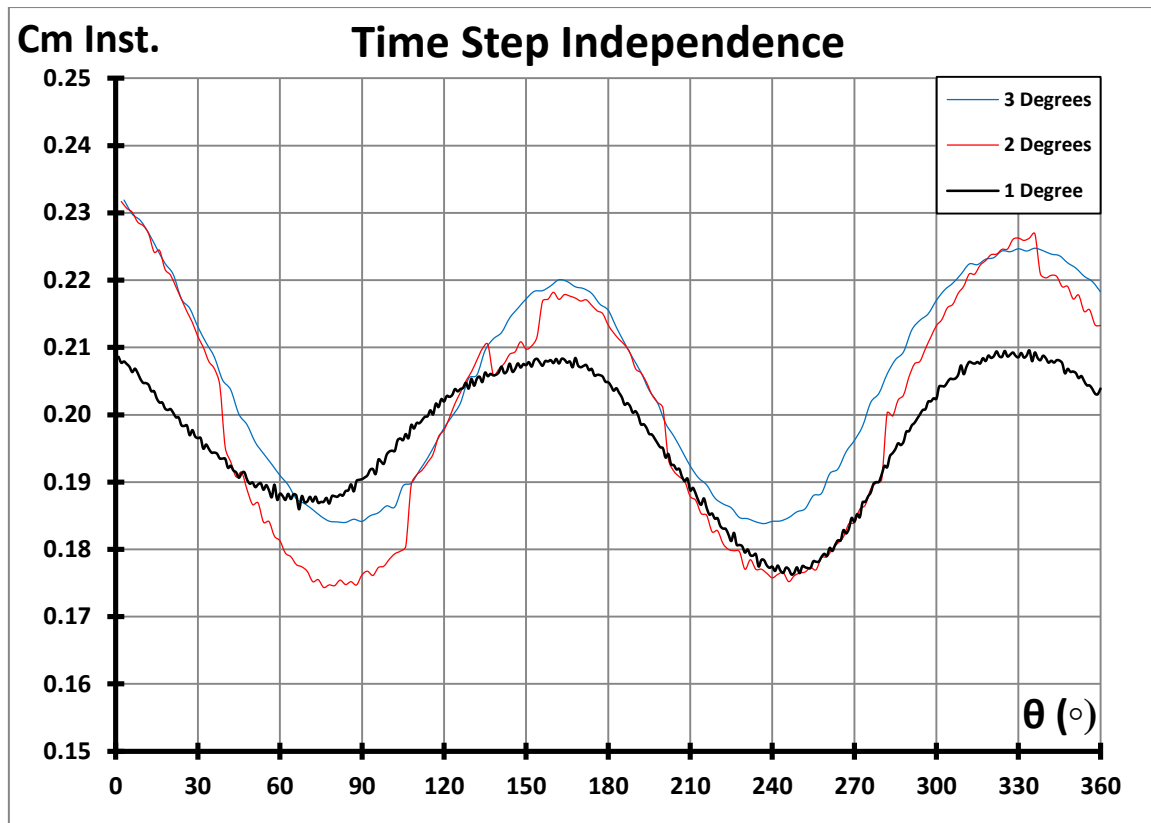
Figure 4.1: Time step independence study

A time step independence study for dynamic mesh technique is not required as the time step size for dynamic meh technique is significantly shorter as compared to the sliding mesh technique, in order to maintain the mesh quality.

4.3   Benchmark Tests

For verification of the solver settings used in the present study, a standard Savonius VAWT model has been numerically generated, which is the same as considered by Alexander and Holownia in 1978 [12] for experimental investigations.

The dimensionless ratios for the standard Savonius model, made for the validation purpose, are the gap ratio of 0.07, overlap ratio of 0.22 and aspect ratio of 5, while the diameter of the end plates is 20% bigger than the diameter of the rotor. Furthermore, the height H of the VAWT is equal to 2.5m, the chord length c is equal to 0.5m, the overlap distance X is 0.11m, the gap distance Y is equal to 0.035m, the rotor diameter Dr is equal to 0.88m, the rotor radius R is 0.44m, and the rotor end plates have diameter De equal to 1.1m. A 3D view of the design can be seen in figure 4.2.

The standard Savonius VAWT design has been simulated at various TSR values ranging from 0.4 to 1 to cover a wide range for verification of the CFD predicted results, which are presented in table 4.3.
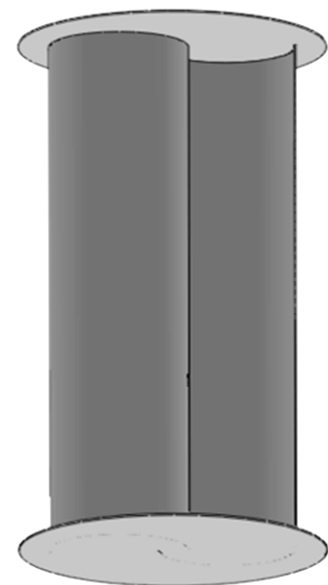
Figure 4.2: 3D Savonius VAWT

Table 4.3: CFD predicted results

λ (TSR)	Coefficient of Power	Coefficient of Moment
0.4	0.122	0.304
0.5	0.130	0.260
0.6	0.138	0.230
0.7	0.142	0.203
0.8	0.140	0.175
0.9	0.127	0.141
1	0.107	0.107

Alexander and Holownia's VAWT model shows peak coefficient of power of 14.5%, while the numerical model of the same show peak coefficient of power of 14.21%, which are 2% different to each other, hence showing that the solver settings used in the present study are capable of predicting the performance parameters of VAWTs with reasonable accuracy. The standard Savonius VAWT has also been tested by other researchers, both experimentally and numerically, such as Fernando in 1987 [38], Aldoss and Kotb in 1991 [39], Fujisawa and Gotoh in 1992 [40], and Yaakob et al. in 2009 [46], all achieving similar values of maximum coefficient of power (Cp_{max}) of around 14-15%.

The standard Savonius VAWT model consider here is treated as the baseline model throughout the study for comparison purposes. In the next section, a detailed qualitative and quantitative analysis of the flow structure and performance output of the baseline model is presented.

4.4   Performance evaluation of the Baseline Model

The performance evaluation of the baseline model has been carried out at TSR of 0.7, which corresponds to its maximum coefficient of power, as shown in table 4.3. Figure 4.3 depicts the variations of static gauge pressure in the vicinity of the baseline model at TSR of 0.7. It can be seen that the highest pressure zone is at the tip of the returning blade, while the lowest pressure zone is at the rear of the same blade. It can also be seen that there is a circular zone of lower pressure downstream the VAWT.
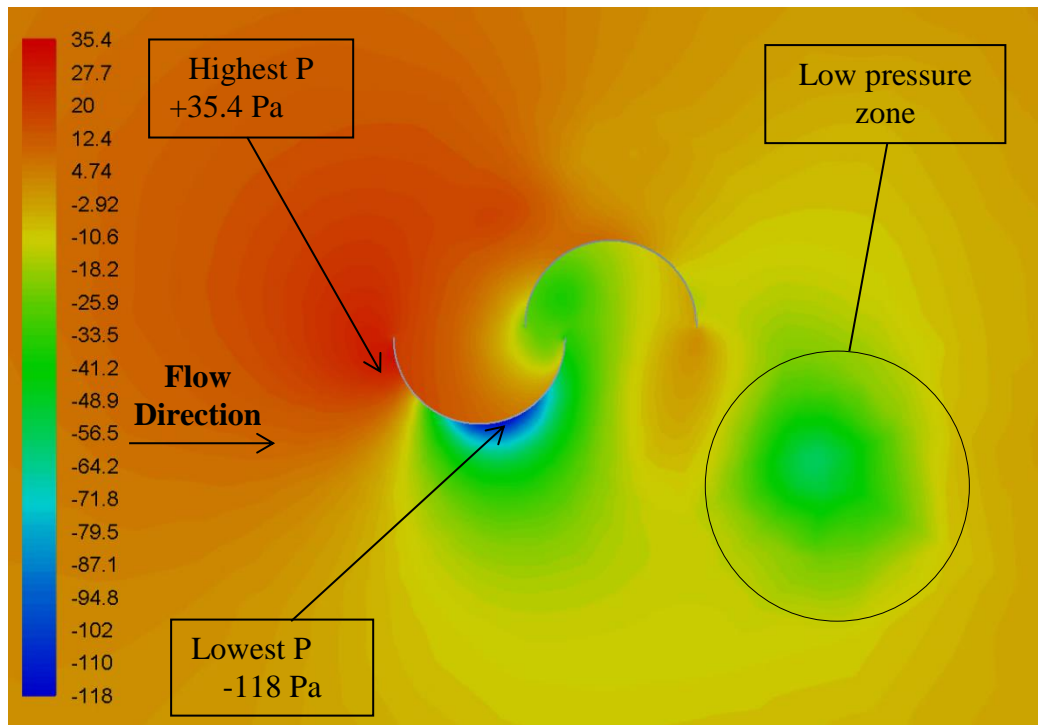
Figure 4.3: Static gauge pressure (Pa) variations in the vicinity of the baseline model

Figure 4.4 depicts the variation in the flow velocity magnitude in the vicinity of the baseline model at TSR of 0.7. It can be seen that although the free stream velocity is 8m/s, the local flow velocity at the rear of the returning blade is much higher, reaching values of upto 13.9m/s. It can also be seen that there is a zone of high velocity downstream the VAWT, corresponding to the low pressure zone, indicating recirculation.
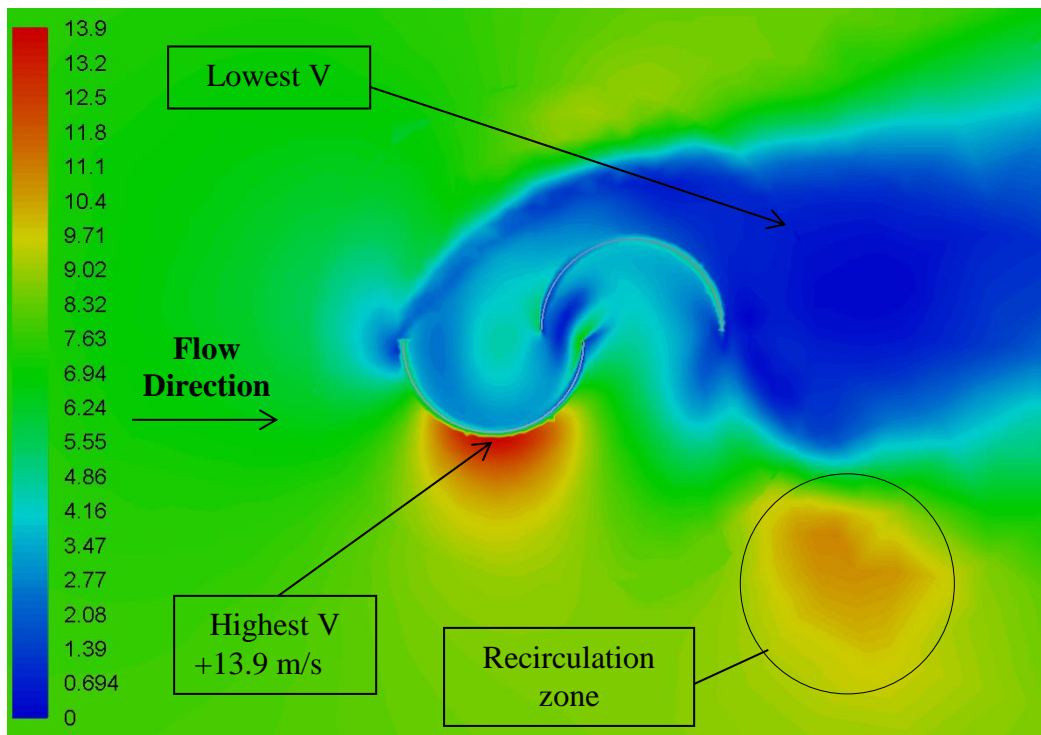
Figure 4.4: Velocity magnitude (m/s) variation in the vicinity of the baseline model

Once the detailed flow analysis of the local flow features in the vicinity of the baseline model has been carried out, the variations of instantaneous coefficients of moment and power have been analysed, as shown in figure 4.5. It can be seen that there is cyclic variation of both the two coefficients, where the positive and negative peaks are equal to the number of blades of the VAWT. Same trends have previously been documented by other researchers [58-61]. It can be seen that the coefficient of moment can reach a value upto 0.45, while coefficient of power reaches a maximum value of 0.32.
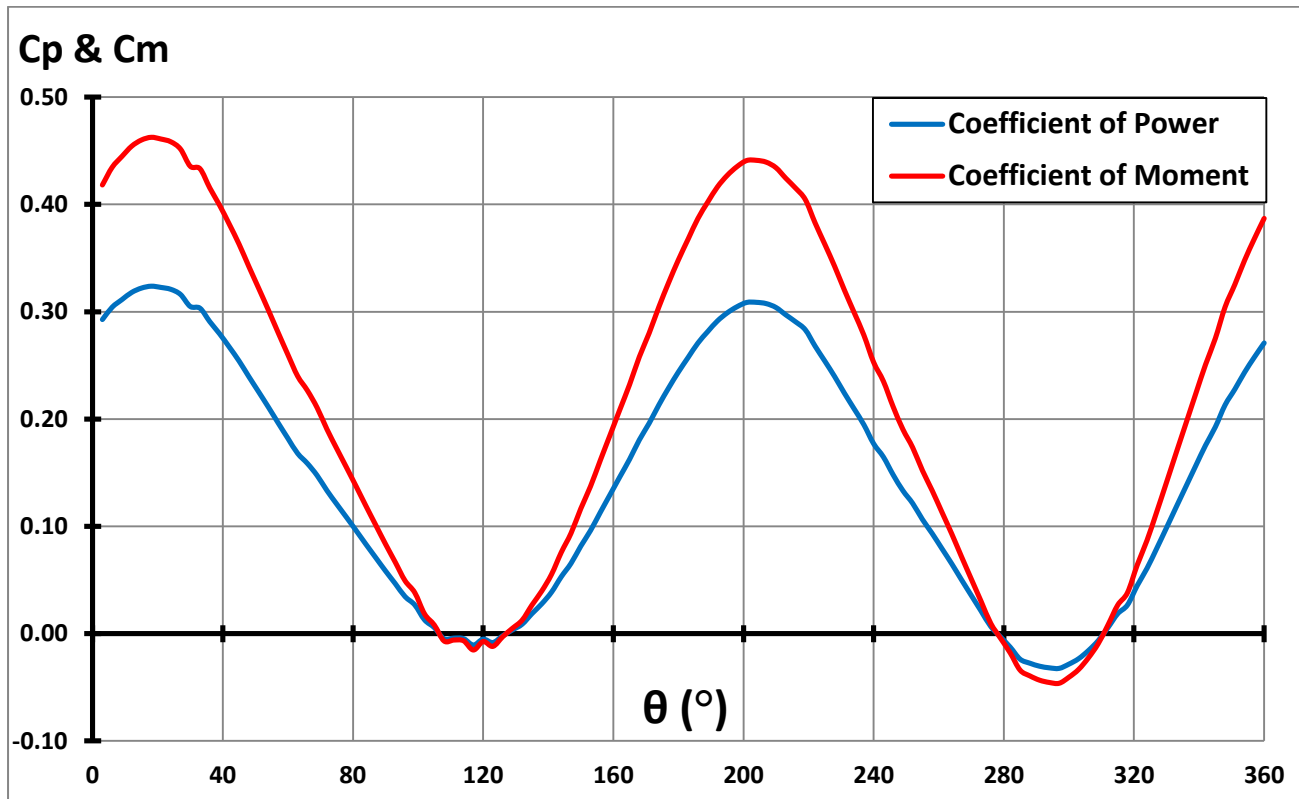
Figure 4.5: Instantaneous coefficients of moment (Cm) and power (Cp) over a complete revolution of the baseline model

The next section highlights the effects of internal guide vanes on the performance of the VAWT.

4.5 Effects of Internal Guide Vanes on the performance of the VAWT

Internal guide vanes are inclined, semi-circular surfaces attached to the inner surfaces of the blades to guide the flow in a certain direction within the VAWT. There are two main geometrical parameters characterizing the design of the guide vanes i.e. the inclination angle and the thickness of the guide vanes (in percentage). Three different guide vane models have been numerically generated, with 10°, 20° and 30° inclination angle at a constant guide vane thickness of 10%. Two additional guide vane models have been numerically generated with 50% and 90% guide vane thickness at 30° inclination angle. The five different guide vanes configurations are shown in figure 4.6.

(a)   (b)   (c)

(d)   (e)
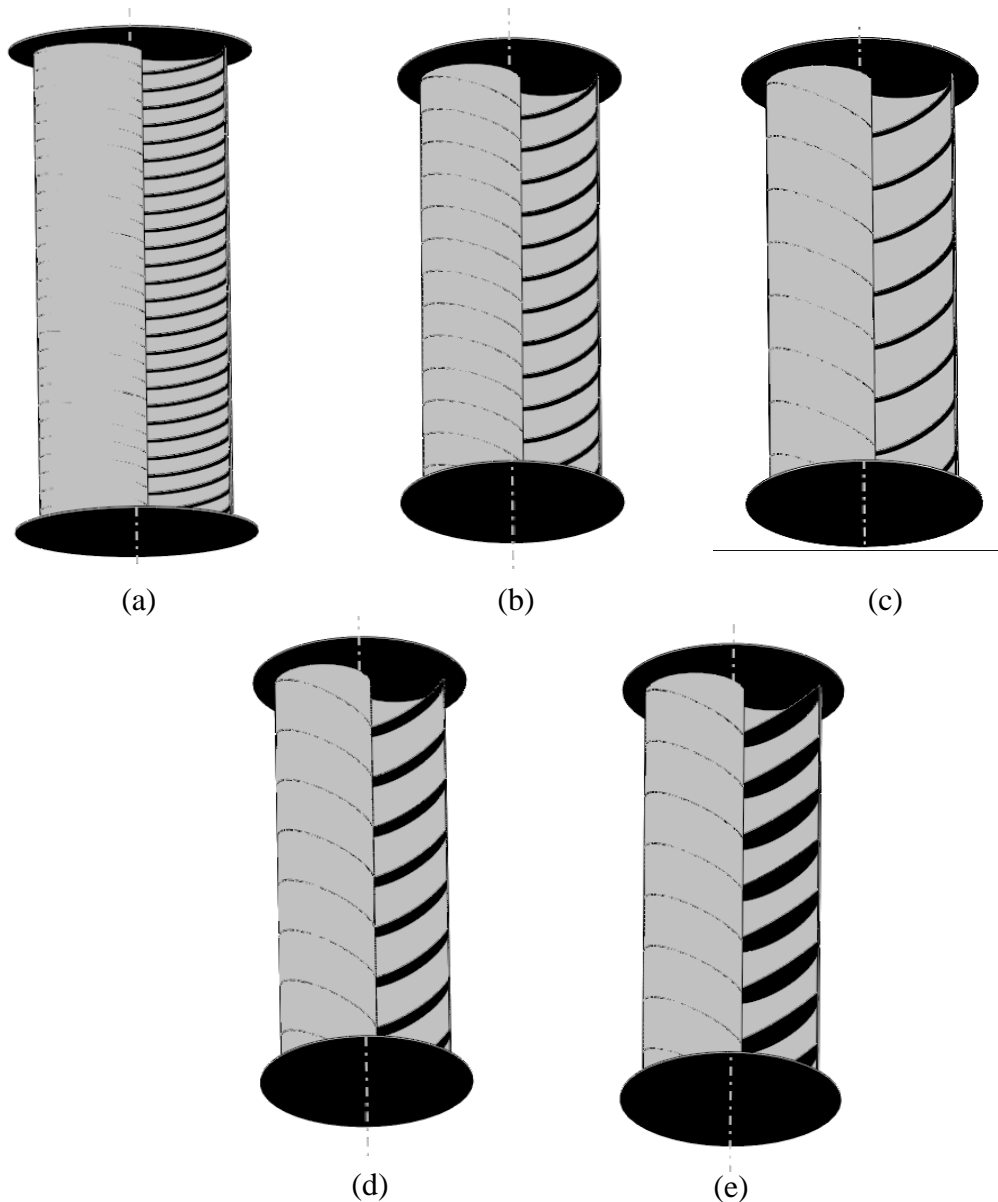
Figure 4.6: Guide vanes models (a) 10° inclination angle and 10% thickness (b) 20° inclination angle and 10% thickness (c) 30° inclination angle and 10% thickness (d) 30° inclination angle and 50% thickness (e) 30° inclination angle and 90% thickness

Each of the five guide vanes models have been analysed at three different TSR values i.e. 0.7, one above and one below TSR of 0.7 (TSR of 0.7 being the highest efficiency point of the baseline model).

Figure 4.7 depicts the variation of static gauge pressure in the vicinity of the three guide vane models at TSR of 0.7. The scale for each of the three guide vane models is kept constant for comparison purposes. It can be seen that the high pressure zone at the tip of the advancing blade is almost the same in the three cases discussed. It can also be seen that the high pressure zone at the tip of the returning blade is similar for 10° and 30° inclination angle models, while for the model with 90% thickness, this zone is much larger in size.

Flow Diagnostics and Optimal Design of Vertical Axis Wind Turbines for Urban Environments
By Martin Zahariev, School of Computing and Engineering, University of Huddersfield, UK (2016)

48

(a)

(b)

Flow Diagnostics and Optimal Design of Vertical Axis Wind Turbines for Urban Environments
By Martin Zahariev, School of Computing and Engineering, University of Huddersfield, UK (2016)

49

(c)

Figure 4.7: Static gauge pressure (Pa) variations in the vicinity of different guide vanes models (a) 10° inclination angle and 10% thickness (b) 30° inclination angle and 10% thickness (c) 30° inclination angle and 90% thickness

Figure 4.8 depicts the variation in the flow velocity magnitude in the vicinity of the guide vanes models at TSR of 0.7. The scale is again kept constant for effective comparison. It can be seen that the high velocity zone at the advancing blade is same for each of the guide vanes models. It can also be seen that the high velocity zone in the middle of the VAWT is similar only for the models with 10° and 30° incline angle, while for the model with 90% thickness, this zone is much smaller, indicating that less air flow is passing through the VAWT model with the guide vanes with 90% thickness.

(a)

(b)

Flow Diagnostics and Optimal Design of Vertical Axis Wind Turbines for Urban Environments
By Martin Zahariev, School of Computing and Engineering, University of Huddersfield, UK (2016)

51
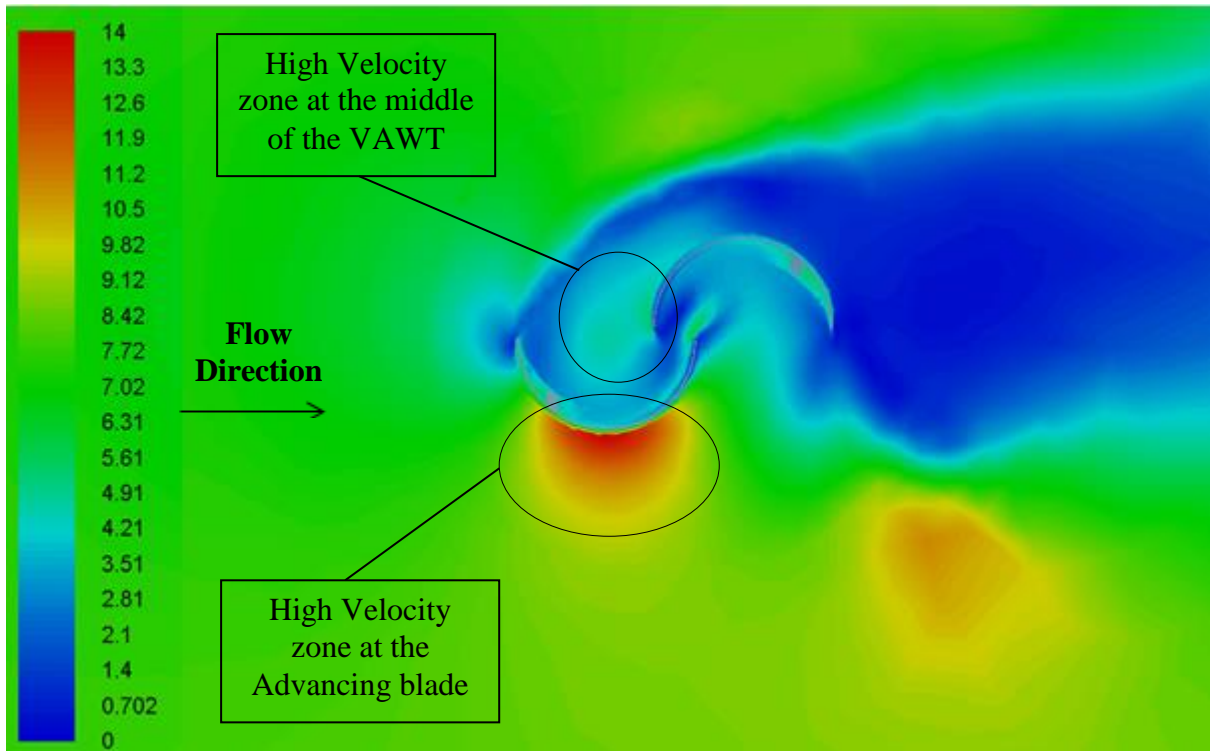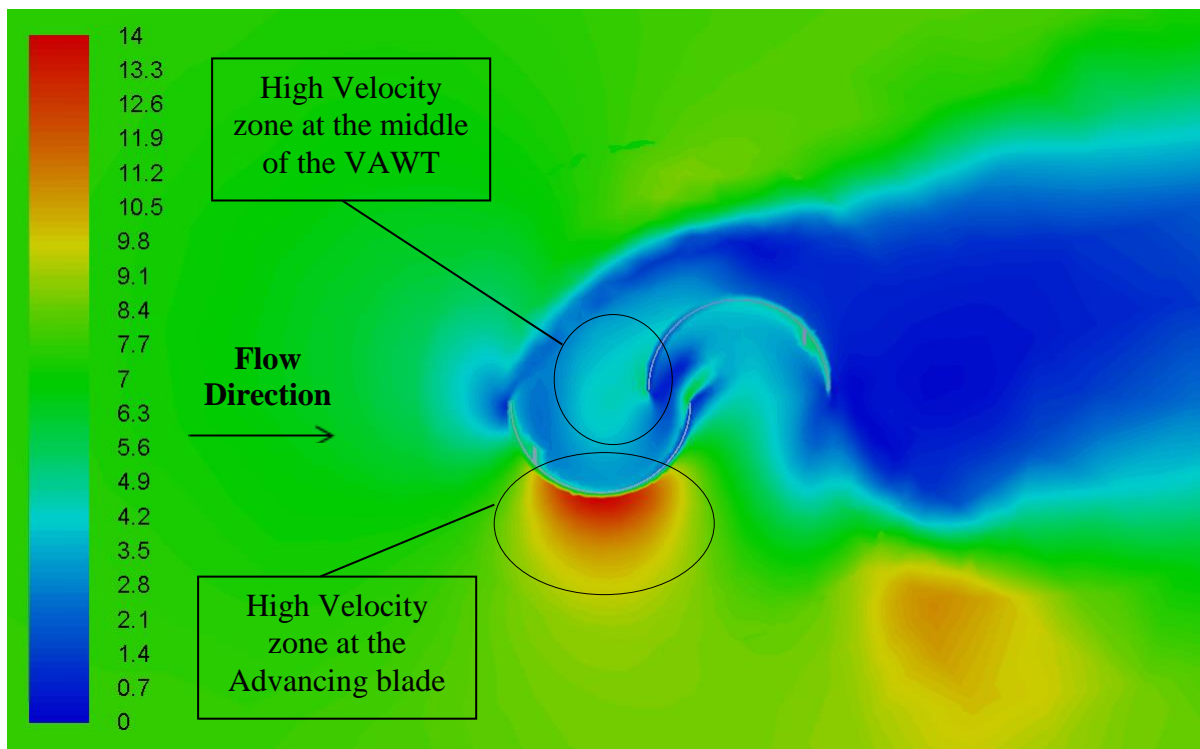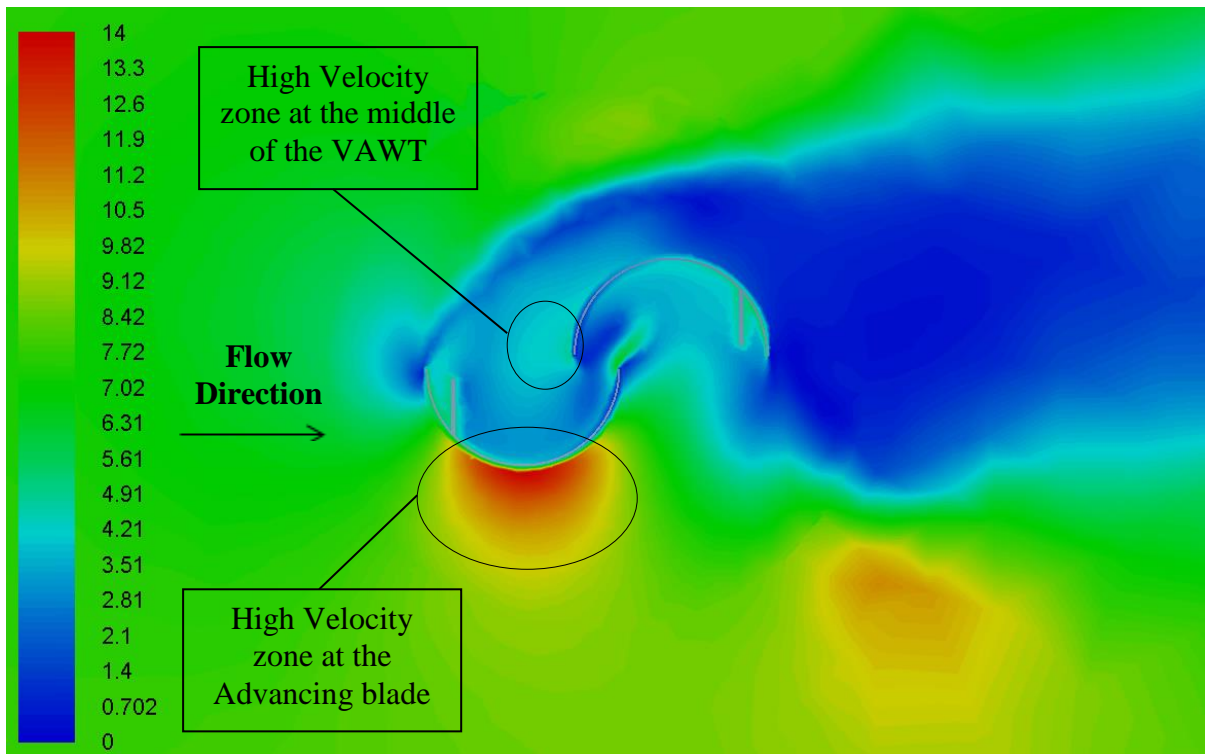
(c)

Figure 4.8: Velocity magnitude (m/s) variation in the vicinity of different guide vanes models (a) 10° inclination angle and 10% thickness (b) 30° inclination angle and 10% thickness (c) 30° inclination angle and 90% thickness

Once the detailed flow analysis of the local flow features in the vicinity of the guide vanes models has been carried out, the variations of the instantaneous coefficients of moment and power in 10°, 20° and 30° inclination angle models have been analysed, as shown in figure 4.9. The cyclic variations in Cm are similar to the one observed in case of the baseline model, indicating that inclination angle of internal guide vanes has negligible effects on the coefficient of moment and power of the VAWT. However, it is noteworthy that both the coefficients are 6.4% less (on average) compared to the baseline model, suggesting that addition of internal guide vanes with different angles decreases the performance output of the VAWT.

Figure 4.10 depicts the variations in the instantaneous coefficients of moment and power over a complete revolution of the guide vanes models having 10%, 50% and 90% thickness, to emphasize on the effects caused by changing the guide vanes' thickness. It can clearly be seen that all three of the models have similar cyclic variations; however, the model with lower percentage of guide vane thickness shows higher Cm and Cp values. Average Cm and Cp values for the three configurations considered here are summarised in table 4.4.

Table 4.4: Average coefficients of moment and power for different guide vanes thicknesses

Guide Vane Thickness (%)	Coefficient of Power	Coefficient of Moment
10	0.133	0.19
50	0.129	0.185
90	0.126	0.18

Flow Diagnostics and Optimal Design of Vertical Axis Wind Turbines for Urban Environments
By Martin Zahariev, School of Computing and Engineering, University of Huddersfield, UK (2016)

52
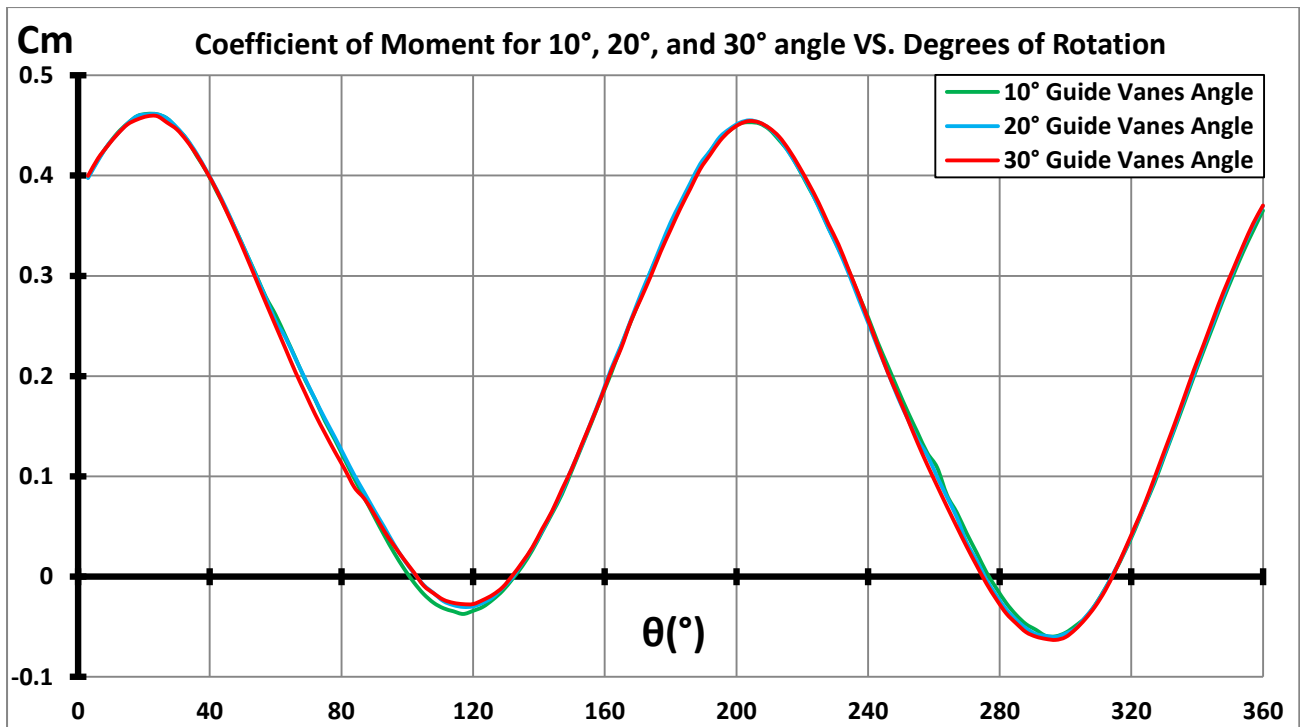
(a)
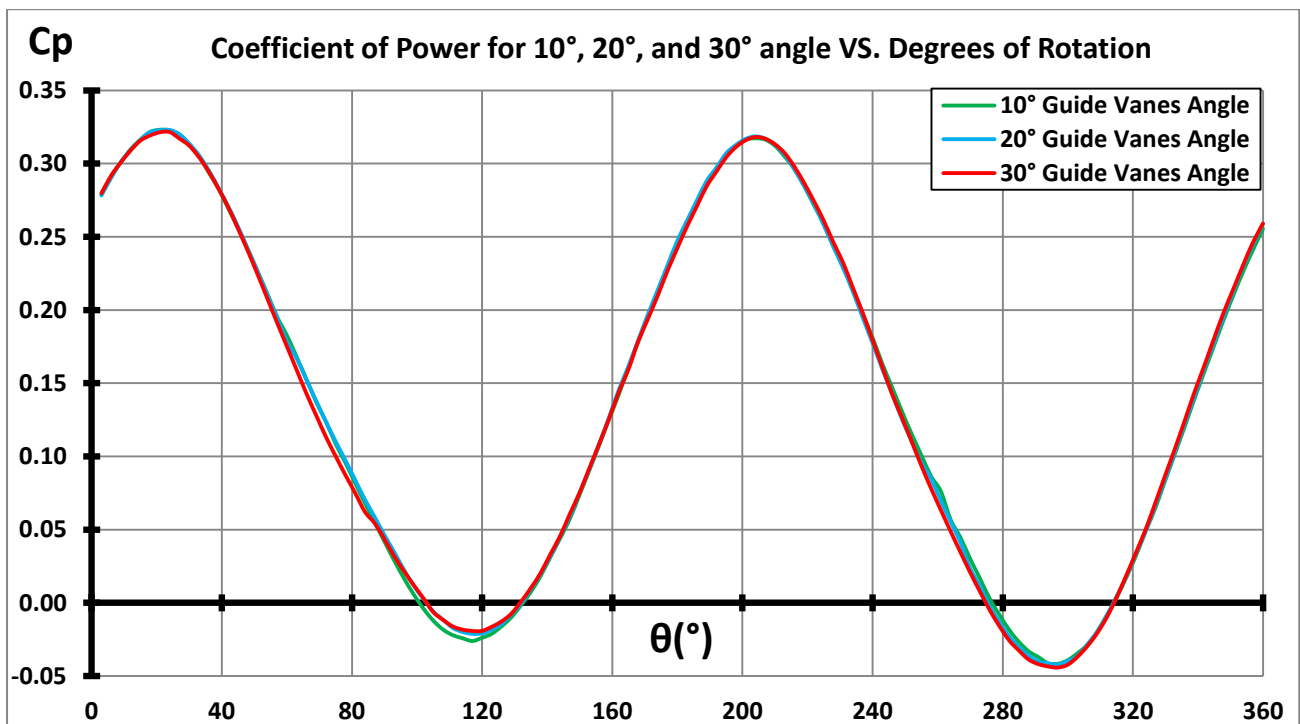
(b)

Figure 4.9: Variations in the instantaneous coefficients of (a) moment (Cm) and (b) power (Cp), over a complete revolution of the guide vanes models having 10°, 20° and 30° inclination angles

Flow Diagnostics and Optimal Design of Vertical Axis Wind Turbines for Urban Environments
By Martin Zahariev, School of Computing and Engineering, University of Huddersfield, UK (2016)

53
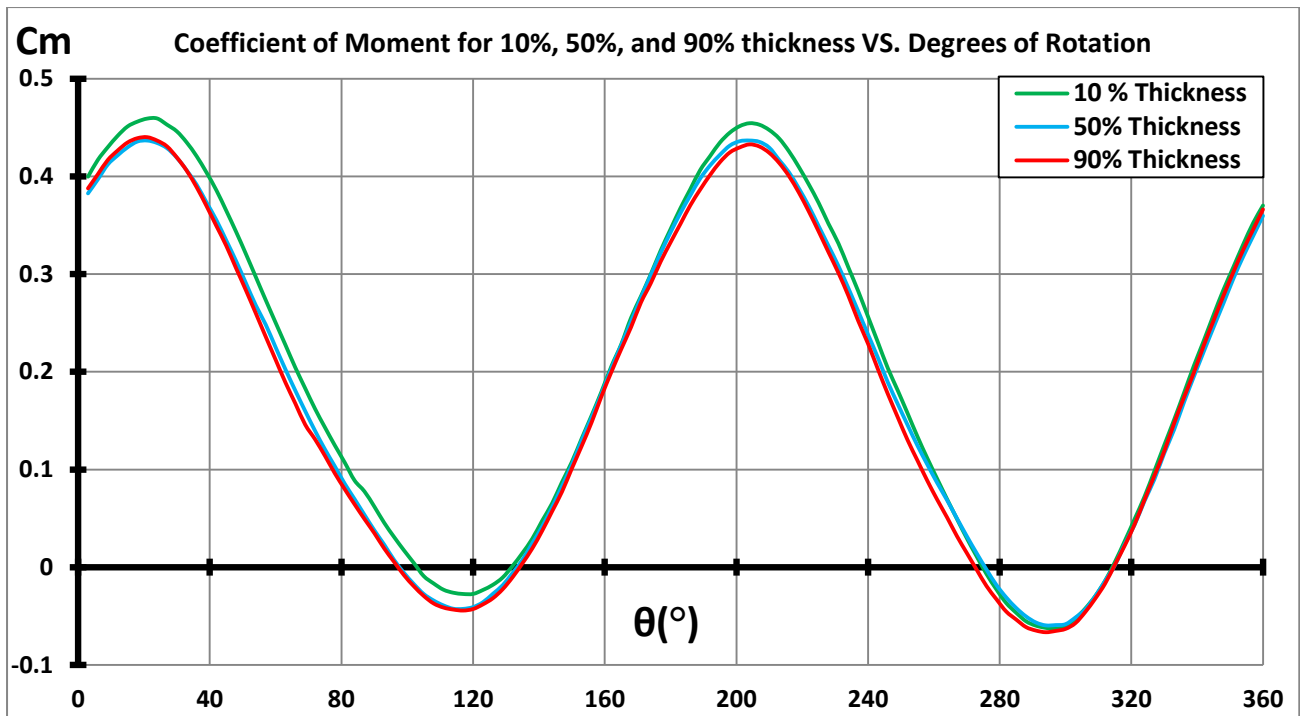
(a)
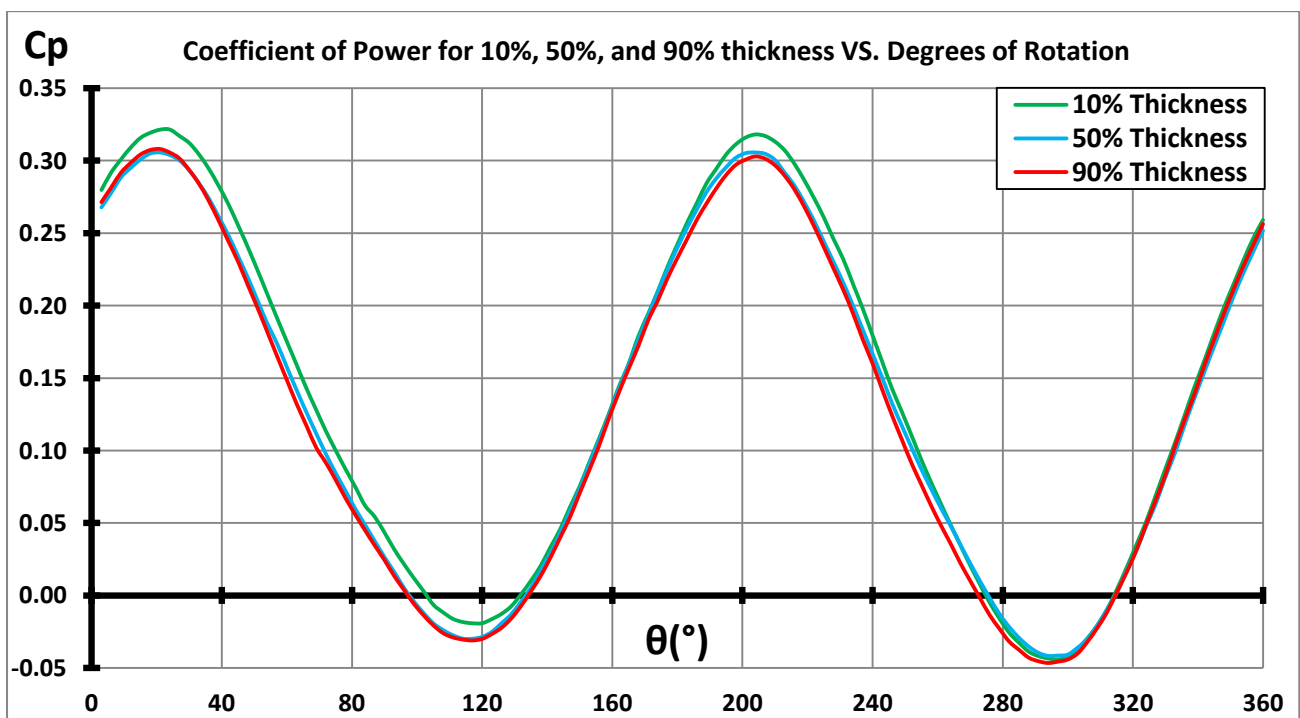
(b)

Figure 4.10: Variations in the instantaneous coefficients of (a) moment (Cm) and (b) power (Cp), over a complete revolution of the guide vanes models having 10%, 50% and 90% thickness

The averaged results for coefficient of moment and coefficient of power over an entire revolution are summarized in table 4.4, where it can be seen that the averaged coefficients of moment and power are decreasing with the increase in guide vane thickness.

Flow Diagnostics and Optimal Design of Vertical Axis Wind Turbines for Urban Environments
By Martin Zahariev, School of Computing and Engineering, University of Huddersfield, UK (2016)

54

The addition of internal guide vanes forces the air flow passing through the VAWT to take an inclined route for propagation. The amount of air passing through this incline route depends on the guide vanes' thickness. Therefore, by increasing the guide vanes' thickness, the amount of air passing through the VAWT is increased. The detailed qualitative and quantitative analysis of the guide vanes models indicate that the efficiency of the VAWT decreases as more air flow is forced to take the longer incline route through the VAWT. This is consisting with previous knowledge regarding the aspect ratio of a drag based VAWT, where it is stated that increase in the aspect ratio of a drag based VAWT increases the VAWT's efficiency. Higher aspect ratio turbines are tall and thin; hence the incoming air flow is passing faster through the turbine, as it passes shorter distance associated with lower width turbines [62].

The addition of internal guide vanes is in-fact increasing the time the air flow takes to propagate through the VAWT, as it travels at lower velocity (see figure 4.11). It also increases the distance the incoming air flow must pass through the VAWT, as it takes the inclined route through the VAWT. This causes the same effect as in lower aspect ratio VAWTs i.e. making the distance longer, which leads to high-torque, low-velocity and low coefficient of power characteristics. To further emphasis on this, figure 4.11 depicts the variations in air velocity and coefficient of power of VAWTs for various guide vanes' thicknesses.
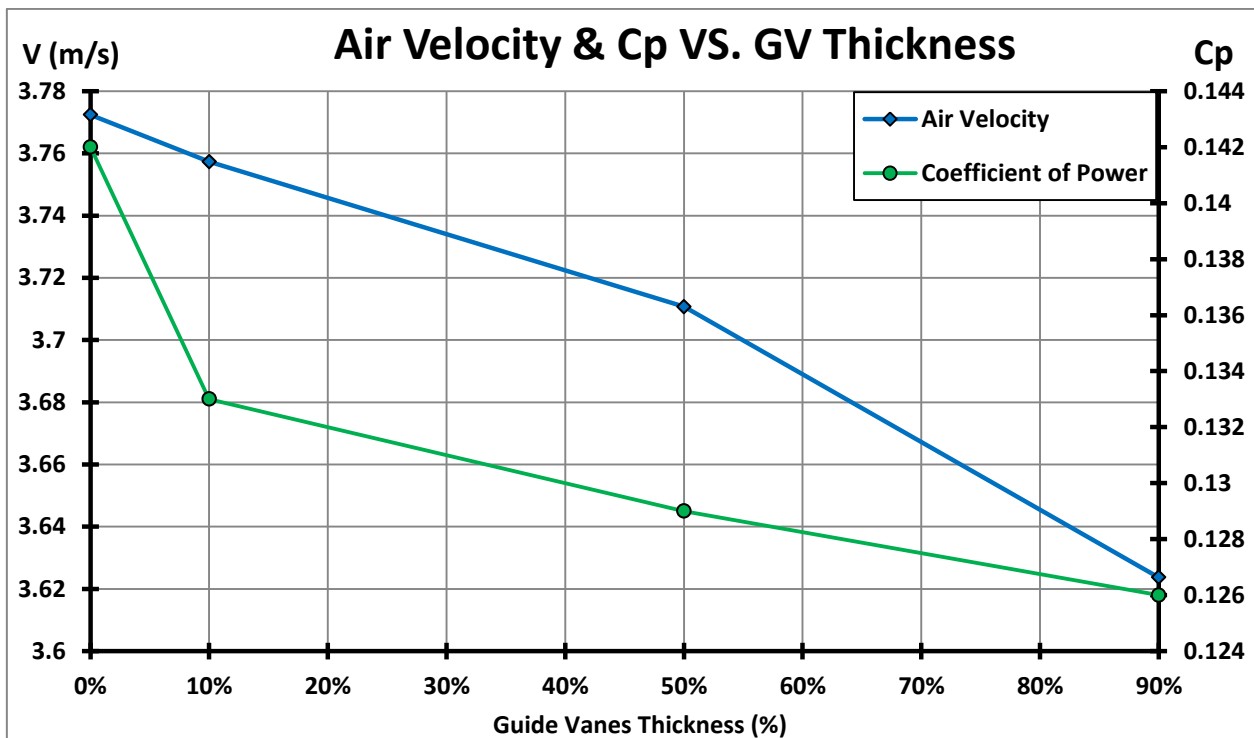
Figure 4.11: Air velocity and coefficient of power variations for different guide vanes' thicknesses

The next section highlights the effects of tapering the blades on the performance of the VAWT.

Flow Diagnostics and Optimal Design of Vertical Axis Wind Turbines for Urban Environments
By Martin Zahariev, School of Computing and Engineering, University of Huddersfield, UK (2016)

55

4.6 Effect of Blade Tapering on the performance of the VAWT

In the present study, three different VAWT models with various blade tapering applied have been analysed. These designs correspond to X-shaped blades, Delta-shaped blades and Rhomb-shaped blades, as shown in figure 4.12. The overlap and gap ratios have been kept constant, meaning that where the blade profile reduces in size, the gap and overlap distances are reduced proportionally to keep these ratios same.

(a)   (b)   (c)
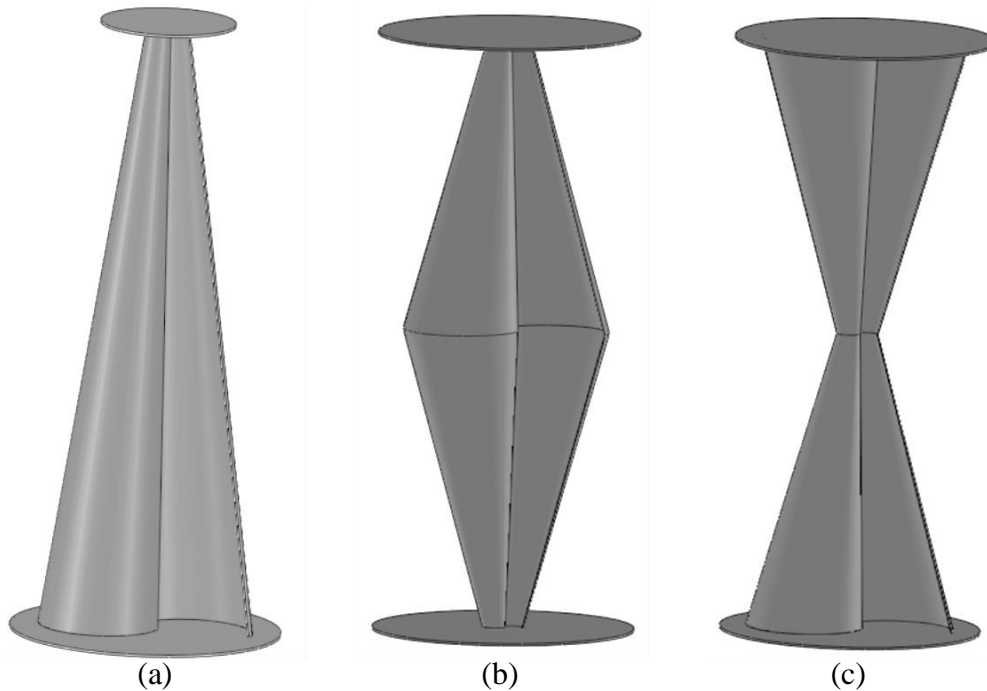
Figure 4.12: Tapered VAWT models (a) Delta-Shape (b) Rhomb-Shape (c) X-Shape

The swept area and the rotor radius of these turbines are different to the baseline model. The swept area and the rotor radius have been calculated, as shown in figure 4.13. The mean rotor radius (Rm) has been calculated based on the radii of the smaller blade side (Rs) and the bigger blade side (Rb). Each of the three tapered blade models have been analysed at three different TSR values i.e. 0.7, one above and one below 0.7 in order to ensure that the peak efficiency point is accurately captured.
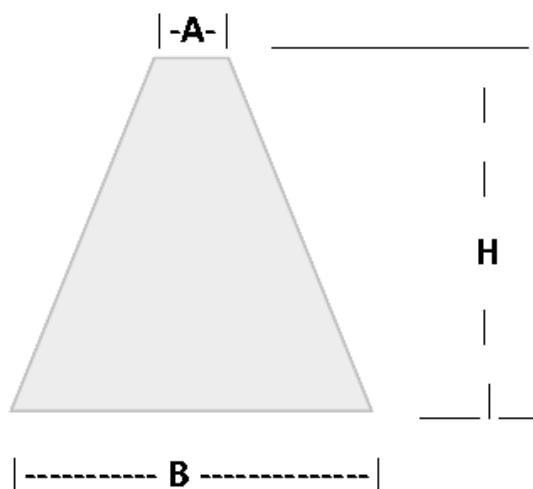
A = 176 mm = 0.176 m

B = 880 mm = 0.88 m

H = 2500 mm = 2.5 m

Rs = 88 mm

Rb = 440 mm

Rm = (88 + 440)/2 = 264 mm = 0.264 m

$$\text{Area} = \frac{A+B}{2} \times H = [(0.176 + 0.88)/2] \text{ x } 2.5 = 1.32 \text{ m}^2$$

Figure 4.13: Area of trapezoid

Figure 4.14 depicts the variation in static gauge pressure in the vicinity of the three tapered blade models at TSR of 0.7. The scale of the pressure distribution has been kept the same for all the three models considered here for effective comparison purposes. It can be seen that for the Rhomb-shaped model, the low pressure zone downstream the VAWT is smaller than the one for the Delta-shaped model. It can also be noticed for the X-shape model that there are two low pressure zones downstream the VAWT, which indicates that as the blades grow in size from the middle of the VAWT towards the end plates, the disturbance generated affects the middle region. It can also be seen that the Rhomb-shaped model has larger high pressure zones, acting on both advancing and returning blades, compared to the Delta-shaped and X-shaped models.

(a)

(b)

Flow Diagnostics and Optimal Design of Vertical Axis Wind Turbines for Urban Environments
By Martin Zahariev, School of Computing and Engineering, University of Huddersfield, UK (2016)

57

(c)
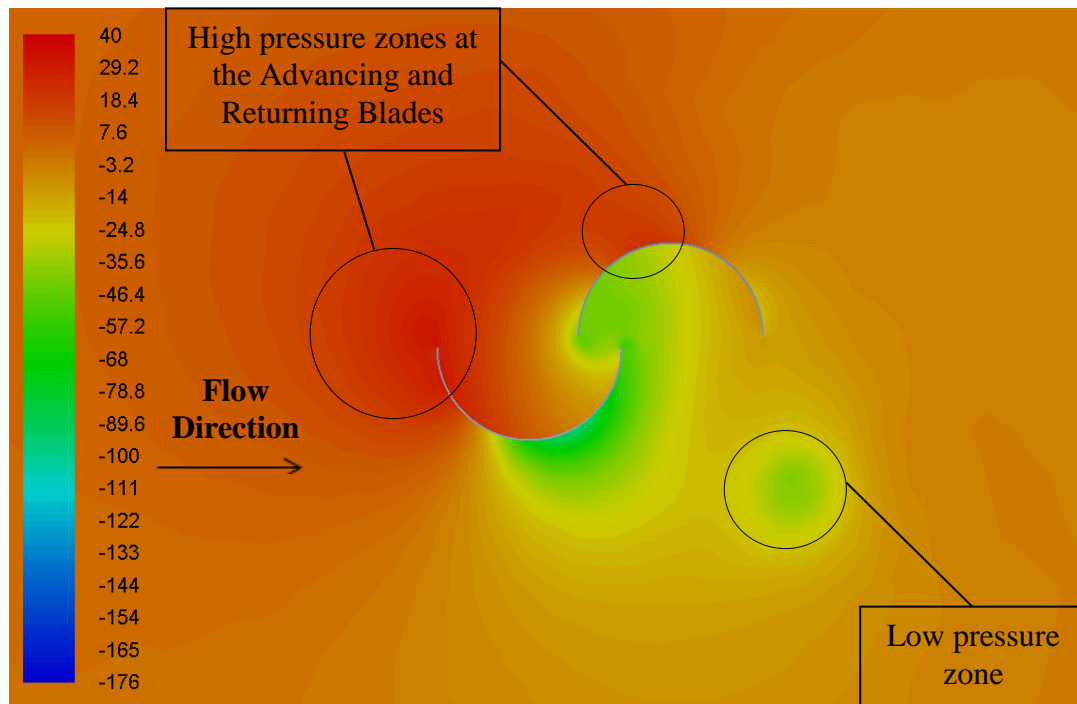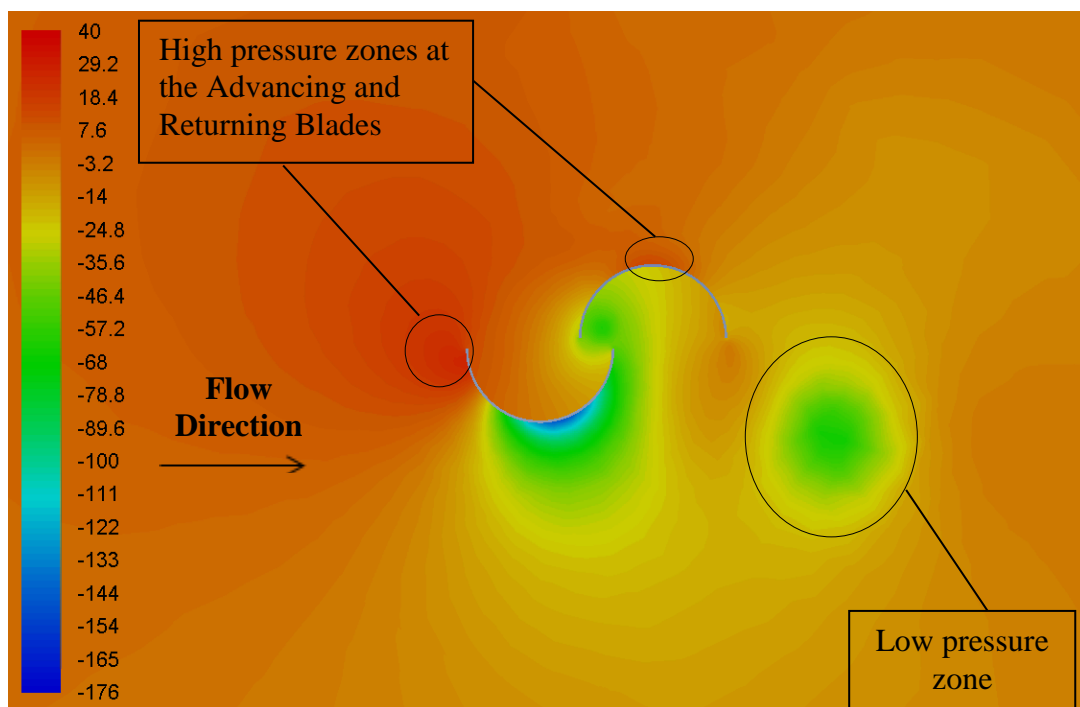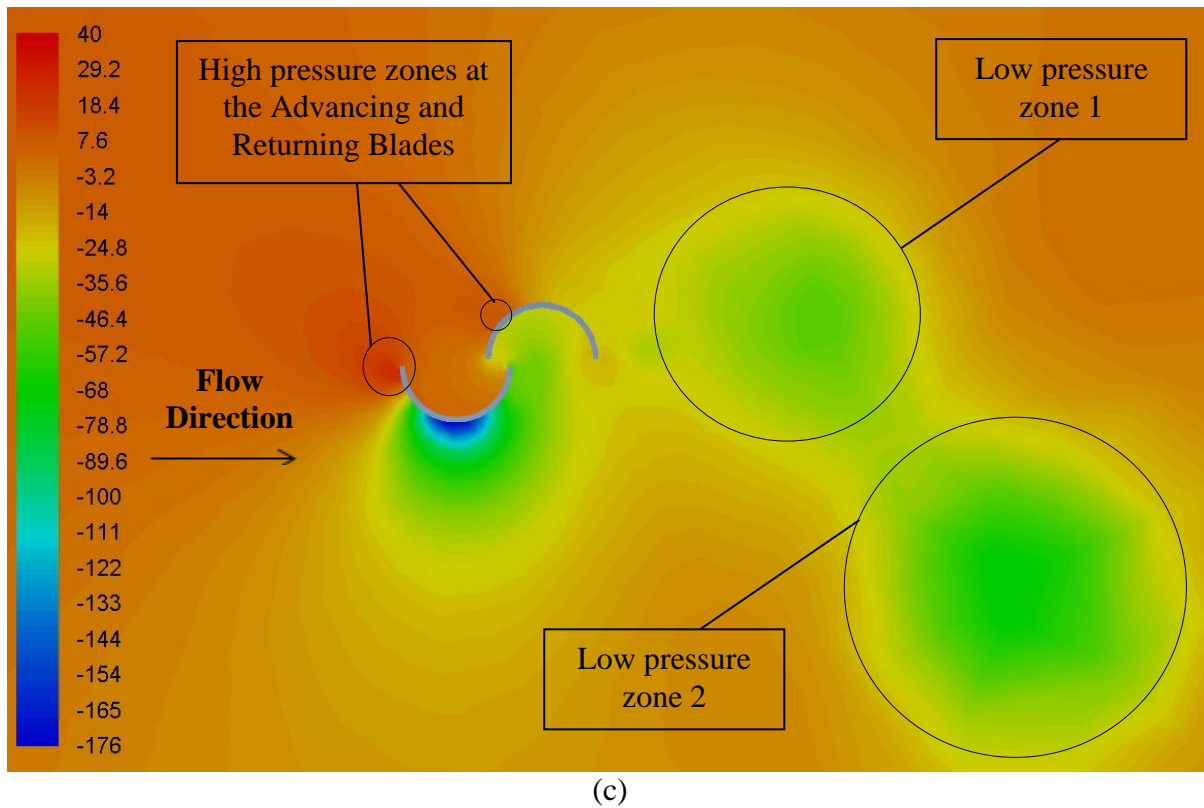
Figure 4.14: Static gauge pressure (Pa) variations in the vicinity of the tapered blades models (a) Rhomb-shaped model (b) Delta-shaped model (c) X-shaped model

Figure 4.15 depicts the variation in the flow velocity magnitude in the vicinity of the tapered blades models at TSR of 0.7. It can be seen that for the Rhomb-shaped model, the high velocity zone in front of the advancing blade is much smaller, and lower in velocity value, than the one for the Delta-shaped model. It can also be seen that for the Rhomb-shaped model, the velocity in the overlap zone is lower than for the Delta-shaped model. The Rhomb-shaped model and the Delta-shaped model have different, in velocity value and size, recirculating flow regions downstream the VAWT, whereas the high velocity recirculating flow region is larger and of higher velocity value for the Delta-shaped model. It can also be observed that the high velocity zone in front of the advancing blade of the Delta-shaped model is similar to the one for the X-shaped model; however, the X-shaped model does not depict the high velocity region in the overlap zone.

Flow Diagnostics and Optimal Design of Vertical Axis Wind Turbines for Urban Environments
By Martin Zahariev, School of Computing and Engineering, University of Huddersfield, UK (2016)

58

(a)

(b)

Flow Diagnostics and Optimal Design of Vertical Axis Wind Turbines for Urban Environments
By Martin Zahariev, School of Computing and Engineering, University of Huddersfield, UK (2016)

59

(c)

Figure 4.15: Velocity magnitude (m/s) variation in the vicinity of the tapered blades models (a) Rhomb-shaped models (b) Delta-shaped model (c) X-shaped model

Once the detailed flow analysis of the local flow features in the vicinity of the tapered blades models has been carried out, the variations of the instantaneous coefficients of moment and power in one complete revolution have been analysed, as depicted in figure 4.16. It can clearly be seen that all three models have similar cyclic variations, but the Delta-shaped model exhibits higher coefficients of moment and power. Performance coefficients of X-shaped model are lower than the Delta-shaped model at the positive peak points. This means that the average coefficients of moment and power of the X-shape model is lower than the Delta-shaped model, but higher that the Rhomb-shaped model, as summarised in table 4.5.

Flow Diagnostics and Optimal Design of Vertical Axis Wind Turbines for Urban Environments
By Martin Zahariev, School of Computing and Engineering, University of Huddersfield, UK (2016)

60
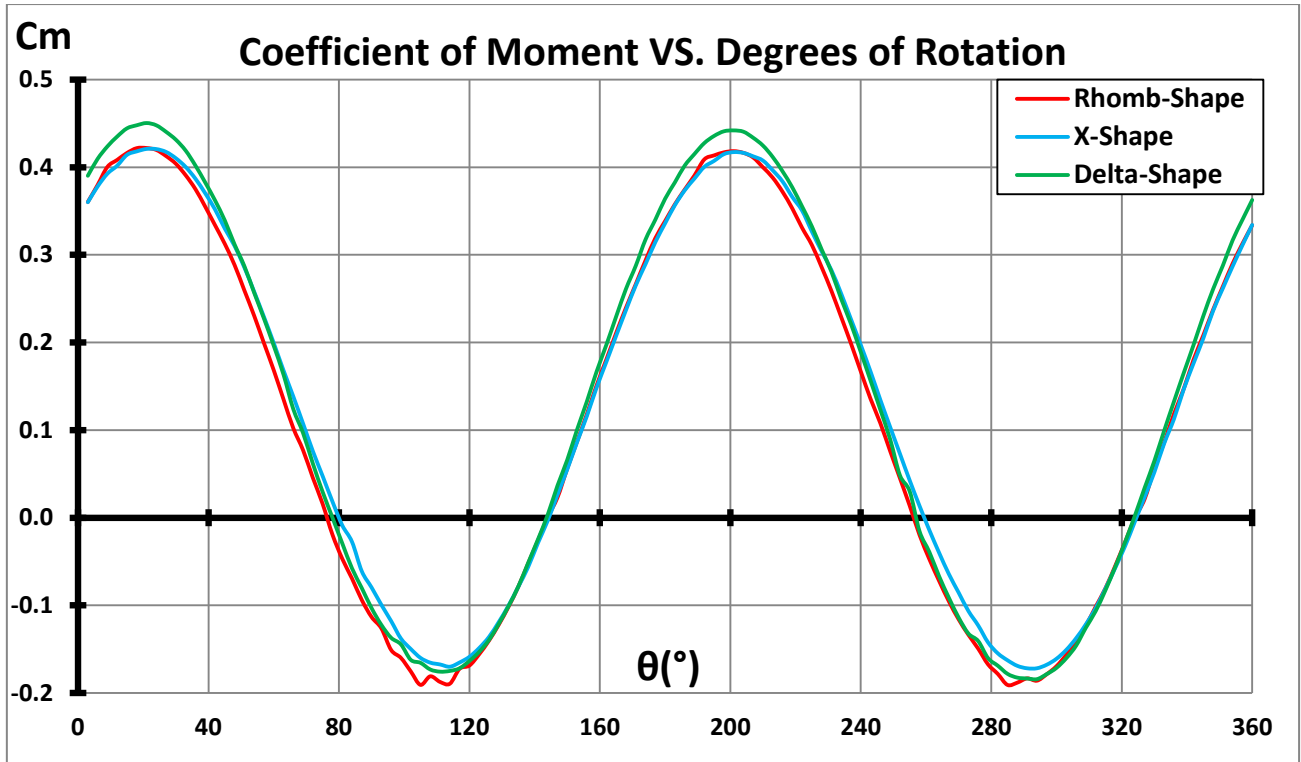
(a)
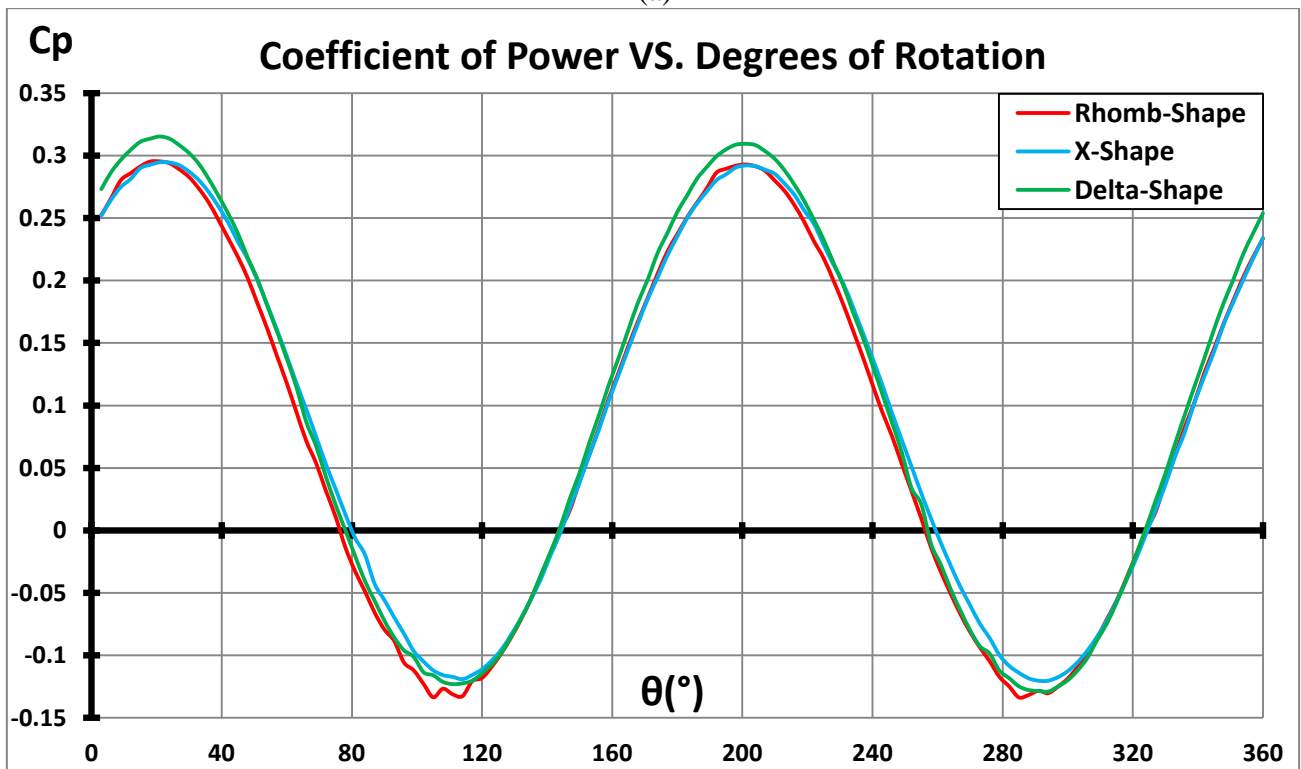
(b)

Figure 4.16: Variations in the instantaneous coefficients of (a) moment (Cm) and (b) power (Cp), over a complete revolution of the tapered blades models

Flow Diagnostics and Optimal Design of Vertical Axis Wind Turbines for Urban Environments
By Martin Zahariev, School of Computing and Engineering, University of Huddersfield, UK (2016)

61

Table 4.5: Average coefficients of moment and power for different tapered blade models

	Coefficient of Moment	Coefficient of Power
Delta-shape	0.129	0.0903
Rhomb-shape	0.114	0.0798
X-shape	0.127	0.0889

It can be further seen in table 4.5 that the average coefficient values are lower than the baseline model, which has coefficient of power of 0.142, leading to the conclusion that tapering of the blades has adverse effects on the performance of the VAWT. Between the three models, it can be observed that the delta and X shaped models are more efficient than the Rhomb shaped model. As the Delta-shaped model is the most efficient of the three tapered blade models, it has been further analyzed to determine the reason for its lower efficiency compared to the baseline model. In figure 4.17, the static gauge pressure distribution across the blades of the delta-shaped VAWT is shown.
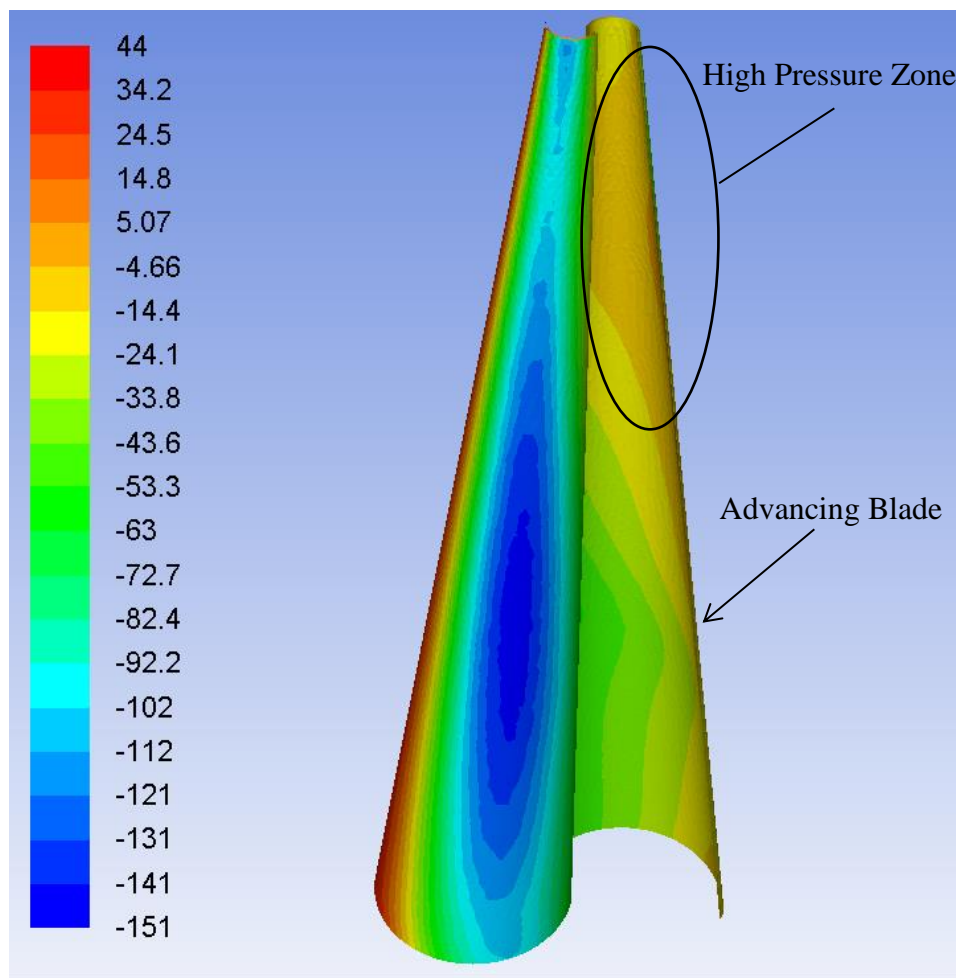
Figure 4.17: Pressure distribution on the blades of the delta-shaped blades model

It can clearly be seen in figure 4.17 that the high pressure zone at the advancing blade is only at the top of the VAWT, where the relative aspect ratio is higher. When analysed as a 3D structure, it is clear that most of the VAWT, where the radius is larger and the relative aspect ratio is lower, is not exhibiting this high pressure. In order to further validate this, the drag force acting on the blades of the Delta-shaped model has been calculated to be 33.4N, while the baseline model has a drag force of 49.7N. Therefore, as this is a drag based VAWT, the torque is heavily dependent on the drag force, meaning that the power output will be lower resulting in overall lower efficiency.

Flow Diagnostics and Optimal Design of Vertical Axis Wind Turbines for Urban Environments
By Martin Zahariev, School of Computing and Engineering, University of Huddersfield, UK (2016)

62

The theoretical reason for the lower efficiency is again the Aspect Ratio, as it has been experimentally and theoretically proven that increase in the Aspect Ratio of a Drag Based VAWT increases VAWT's efficiency. Higher Aspect Ratio turbines are tall and thin and have higher efficiencies [62]. In the case of the tapered blade models, at some parts of the VAWT, the rotor radius is bigger that the baseline model, indicating that at these parts, the VAWT is working at lower Aspect Ratio, hence lower efficiency. In other parts of the VAWT, the rotor radius is smaller than the baseline model, indicating that the VAWT is working at higher Aspect Ratio at those parts, hence higher efficiency. The overall lower efficiency is due to the fact that in case of a trapezoid, 66.7% of the VAWT's swept area is in the lower Aspect Ratio region; while only 33.3% of the VAWT's swept area is in the higher Aspect Ratio region. This means that 66.7% of the VAWT is working at lower efficiency than the baseline model. In figure 4.18, calculations are shown explaining these area-based discussions for a trapezoid (Delta-shaped model).
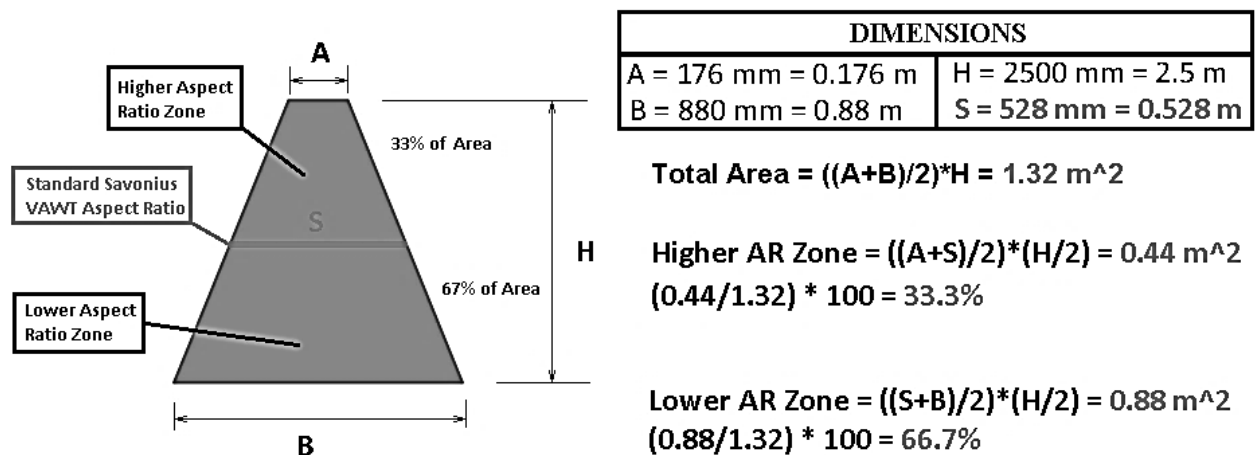
Figure 4.18: Area calculations for the Delta-shaped model

In order to validate that the power production of the VAWT is the way that it has been explained here i.e. based on the swept area, localized post-processing of the results has been carried out, where the blades have been divided into 10 equally spaced zones. Corresponding static pressures in these zones have been calculated. In figure 4.19, these 10 zones of the VAWT are shown. The static pressure values at the back and front of a given blade, for each zone, have been computed, together with the associated area of each zone. The static pressure values, and the areas, have then been used to calculate the forces acting on the blade for that particular zone. The same process has been repeated for the other blade, resulting in a set of forces for blades 1 and 2, for each of the 10 zones. The results have then been used to calculate the torque generated by the blades for each of the zones. Examples of these calculations for zone 10 are shown in table 4.6.

Flow Diagnostics and Optimal Design of Vertical Axis Wind Turbines for Urban Environments
By Martin Zahariev, School of Computing and Engineering, University of Huddersfield, UK (2016)

63
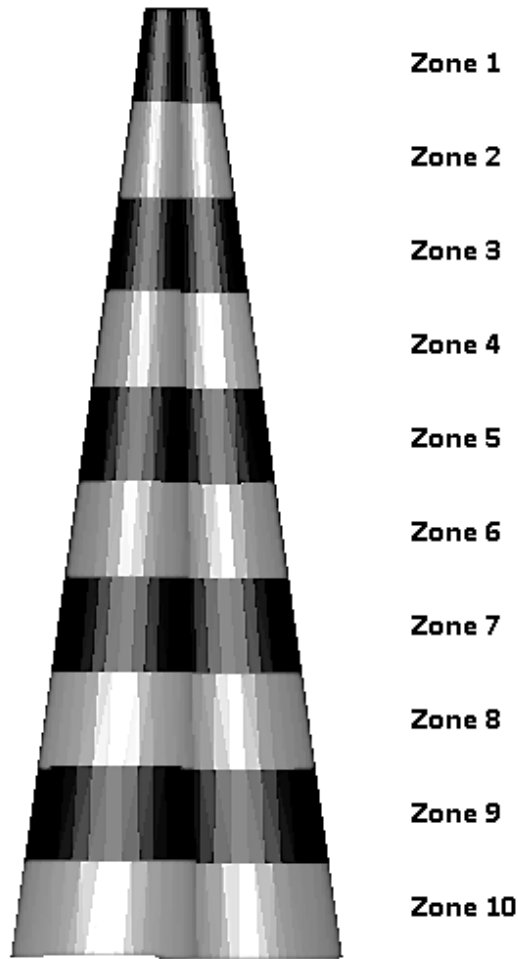
Figure 4.19: Blade Zones

Table 4.6: Calculations for Zone 10

ZONE 10 (Radius 0.1824m)				
	In Front of Blade 1	At The Back of Blade 1	In Front of Blade 2	At The Back of Blade 2
Area (m^2)	0.184	0.190	0.184	0.190
Static Pressure (Pa)	-33.70	-5.97	9.12	-46.29
Force (N)	-6.21	-1.14	1.68	-8.80
	Blade 1		Blade 2	
Force (N)	-5.07		10.48	
Torque (Nm)	-0.925		1.91	
	TOTAL			
Torque (Nm)	0.987			

The results for the rest of the zones have been calculated using the same principle described in table 4.6, and are summarized in table 4.7.

Flow Diagnostics and Optimal Design of Vertical Axis Wind Turbines for Urban Environments
By Martin Zahariev, School of Computing and Engineering, University of Huddersfield, UK (2016)

64

Table 4.7: Calculated results for each of the ten zones

	Total Torque (Nm)		Total Torque (Nm)
Zone 1	0.111	Higher Aspect Ratio VAWT Zone	1.773
Zone 2	0.218		
Zone 3	0.351		
Zone 4	0.485		
Zone 5	0.609		
Zone 6	0.711	Lower Aspect Ratio VAWT Zone	4.148
Zone 7	0.739		
Zone 8	0.799		
Zone 9	0.913		
Zone 10	0.987		

The total instantaneous torque output of the VAWT is 5.92 Nm; therefore, the percentage of the torque from the higher aspect ratio zone is 29.95%, while the percentage of the torque produced from the lower aspect ratio zone is 70.05%. This is consistent with the explanation based on the swept area. The percentage of instantaneous torque per each zone has been calculated as well, and presented in figure 4.20.
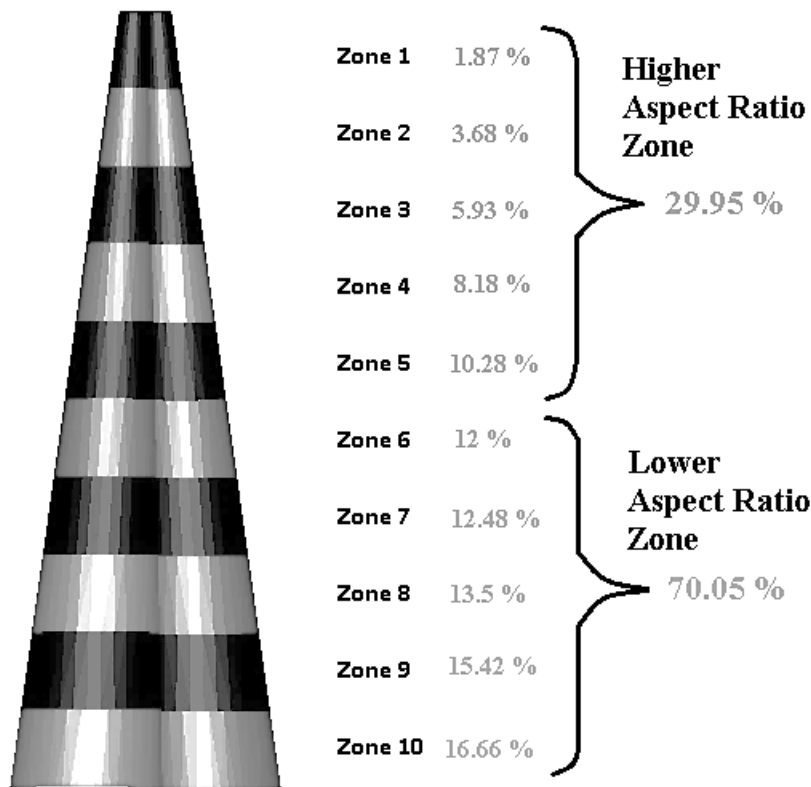
Figure 4.20: Torque distribution per zone for the Delta-shaped model

It can clearly be seen that the actual results extracted and analysed from the CFD solver are matching the swept area based prediction for the power production per zone of the tapered blade VAWTs. Therefore, it can be concluded that as 70% of the torque generation is at lower aspect ratio, the efficiency of this 70% region is lower than the baseline model. 30% of the torque generation is at higher aspect ratio, and have higher local efficiency than the baseline model. The overall aspect ratio of the tapered model is lower than the baseline model, resulting in lower overall efficiency.

Flow Diagnostics and Optimal Design of Vertical Axis Wind Turbines for Urban Environments
By Martin Zahariev, School of Computing and Engineering, University of Huddersfield, UK (2016)

65

4.7   Effect of Helically Twisted Blades on the VAWT's performance

Five different models with varying levels of helical twists have been generated, where the helical twist level is defined as the number of revolutions a blade make around its axis from one end to the other. The five models have twists of 0.25, 0.5, 1, 1.5 and 2 revolutions, as shown in figure 4.21.

(a)   (b)   (c)

(d)   (e)   (f)
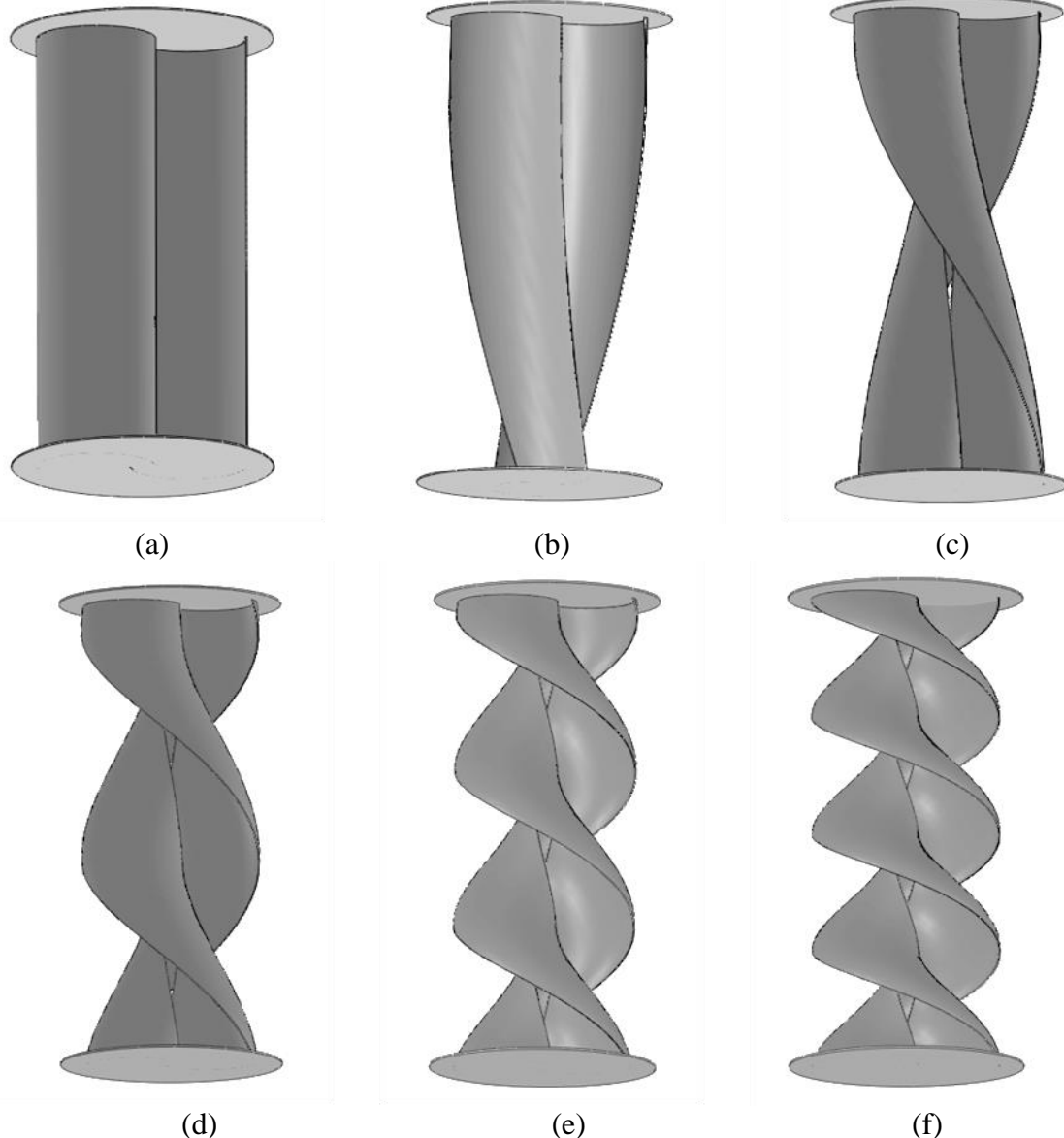
Figure 4.21: Helically twisted models (a) Baseline model with 0 revolutions of twist (b) 0.25 revolution of twist (c) 0.5 revolutions of twist (d) 1 revolution of twist (e) 1.5 revolutions of twist (f) 2 revolutions of twist

As the blades chord lengths do not change due to the helical twist, another way of calculating the solidity has been used. By introducing helical twist to the blades, the blades' surface areas increase with the increasing level of twist. Therefore, as the core definition of rotor solidity is the difference between the rotor's swept area and the area of the blades, it can be concluded that the helical twist increases the solidity of the VAWT. The solidity variations are summarized in table 4.8.

Flow Diagnostics and Optimal Design of Vertical Axis Wind Turbines for Urban Environments
By Martin Zahariev, School of Computing and Engineering, University of Huddersfield, UK (2016)

66

Table 4.8: Helically twisted models' solidity

	VAWT Swept Area (m^2)	Blades Surface Area (m^2)	Solidity (%)
Baseline Model	2.2	3.888	43.41
0.25 Revolutions Twist	2.2	3.902	43.61
0.5 Revolutions Twist	2.2	3.943	44.20
1 Revolution Twist	2.2	4.102	46.37
1.5 Revolutions Twist	2.2	4.356	49.50
2 Revolutions Twist	2.2	4.657	52.76

It can be seen that the solidity of the rotor changes by a small fraction for the 0.25 and 0.5 revolutions of twist models, while for 1, 1.5 and 2 revolutions of twist models, the solidity increases significantly. Therefore, as rotors with higher solidity usually depict peak efficiency at lower TSR values, compared to rotors with lower solidity, the 1, 1.5 and 2 revolutions of twist models have been numerically analysed at TSRs ranging from 0.4 to 0.7, as they have higher solidity. The 0.25 and 0.5 revolutions of twist models have solidity similar to the baseline model; therefore, they have been numerically tested at TSR values of 0.7, one above and one below TSR of 0.7, to confirm their peak efficiency is at TSR of 0.7, as in the case of the baseline model.

From numerical examinations, it has been found that the models with 0.25 and 0.5 revolutions of twist depict peak in efficiency at TSR of 0.7, while the models with 1, 1.5 and 2 revolutions of twist have been found to depict peak in efficiency at TSR of 0.5; lower than the baseline model as their solidity is noticeably higher. Both qualitative and qualitative analysis of the helically twisted models has been carried out at their peak efficiency TSRs. Figure 4.22 depicts the variation of static gauge pressure in the vicinity of the helically twisted models. It can be seen that the model with 0.25 revolutions of twist has a zone of low pressure at the tip of the advancing blade, which is lower in value compared to the model with 0.5 revolutions of twist. It can also be observed that the model with 1 revolutions of twist has a low pressure zone at the tip of the advancing blade, which is smaller than the model with 0.5 revolutions of twist. It can also be noted that the model with 1 revolution of twist has a second zone of low pressure, probably caused by the returning blade, due to the high level of helical twist. It can also be observed that the model with 1.5 revolutions of twist has even smaller zone of low pressure at the tip of its advancing blade than the model with 1 revolution of twist. It can also be seen that the model with 1.5 revolutions of twist has a zone of low pressure behind the returning blade. It can also be observed that the model with 2 revolutions of twist has the smallest zone of low pressure at the tip of its advancing blade. It can be noticed that the model with 2 revolutions of twist has larger zone of low pressure behind its returning blade compared to the model with 1.5 revolutions of twist.

Generally, it can be concluded that the zone of low pressure at the tip of the advancing blade reduces in size with the increase of the level of helical twist applied to the blades. It can also be concluded that above helical twist of 1 revolution the shape of the VAWT gets excessively distorted causing undesirable effects behind the returning blades, which reduces the beneficial effects of the flow that passes through the overlap zone.

Flow Diagnostics and Optimal Design of Vertical Axis Wind Turbines for Urban Environments
By Martin Zahariev, School of Computing and Engineering, University of Huddersfield, UK (2016)

67

(a)

(b)

Flow Diagnostics and Optimal Design of Vertical Axis Wind Turbines for Urban Environments
By Martin Zahariev, School of Computing and Engineering, University of Huddersfield, UK (2016)

68

(c)

(d)

Flow Diagnostics and Optimal Design of Vertical Axis Wind Turbines for Urban Environments
By Martin Zahariev, School of Computing and Engineering, University of Huddersfield, UK (2016)

69

(e)

Figure 4.22: Static gauge pressure (Pa) variations in the vicinity of the helically twisted models with revolutions of twist of (a) 0.25 (b) 0.5 (c) 1 (d) 1.5 (e) 2

Figure 4.23 depicts the variation in the flow velocity magnitude in the vicinity of the helically twisted models. It can be seen in figure 4.23 that the model with 0.25 revolutions of twist has a high velocity zone at the tip of the advancing blade, which is larger in size and higher in value than the model with the 0.5 revolutions of twist. It can also be observed that the downstream low velocity zone of the model with 0.25 revolutions of twist is larger than the corresponding zone of the model with 0.5 revolutions of twist. It can be noticed that the model with 1 revolution of twist has a high velocity zone at the tip of the advancing blade, which is smaller in size and lower in value than the model with 0.5 revolutions of twist. The downstream low velocity zone of the model with 1 revolution of twist is smaller than the model with 0.5 revolution of twist. It can also be seen that the model with 1.5 revolution of twist has a high velocity zone at the tip of the advancing blade, which is smaller in size and lower in value than the model with 1 revolution of twist. The downstream low velocity zone of the model with 1.5 revolution of twist is smaller than the model with 1 revolution of twist. The model with 1.5 revolution of twist also has a high velocity zone at the back of the advancing blade immediately after the overlap zone. It can also be observed that the model with 2 revolutions of twist has a high velocity zone at the tip of the advancing blade, which is the smallest in size and lowest in value compared to the rest of the models. The high velocity zone at the back of the advancing blade immediately after the overlap zone of the model with 2 revolutions of twist is larger in size compared to the model with 1.5 revolutions of twist.

In general, it can be concluded that high velocity zone at the tip of the advancing blade is reduces in size and decreases in value with the increase of the level of helical twist applied to the blades. It can also be concluded that the downstream low velocity zone decreases with the increase of the level of helical twist.

Flow Diagnostics and Optimal Design of Vertical Axis Wind Turbines for Urban Environments
By Martin Zahariev, School of Computing and Engineering, University of Huddersfield, UK (2016)

70

(a)

(b)

Flow Diagnostics and Optimal Design of Vertical Axis Wind Turbines for Urban Environments
By Martin Zahariev, School of Computing and Engineering, University of Huddersfield, UK (2016)

71

(c)

(d)

Flow Diagnostics and Optimal Design of Vertical Axis Wind Turbines for Urban Environments
By Martin Zahariev, School of Computing and Engineering, University of Huddersfield, UK (2016)

72

(e)

Figure 4.23: Velocity magnitude (m/s) variation in the vicinity of the helically twisted models with revolutions of twist of (a) 0.25 (b) 0.5 (c) 1 (d) 1.5 (e) 2

Once the detailed flow analysis of the local flow features in the vicinity of the helically twisted models has been carried out, the variations of the instantaneous coefficients of moment for the models with highest efficiency point at TSR 0.5 and the models with highest efficiency point at TSR 0.7 have been depicted in figure 4.24 (a) and (b).

It can clearly be seen in figure 4.24 (a) that for the models with highest efficiency point at TSR 0.5, the cyclic variations of the instantaneous coefficient of moment for each of the models are similar. However, with the increase in level of twist, the average coefficient of moment decreases (0.245 at 1 revolution of twist, 0.179 at 1.5 revolution of twist and 0.139 at 2 revolutions of twist). It can also be noticed that amplitude of the variations of the instantaneous coefficient of moment slightly reduces with the increase of the level of helical twist.

It can clearly be seen in figure 4.25 (b) that for the models with highest efficiency point at TSR 0.7, the cyclic variations of the instantaneous coefficient of moment for each of the models are similar, having the same period, but different amplitudes. It can also be observed that with the increase of the level of helical twist, the amplitude of the variations of the instantaneous coefficient of moment reduces significantly.

Flow Diagnostics and Optimal Design of Vertical Axis Wind Turbines for Urban Environments
By Martin Zahariev, School of Computing and Engineering, University of Huddersfield, UK (2016)

73
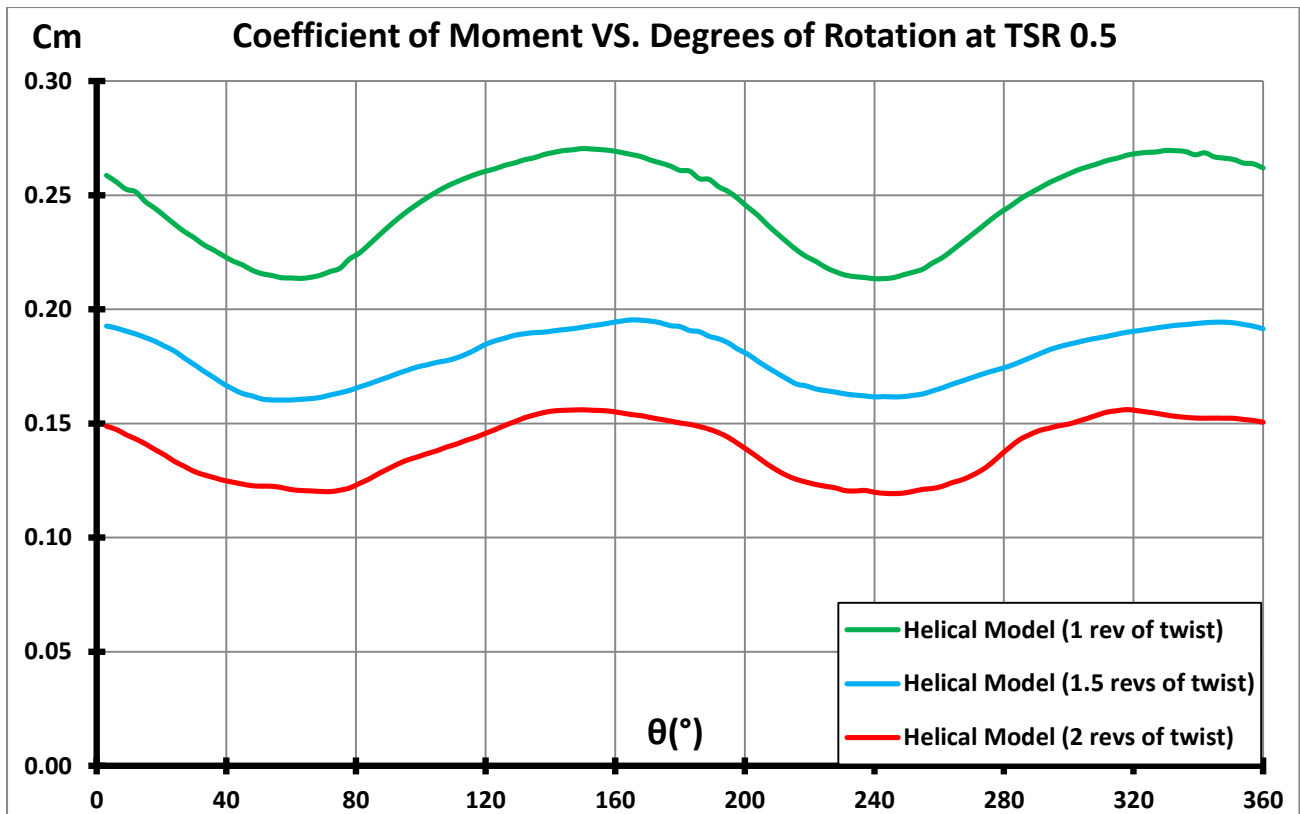
(a)
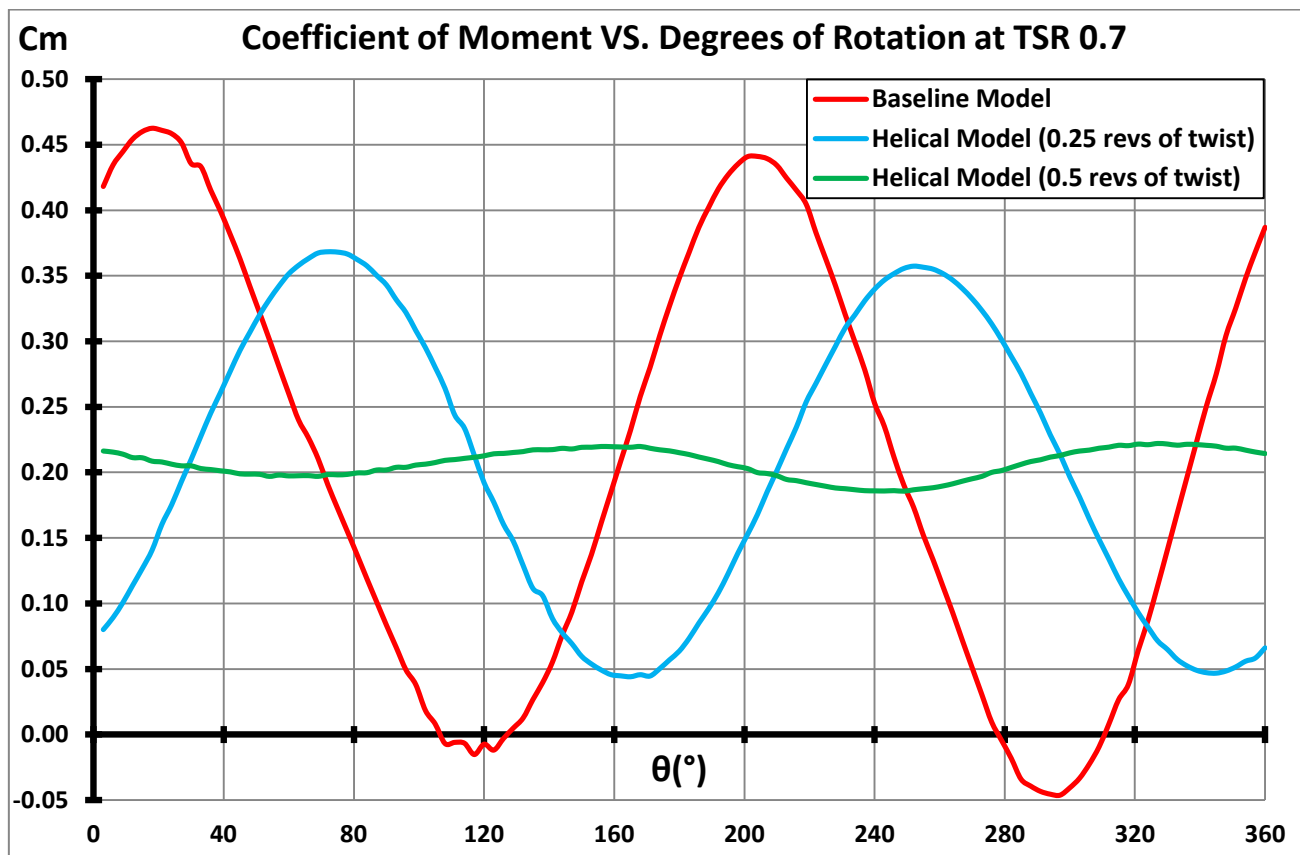
(b)

Figure 4.24: Variation of the instantaneous coefficient of moment (Cm) over a complete revolution of the helically twisted models with highest efficiency point at (a) TSR 0.5 (b) TSR 0.7

Flow Diagnostics and Optimal Design of Vertical Axis Wind Turbines for Urban Environments
By Martin Zahariev, School of Computing and Engineering, University of Huddersfield, UK (2016)

74

In order to compare the cyclic variations at the same scale for all of the models (the helical models with highest efficiency point at TSR 0.5 and the helical models with highest efficiency point at TSR 0.7), instead of instantaneous coefficient of moment, the instantaneous coefficient of power has been calculated. Using the instantaneous coefficient of power sets the values at the same scale and enables easier comparison, as the coefficient of power can be express as coefficient of moment multiplied by the TSR. The variations of the instantaneous coefficients of power for all of the helically twisted models and the baseline model at the TSR values at which they achieve highest efficiency, have been depicted in figure 4.25. It can clearly be seen in figure 4.25 that the cyclic variations of the instantaneous coefficient of power for each of the models are similar with two negative and two positive peaks. For the baseline model (0 revolution of twist) and the helical models with 0.25 and 0.5 revolution of twist the amplitude of the variations of the instantaneous coefficient of power reduces significantly with the increase in the level of twist. For the models with 0.5, 1, 1.5 and 2 revolutions of twist the amplitude of the variations of the instantaneous coefficient of power reduces with a small amount compared to the change of the level of helical twist. For the models with 0.5, 1, 1.5 and 2 revolution of twist the average value of the coefficient of power decreases significantly with the increase in the level of twist. Therefore, it can be summarized that application of helical twist above 0.5 revolution of twist, has a minor positive effect on the amplitude of the instantaneous coefficient of power, but has a significant negative effect on the average coefficient of power generated by the VAWT. This leads to a conclusion that the model with 0.5 revolutions of twist is the optimal configuration as its averaged coefficient of power is higher than the baseline model, and the cyclic variations of both instantaneous coefficient moment and power, have smaller amplitude than the baseline model.
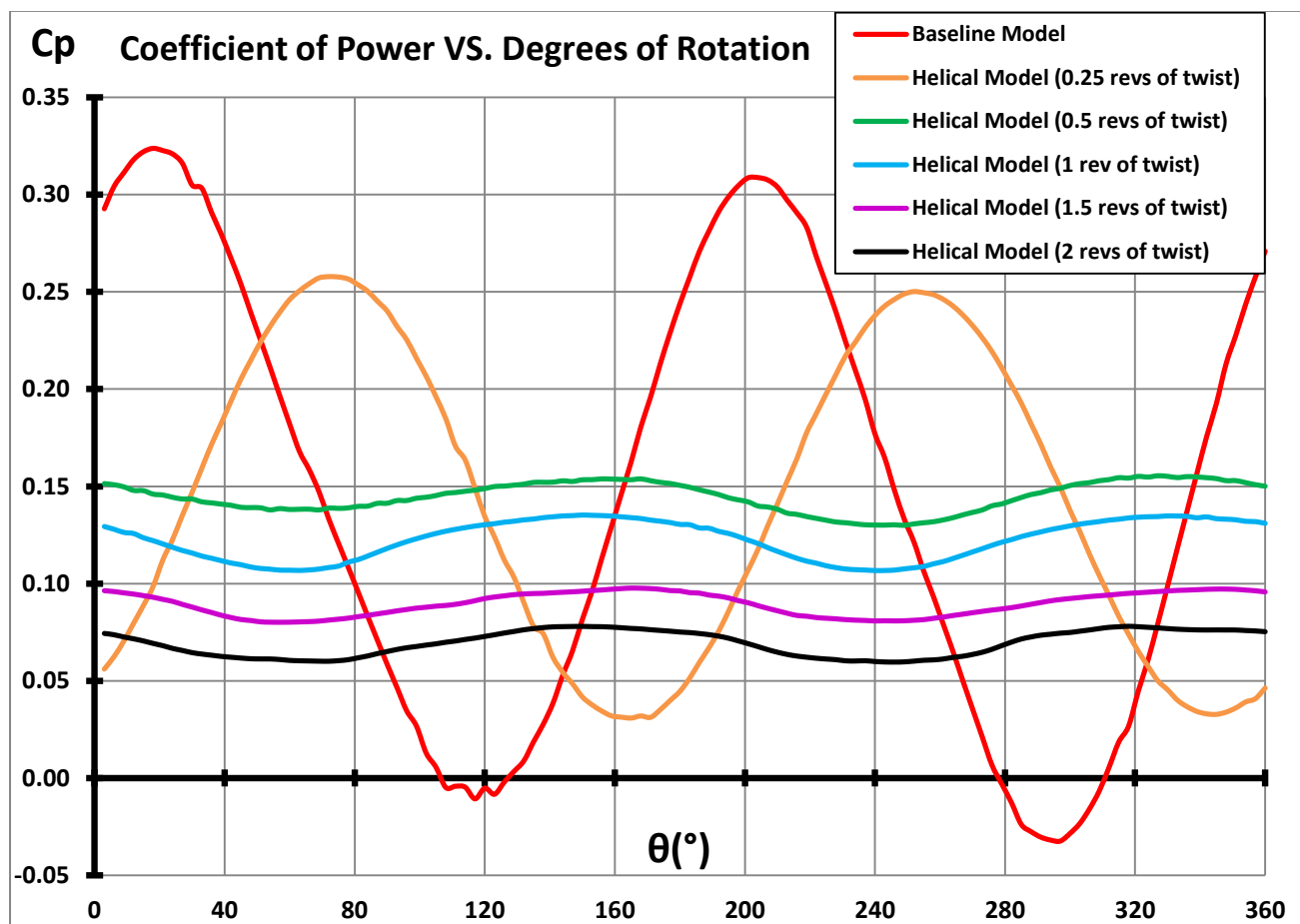
Figure 4.25: Variation of the instantaneous coefficient of power (Cp) over a complete revolution of all of the helically twisted models and the baseline model

The average coefficient of power at each of the numerically examined TSR values for all of the helically twisted models including the baseline model, have been summarized in figure 4.26. It ca clearly be seen in the figure 4.26 that the baseline model and the helically twisted models with 0.25 and 0.5 revolutions of twist have highest efficiency point at TSR 0.7, while the models with 1, 1.5 and 2 revolutions of twist have highest efficiency point at TSR 0.5. It can also be noticed that the model with 0.5 revolutions of twist has the highest coefficient of power followed by the model with 0.25 revolutions of twist than the baseline model.
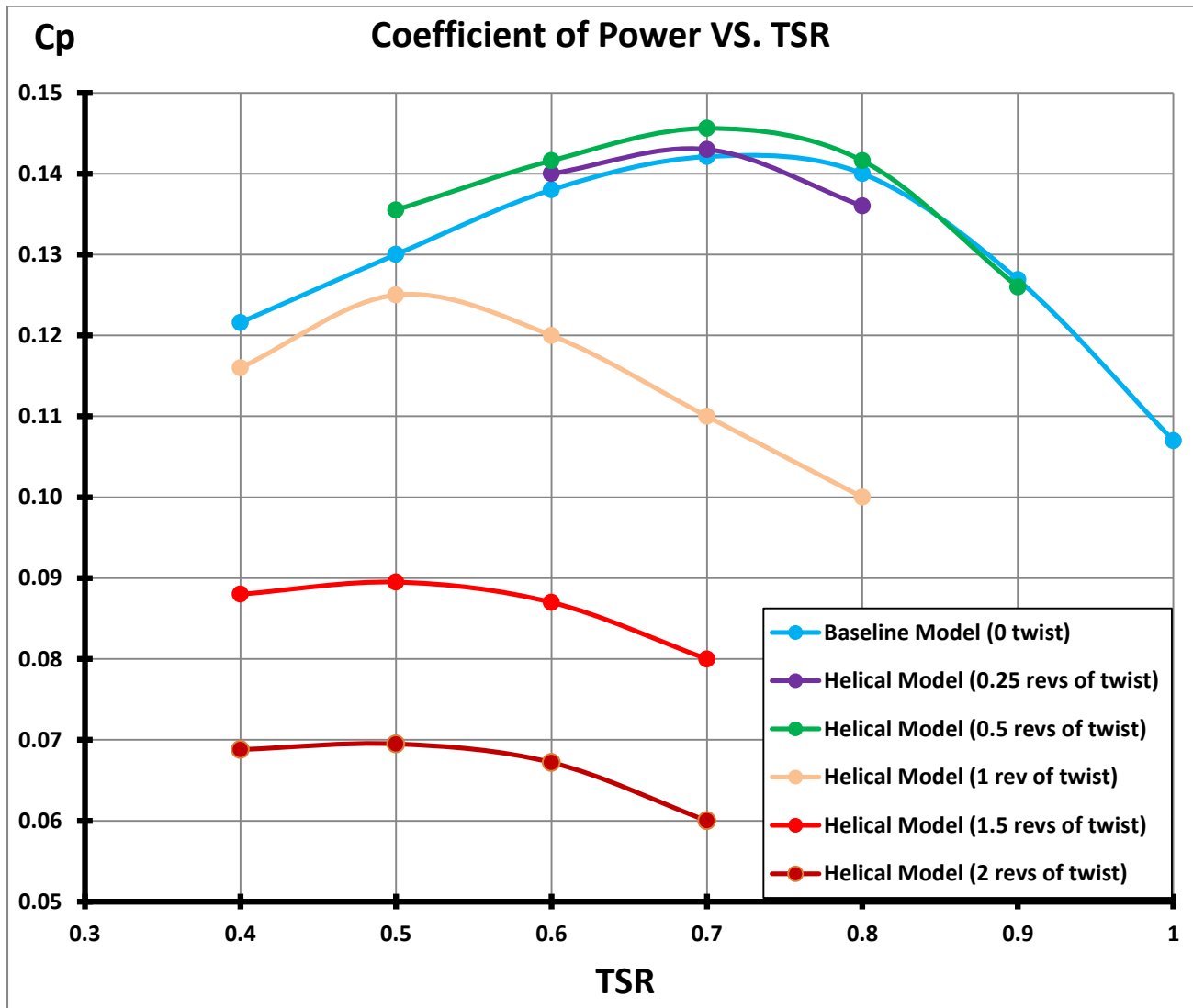
Figure 4.26: Average coefficient of power (Cp) against tip speed ratio (TSR) for all of the helically twisted models and the baseline model

Based on the detailed qualitative and quantitative analysis the helically twisted VAWT with 0.5 revolutions of twist has been established to be the optimal design configuration, as it has the highest efficiency and a small amplitude of the torque variation. Therefore, in the next section the complete performance spectrum and the accelerating behaviour (start-up process) of the optimal design has been critically analysed using the advanced CFD technique dynamic mesh.

Flow Diagnostics and Optimal Design of Vertical Axis Wind Turbines for Urban Environments
By Martin Zahariev, School of Computing and Engineering, University of Huddersfield, UK (2016)

76

4.8 Critical Flow Field analysis using Dynamic Mesh Technique

The sliding mesh technique used to analyse the performance of the helically twisted VAWT assumes that the VAWT is operating at constant operating point. Hence, it cannot predict the complete performance spectrum of the VAWT, which includes the start-up process where the VAWT is accelerating. Therefore, in the present study, the helical VAWT with 0.5 revolutions of twist has been considered for generating its complete performance spectrum. The advanced CFD technique dynamic mesh has been used for this purpose.

The numerical analysis using the dynamic mesh technique has achieved steady state of operation in around 26 seconds of VAWT operation. At steady operating point, the torque values start to approach zero. This gives an operating range from 0 to 17.5m/s, which corresponds to TSR ranging from 0 to 0.96. This also confirms the choice of TSR range selected for analysis in the present study i.e. 0.4 to 1. The changes to the TSR with respect to time can be seen in figure 4.27, where it can clearly be seen that the TSR changes rapidly at the beginning of the simulation when the VAWT is accelerating. The TSR variations at around 15 seconds of operation become almost steady with value of 0.96.
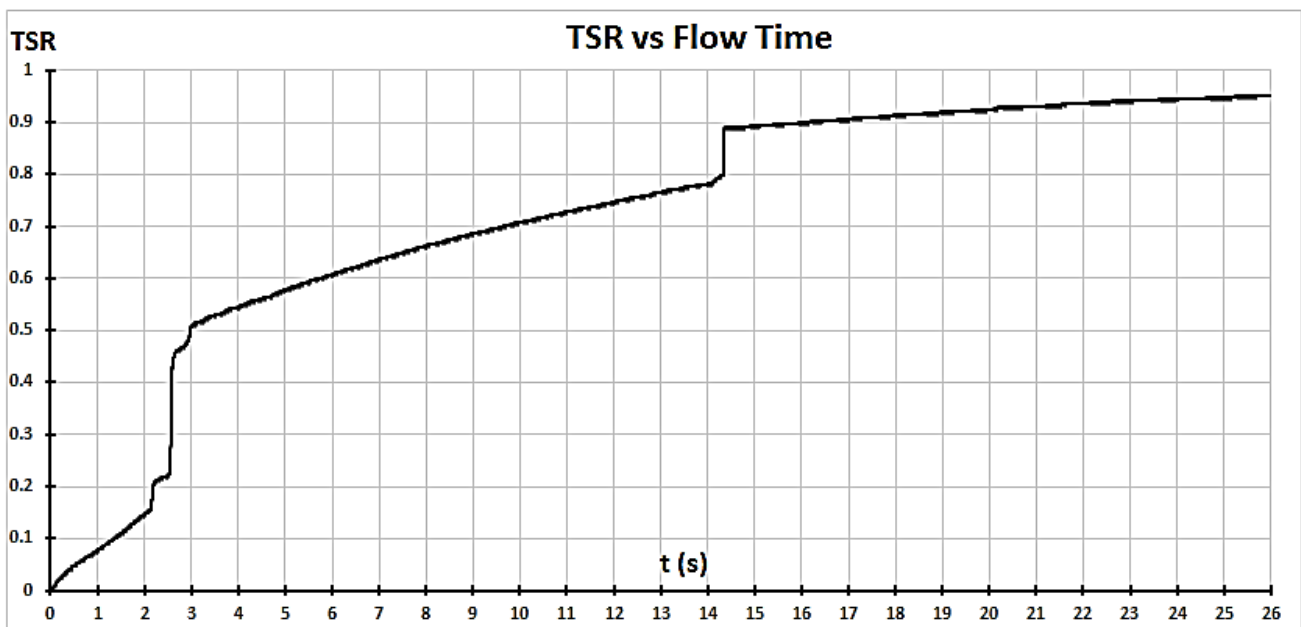
Figure 4.27: Variation of tip speed ratio with respect to operational time.

In figure 4.29 (a), it can clearly be seen that the torque variations start to approach zero at operational time of 26.2 seconds, and at that time, the variations of angular acceleration are very small indicating that the helical VAWT has achieved steady state of operation. In figure 4.29 (b), it can be noticed that the 26.2 seconds of operational time translates into 19800° of rotation. The 19800° of rotation result in 55 complete revolutions of the VAWT, based on 360° per revolution. Hence, 55 complete revolutions are required until the acceleration starts to approach zero, and the steady state of operation is reached. In figure 4.29 (a) and (b), it can clearly be observed that the torque values are not always converged especially in the beginning of the numerical analysis. It can also be noticed that the torque becomes irregular at places well towards the end of the numerical analysis. These irregularities towards the end of the numerical analysis can be attributed to the fact that the dynamic mesh technique is moving the mesh from time step to time step, based on the acceleration values calculated within the solver. This movement of the mesh eventually distorts the local mesh cells and causes the mesh quality check to fail, which starts the pre-set automatic mesh repair function.

Once the pre-set automatic mesh repair function finishes the newly made mesh meets the pre-set mesh quality criteria, and then the solver can continue to move the mesh to the next position. However, when the solver makes a complete revolution, it does not take the original mesh and start the new revolution, but rather continues to move the repaired mesh and further repairs it when necessary. This continues repairs to the mesh results in accumulation of errors in repetitive motion problems such as rotation. The accumulation of errors, due to continues mesh repairs, makes the results towards the end of the numerical analysis less representative and causes the torque to get out of convergence, for brief periods, towards the end of the numerical analysis.
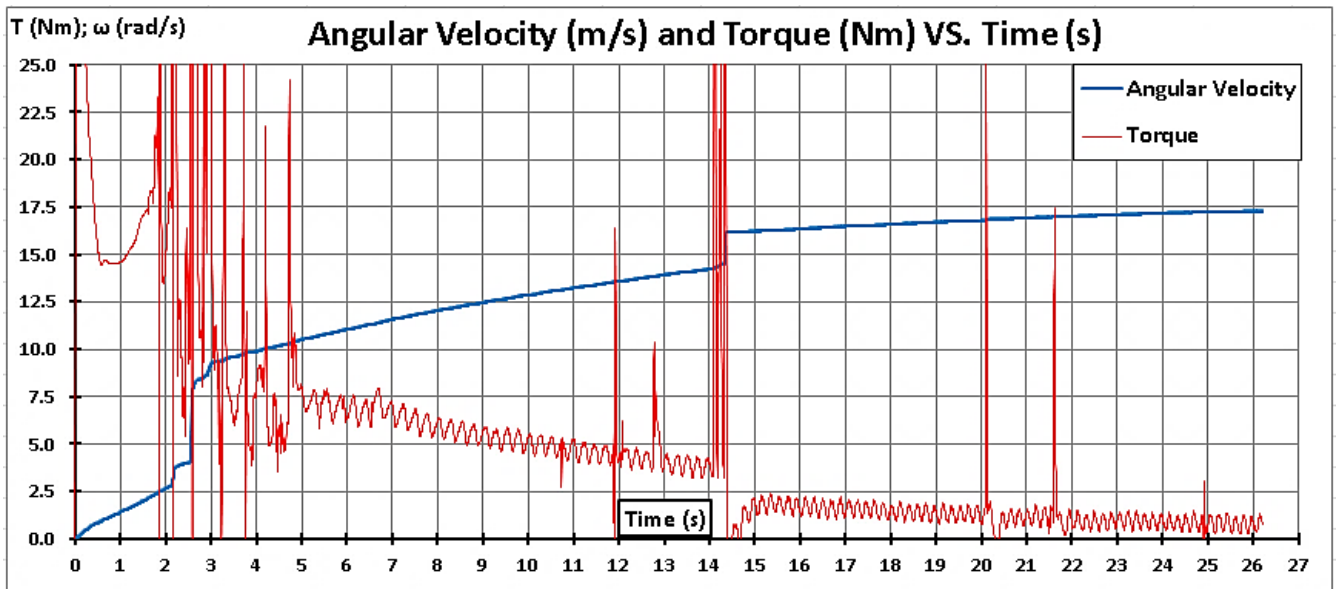
(a)
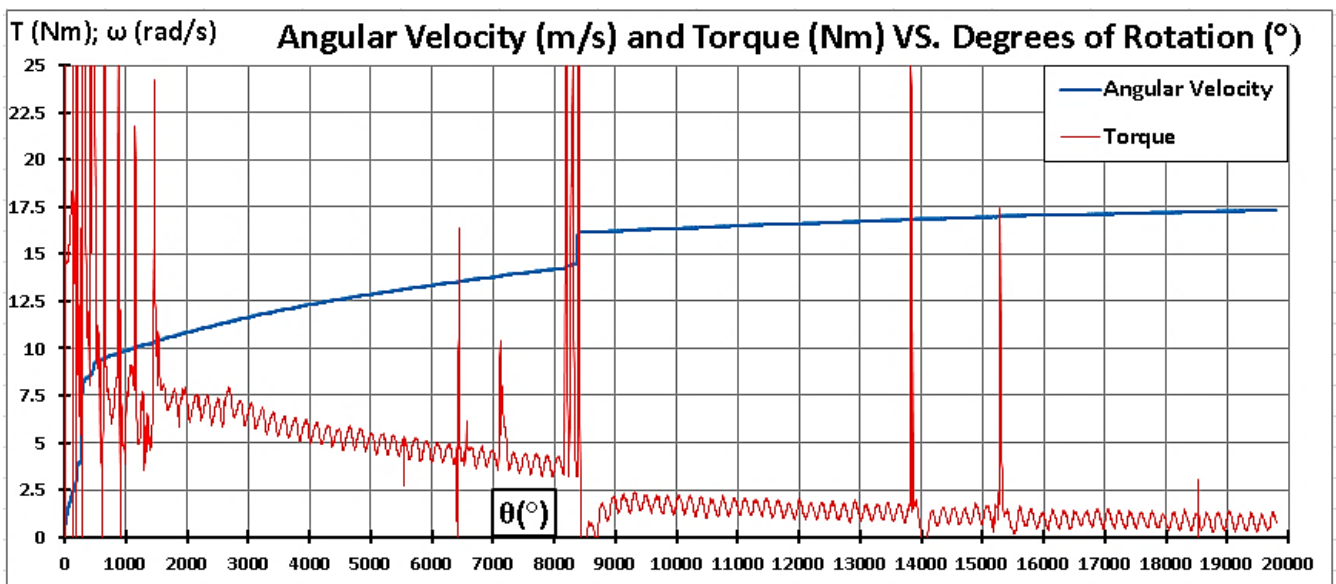
(b)

Figure 4.28: Variation of instantaneous torque and angular velocity with respect to (a) time (s) (b) degrees of rotation (°).

Flow Diagnostics and Optimal Design of Vertical Axis Wind Turbines for Urban Environments
By Martin Zahariev, School of Computing and Engineering, University of Huddersfield, UK (2016)

78

The nature of the dynamic mesh technique is such that it is starts at 0 rad/s angular velocity and increases to the maximum (17.5rad/s). Hence, the instantaneous torque is at a different TSR value at each individual time step. This indicates that the average torque per complete revolution is at different TSR values throughout that revolution, where the torque obtained using the sliding mesh technique is at constant TSR during the entire revolution. The torque obtained using the sliding mesh technique varies based on the position of the blades during an entire revolution at a constant TSR value. Therefore, the minimum and maximum torque values, achieved during an entire revolution of the VAWT using the sliding mesh technique, have been selected as the torque range of the VAWT at that TSR value. The instantaneous torque obtained using the dynamic mesh technique, at that exact TSR value, has been extracted and compared against the torque range obtained using the sliding mesh technique. An example at TSR 0.6 is shown below.

Sliding mesh numerical results

- Angular Velocity = 10.91 rad/s (TSR = 0.6)

- Minimum torque during an entire revolution = 7.73 Nm

- Maximum torque during an entire revolution = 10.41 Nm

- Torque range at TSR 0.6 = 7.73 to 10.41 Nm

Dynamic mesh numerical results

- Angular velocity = 10.93 rad/s (TSR =0.6)

- Instantaneous Torque = 7.91 Nm

The instantaneous torque of 7.91Nm, obtained using the dynamic mesh technique, is within the torque range obtained using the sliding mesh technique. This indicates that the dynamic mesh technique is as accurate as the sliding mesh technique. The same sort of comparisons is not possible at very low TSR values, as the torque of the dynamic mesh numerical analysis at that stage, is not yet converged. Also at some of the very high TSR values the instantaneous torque values, obtained using the dynamic mesh technique, are also not comparable. The values are not comparable, because the torque is getting out of convergence at some parts of the numerical analysis, due to the accumulation of errors caused by the repeated re-meshing. In general, the angular velocity and torque values obtained using the dynamic mesh technique are similar to the values obtained using the sliding mesh technique. The notable difference is that the dynamic mesh technique also provides data on the star-up process and allows analysis of the complete performance spectrum to be carried out.

In figure 4.29, the angular acceleration has been presented with respect to operational time, to emphasize on the acceleration behaviour of the helical VAWT. The results presented in figure 4.29 have been plotted using a 3rd order polynomial equation in order for better visualization of the acceleration of the VAWT, with respect to time. In figure 4.29, it can clearly be seen that the acceleration is higher at the beginning of the numerical analysis and then it reduces as the variation between the results towards the end of the numerical analysis are getting smaller. It can also be observed that the angular acceleration reduces around 10s of operational time, which is where the VAWT reaches high efficiency at the optimal TSR value. This indicates that the acceleration of the VAWT remains high until the optimal operating point is reached, which is also indicative of the self-starting ability the helical VAWT.
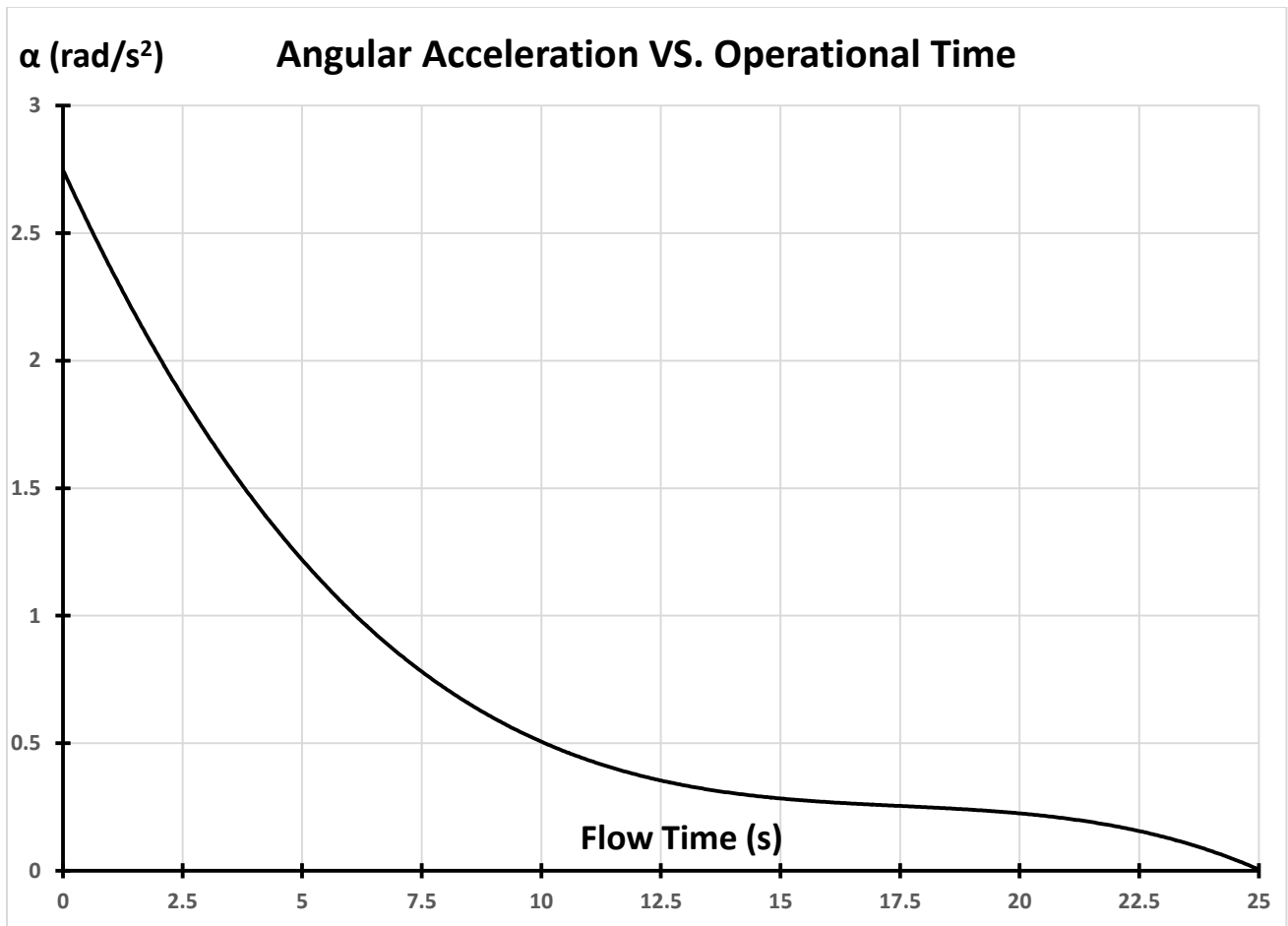
Figure 4.29: Variation of angular acceleration with respect to operational time

The variation of the instantaneous coefficient of power, with respect to operational time, has been depicted in figure 4.30, using a polynomial equation. In figure 4.30, it can clearly be seen that the maximum instantaneous coefficient of power achieved by the VAWT is 0.145. It can also be noticed that he maximum value of instantaneous coefficient of power is achieved around flow time of 10s, which is where the TSR value of the VAWT is equal to 0.7. This confirms the results of the sliding mesh technique, where the maximum coefficient of power is 0.1456 and it is obtained at the same TSR value of 0.7.

Flow Diagnostics and Optimal Design of Vertical Axis Wind Turbines for Urban Environments
By Martin Zahariev, School of Computing and Engineering, University of Huddersfield, UK (2016)

80
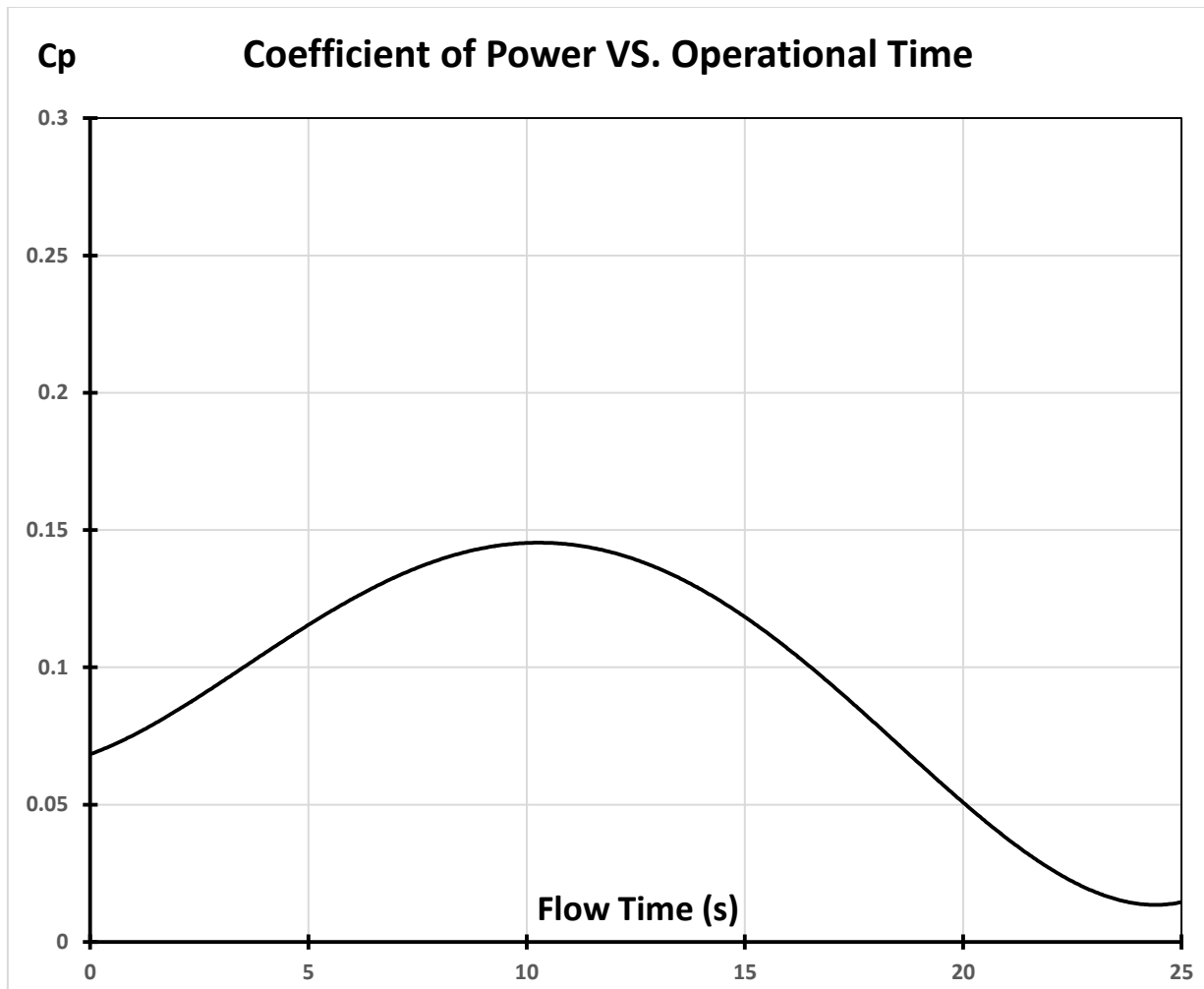
Figure 4.30: Variation of the instantaneous coefficient of power with respect to operational time

It can be summarized that the dynamic mesh technique predicts the complete performance spectrum of the helical VAWT with 0.5 revolutions of twist. It has been establish that the dynamic mesh numerical analysis allows for the performance of the VAWT to be accurately predicted at different points of the performance spectrum. The dynamic mesh technique also allows for the analysis of the start-up process to be carried out, where it has been found that the acceleration is very high at the beginning of the numerical analysis which confirms the self-starting ability of the VAWT. The dynamic mesh technique also allows for the instantaneous coefficient of power to be established, with respect to time, which provides data for the coefficient of power at different TSR values. Hence, allows for the maximum coefficient of power and the optimal TSR value to be determined. It has also been established that the maximum coefficient of power (0.145) and the optimal TSR value (0.7), obtained using the dynamic mesh technique, are in close agreement with the corresponding values, obtained using the sliding mesh technique.

4.9   Summary of the work

The guide vanes models have been numerically tested at various inclined angles and thicknesses. It has been shown that the addition of internal guide vanes increases the time and distance the air flow takes to pass through the VAWT, which has negative effect on the VAWTs performance. Various tapered blades models have been numerically tested showing that 70% of the VAWT is working at lower aspect ratio (at lower efficiency), while the remaining 30% of the VAWT is working at higher aspect ratio (at higher efficiency). Once combined it has been shown that the 30% working at higher efficiency cannot offset the 70% working at lower efficiency and the overall efficiency of the entire VAWT is lower, indicating that applying tapering has negative effect on the performance of the VAWT. The helically twisted models with various level of helical twist applied to the blades have been numerically tested. It has been shown that only a moderate level of helical twist (0.5 revolutions of twist) has a beneficial effect on the performance of the VAWT. Furthermore, it has been established that by applying helical twist, the torque variations of the VAWT are significantly reduced.

In this chapter, as the sliding mesh technique assumes that the VAWT is being constantly operating at particular operation point as previously discussed in detail, the advanced CFD technique dynamic mesh has been employed. The dynamic mesh technique has been used to determine the complete performance spectrum of the helically twisted VAWT with 0.5 revolutions of twist and analyse its accelerating behaviour. It has been established that the dynamic mesh numerical analysis allows for the entire performance spectrum of the VAWT to be determined and for the performance of the VAWT to be accurately predicted at different points of its performance spectrum. The dynamic mesh technique has also being used to analyse the start-up process of the helical VAWT, where it has been found that the acceleration is very high at the beginning of the numerical analysis which confirms the self-starting ability of the helical VAWT. The dynamic mesh technique has also being used to determine the instantaneous coefficient of power and the TSR values, with respect to time. This allows for the maximum coefficient of power and the optimal TSR value to be established.

In the next chapter, an in-house CFD package for aerodynamic performance analysis of the helically twisted VAWT with 0.5 revolutions of twist has been developed, based on an existing open source CFD code. The in-house built CFD package has been used to conduct critical flow field analysis of the VAWT and the predicted flow fields and performance data have been compared to commercial CFD solver, where the accuracy and the robustness of the in-house built CFD package have been established.

Chapter 5
Development of a Design Analysis package for Vertical Axis Wind Turbines

In this chapter, an in-house built CFD package for aerodynamic design analysis of VAWTs has been developed, based on already existing open source CFD solver. The in-house built CFD package has been used to conduct critical flow field analysis of VAWTs. The predicted flow fields and performance of the VAWTs, predicted by both commercial and the in-house developed CFD packages, have been critically analysed and found to be in close agreement with each other.

5.1 Development of an In-House CFD package

In this section, an in-house CFD package has been developed, based on existing open source CFD solver for aerodynamic design analysis of the optimal VAWT (from chapter 4). The in-house built CFD package has been used to conduct critical flow field analysis of the helically twisted VAWT with 0.5 revolutions of twist. The predicted flow fields and performance parameters of the VAWT, obtained by using the in-house built CFD package, have been compared against corresponding results obtained using commercial CFD solver. The results obtained using the in-house built CFD package have been found to be in close agreement with the one obtained using commercial CFD solver. The reason for developing an in-house CFD package is the cost of commercial CFD software, which prevents small to medium sized enterprises (SMEs) to take advantage of the advancing CFD methods. This results in a need for an alternative package that provides accurate results at lower cost. Such an alternative are the open source CFD solvers, however their usage is mostly TUI based and extremely complex. Hence in the present study, an in-house built CFD package has been specifically developed for aerodynamic design analysis of VAWTs , based on open source CFD solvers.

The in-house CFD package has been developed by creating files associated with aerodynamic analysis of VAWTs. The description of these files is presented below:

- Domain setup file, where the domain size and location have been specified and type of the domain's individual faces have been set.
- Mesh setup file, where the VAWT's geometry CAD files have been added to the domain and the associated mesh sizes and refinement levels have been set.
- Transport file, where the properties of the fluid and the transport method are specified.
- Turbulence properties file, where the turbulence model and parameters have been specified.
- Velocity file, where the inlet velocity and velocity field have been specified and the blades have been set as moving walls to capture the rotational behaviour of the VAWT.
- Pressure file, where the atmospheric condition have been set and pressure field is specified.
- Turbulence files, where the turbulence kinetic energy and dissipation rate are specified.
- Control file, where the numerical models parameters are set, such as start time, time step size, solver type, monitors etc.
- Solver setup files, where the types of solvers for the individual residuals are specified and the associated residual controls are set together with the calculating schemes.
- Mesh control file, where the application of the sliding mesh technique has been specified, by selecting the rotational domain, the origin and axis of rotation, angular speed and motion type

In figure 5.1, the domain setup file developed for the in-house CFD package has been shown, depicting the size and location of the faces of the domain. The domain has been created with the same size as used in case of the commercial CFD solver. The inlet and outlet faces have been set as patch type, so that boundary conditions, such as velocity, pressure and turbulence can be applied to them. The other four faces of the domain have been set as wall type, as they will not be used as inlets or outlets, therefore wall functions must be applied to them. The number of cells across x, y and z dimensions of the rectangular domain have also been set in this file, so that they can be used later by the mesh setup file as base mesh size, to which refinements has been applied where required.

```
FoamFile
{
    format      ascii;
    class       dictionary;
    location    "constant/polyMesh";
    object      blockMeshDict;
}
// * * * * * * * * * * * * * * * * * * * * * * * * * * * * * * * * * * //
convertToMeters 1;
vertices
(
    ( -8.8 -8.8 -6.35)
    ( 8.8 -8.8 -6.35)
    ( 8.8 8.8 -6.35)
    ( -8.8 8.8 -6.35)
    ( -8.8 -8.8 6.35)
    ( 8.8 -8.8 6.35)
    ( 8.8 8.8 6.35)
    ( -8.8 8.8 6.35)
);
blocks
(
    hex (0 1 2 3 4 5 6 7) (120 120 85 ) simpleGrading (1 1 1)
);
edges ( );
boundary
(
    inlet
    {
        type patch;
        faces
        (
            (0 4 7 3)
        );
    }
    outlet
    {
        type patch;
        faces
        (
            (1 2 6 5)
        );
    }
    wall1
    {
        type wall;
        faces
        (
            (0 1 5 4)
        );
    }
    wall2
    {
        type wall;
        faces
        (
            (3 7 6 2)
        );
    }
```

Flow Diagnostics and Optimal Design of Vertical Axis Wind Turbines for Urban Environments
By Martin Zahariev, School of Computing and Engineering, University of Huddersfield, UK (2016)

85

```
    wall3
    {
        type wall;
        faces
        (
            (0 3 2 1)
        );
    }
    wall4
    {
        type wall;
        faces
        (
            (4 5 6 7)
        );
    }
);
mergePatchPairs ( );
// ********************************************************************* //
```

Figure 5.1: Domain setup file showing the location and size of the domain

In figure 5.2, the mesh setup file developed for the in-house CFD packages has been shown. The refinement of the mesh is included in this file, indicating the mesh quality controls. The mesh setup file shows what type of surfaces (triSurfaceMesh) are created out of the STL CAD files, and their associated names.

In figure 5.2, the castellated mesh controls are first shown, where the location of the mesh, the maximum number of cells, the number of cells between refinement levels, and the refinement levels of the VAWT's surfaces and the interfaces are set. The values are selected as such that the final mesh will have similar number of elements as the mesh used for the commercial CFD solver (approx. 2million), and the refinements are specified to the same zones (blades and interfaces) as for the commercial CFD solver.

The next stage of the meshing process, depicted in the mesh setup file in figure 5.2, shows the snap controls. The snap controls are controlling the snapping process, which removes the jagged edges of the castellated mesh by moving the cell vertices onto the STL surface geometry. The process then continues and solves the relaxation of the internal mesh equations, after which detects the vertices that cause the mesh quality to be violated. Once the vertices of the failed elements have been found, the same process starts all over again until the snapped mesh meets the quality criteria. The snap controls define the tolerances and the maximum number of iterations for the various snapping and relaxation equations, all of which have been selected as such that the mesh meets the same quality criteria as the mesh created for the commercial CFD solver.

The next stage of the meshing process, depicted in the mesh setup file in figure 5.2, shows the mesh quality controls. The mesh controls have been selected as such to generate a mesh that meets the aspect ratio, Jacobian ratio, skewness and the orthogonal quality of the mesh generated for the commercial CFD solver.

Flow Diagnostics and Optimal Design of Vertical Axis Wind Turbines for Urban Environments
By Martin Zahariev, School of Computing and Engineering, University of Huddersfield, UK (2016)

86

```
FoamFile
{
    format      ascii;
    class       dictionary;
    object      snappyHexMeshDict;
}
// * * * * * * * * * * * * * * * * * * * * * * * * * * * * * * * * * * //
    castellatedMesh true;
    snap true;

    geometry
    {
        Blades.stl
        {
            type triSurfaceMesh;
            name Blades;
        }
        EndPlateBOTTOM.stl
        {
            type triSurfaceMesh;
            name EndPlateBOTTOM;
        }
        EndPlateTOP.stl
        {
            type triSurfaceMesh;
            name EndPlateTOP;
        }
        Interface_surface.stl
        {
            type triSurfaceMesh;
            name Interface_surface;
        }
    }

    castellatedMeshControls
    {
        refinementSurfaces
        {
            Blades
            {
                level ( 3 3 );
            }
            EndPlateBOTTOM
            {
                level ( 3 3 );
            }
            EndPlateTOP
            {
                level ( 3 3 );
            }
            Interface_surface
            {
                level ( 4 4 );
            }
        }
        locationInMesh ( 0.61 -2.58 -0.53 );
        maxLocalCells 300000;
        maxGlobalCells 6000000;
        minRefinementCells 0;
        nCellsBetweenLevels 1;
        resolveFeatureAngle 30;
```

Flow Diagnostics and Optimal Design of Vertical Axis Wind Turbines for Urban Environments
By Martin Zahariev, School of Computing and Engineering, University of Huddersfield, UK (2016)

87

```
        allowFreeStandingZoneFaces true;
        planarAngle 30;
        maxLoadUnbalance 0.10;
    }

    snapControls
    {
        nSolveIter 30;
        nSmoothPatch 3;
        tolerance 2.0;
        nRelaxIter 5;
        nFeatureSnapIter 10;
        implicitFeatureSnap false;
        explicitFeatureSnap true;
        multiRegionFeatureSnap false;
    }

    meshQualityControls
    {
        maxNonOrtho 65;
        maxBoundarySkewness 20;
        maxInternalSkewness 4;
        maxConcave 80;
        minFlatness 0.5;
        minVol 1.00E-13;
        minTetQuality 1e-15;
        minArea -1;
        minTwist 0.02;
        minDeterminant 0.001;
        minFaceWeight 0.05;
        minVolRatio 0.01;
        minTriangleTwist -1;
        nSmoothScale 4;
        errorReduction 0.75;
    }

    debug 0;
    mergeTolerance 1E-6;
    autoBlockMesh false;

// ********************************************************************** //
```

Figure 5.2: Mesh setup file showing the mesh size, location, and refinement levels

In figure 5.3, the properties of the fluid used by the in-house built CFD package for the numerical analysis of the VAWT are specified. The transport model is selected as Newtonian, which assumes that the kinematic viscosity of the fluid is constant, and in the case of incompressible numerical analysis, this assumption is correct for predicting the flow behavior. The properties of the fluid are also specified in this file, for the purpose of creating a fluid zone consisting of air. The physical properties of air such as density, dynamic viscosity, specific heat, expansion coefficient, prandtl's number, atmospheric pressure etc. are specified in this file to create a fluid zone that corresponds to air at atmospheric conditions.

Flow Diagnostics and Optimal Design of Vertical Axis Wind Turbines for Urban Environments
By Martin Zahariev, School of Computing and Engineering, University of Huddersfield, UK (2016)

88

```
FoamFile
{
    format      ascii;
    class       dictionary;
    location    "constant";
    object      transportProperties;
}
// * * * * * * * * * * * * * * * * * * * * * * * * * * * * * * * * * * * //

materialName air;

transportModel Newtonian;

NewtonianCoeffs
{
}
    rho rho [1 -3 0 0 0 0 0 ] 1.205;

    mu mu [1 -1 -1 0 0 0 0 ] 1.9137E-5;

    nu nu [0 2 -1 0 0 0 0 ] 1.5881327800829875E-5;

    Cp Cp [0 2 -2 -1 0 0 0 ] 1006.0;

    Cp0 1006.0;

    Prt Prt [0 0 0 0 0 0 0 ] 0.85;

    Pr Pr [0 0 0 0 0 0 0 ] 0.9;

    lambda lambda [1 1 -3 -1 0 0 0 ] 0.024;

    pRef pRef [1 -1 -2 0 0 0 0 ] 101325.0;

    beta beta [0 0 0 -1 0 0 0 ] 0.00333;

    TRef TRef [0 0 0 1 0 0 0 ] 300.0;

// ******************************************************************* //
```

Figure 5.3: Transport file showing the properties of air and the transport model.

In figure 5.4, the turbulence properties files developed for the in-house CFD package has been shown, depicting the type of turbulence models to be used, and specifying the exact model of that type of turbulence models. The type of turbulence models to be used for the in-house built CFD package has been selected as Reynolds-averaged simulation (RAS), which contains the exact turbulence model used for the commercial CFD solver (k-epsilon realizable). In figure 5.4, it has been shown that the RAS models has been specified as realizableKE, which corresponds to the k-epsilon realizable model used for the numerical analysis carrier our with the commercial CFD solver. The turbulence model coefficients have also been set to the same values as used for the commercial CFD solver.

Flow Diagnostics and Optimal Design of Vertical Axis Wind Turbines for Urban Environments
By Martin Zahariev, School of Computing and Engineering, University of Huddersfield, UK (2016)

89

```
FoamFile
{
    format      ascii;
    class       dictionary;
    location    "constant";
    object      turbulenceProperties;
}
// * * * * * * * * * * * * * * * * * * * * * * * * * * * * * * * * * * //

simulationType      RAS;

RAS
{
    RASModel realizableKE;
    turbulence on;
    printCoeffs on;
    realizableKECoeffs
    {
        label "Realizable k-\u03B5";
        fieldMaps
        {
            k k;
            epsilon epsilon;
            nut nut;
        }
        Cmu 0.09;
        A0 4.04;
        C1 1.44;
        C2 1.9;
        alphak 1.0;
        alphaEps 1.2;
        alphah 1.0;
    }

}

// ********************************************************************* //
```

Figure 5.4: Turbulence properties file showing the turbulence model and associated coefficients

In figure 5.5, the velocity file developed for the in-house CFD package has been shown, specifying the initial velocity field and each individual face type and associated value. The internal (initial) velocity field has been specified as 8m/s in x-direction, corresponding to the flow velocity. The type of the VAWT's faces has been set as movingWallVelocity, which corrects the flux due to mesh motion so that the total flux is zero and allows for the rotational (moving) effects to be captured. The inlet face type has been selected as fixed value and set at 8m/s, which is the flow velocity of the numerical analysis. The outlet face type has been set to zero gradient, meaning the velocity values form the internal field are set to the face at zero-gradient conditions. The faces of the walls of the domain are set to slip, as this type of boundary condition considers the effect of the shear stress to be zero, which as the numerical analysis is considering open space is correct. The type at the interface surfaces is set as CyclicAMI, which enforces a cyclic condition between the boundaries and the communication between them is performed using an arbitrary mesh interface (AMI).

Flow Diagnostics and Optimal Design of Vertical Axis Wind Turbines for Urban Environments
By Martin Zahariev, School of Computing and Engineering, University of Huddersfield, UK (2016)

90

```
FoamFile
{
    format      ascii;
    class       volVectorField;
    location    "0";
    object      U;
}
// * * * * * * * * * * * * * * * * * * * * * * * * * * * * * * * * * * * //
dimensions [ 0 1 -1 0 0 0 0 ];
internalField uniform (8.0 0.0 0.0);
boundaryField
{
    inlet
    {
        type fixedValue;
        value uniform (8.0 0.0 0.0 );
    }
    outlet
    {
        type zeroGradient;
        value uniform (0 0 0);
    }
    walls
    {
        type slip;
    }
    Blades
    {
        type movingWallVelocity;
        value uniform ( 0 0 0);
    }
    EndPlateBOTTOM
    {
        type movingWallVelocity;
        value uniform ( 0 0 0);
    }
    EndPlateTOP
    {
        type movingWallVelocity;
        value uniform ( 0 0 0);
    }
    Interface_surface_1
    {
        type cyclicAMI;
        value uniform (0 0 0);
    }
    Interface_surfface_2
    {
        type cyclicAMI;
        value uniform (0 0 0);
    }
}
// ********************************************************************** //
```

Figure 5.5: Velocity file showing the initial field value and the individual faces types and values

Flow Diagnostics and Optimal Design of Vertical Axis Wind Turbines for Urban Environments
By Martin Zahariev, School of Computing and Engineering, University of Huddersfield, UK (2016)

91

In figure 5.6, the pressure file developed for the in-house CFD package has been shown, specifying the initial pressure field and each individual face type and associated value. The internal (initial) pressure field has been specified as 0Pa for the use of the in-house built CFD package. The type of the VAWT's faces is set to zero-gradient, meaning the pressure values form the internal field are set to the faces at zero-gradient conditions. The type at the interface surfaces is set as CyclicAMI, which enforces a cyclic condition between the boundaries and the communication between them is performed using an arbitrary mesh interface (AMI). The type at the outlet face is set as fixed value, where pressure of 0Pa is specified as the value, creating atmospheric conditions at the outlet.

```
FoamFile
{
    format      ascii;
    class       volScalarField;
    location    "0";
    object      p;
}
// * * * * * * * * * * * * * * * * * * * * * * * * * * * * * * * * * * * * * //
dimensions [ 0 2 -2 0 0 0 0 ];
internalField uniform 0.0;
boundaryField
{
    inlet
    {
        type zeroGradient;
    }
    outlet
    {
        type fixedValue;
        value uniform 0;
    }
    walls
    {
        type zeroGradient;
    }
    Blades
    {
        type zeroGradient;
    }
    EndPlateBOTTOM
    {
        type zeroGradient;
    }
    EndPlateTOP
    {
        type zeroGradient;
    }
    Interface_surface_1
    {
        type cyclicAMI;
        value uniform 0;
    }
    Interface_surfface_2
    {
        type cyclicAMI;
        value uniform 0;
    }
}
// ********************************************************************* //
```

Figure 5.6: Pressure file showing the initial field value and the individual faces types and values.

In figure 5.7, the turbulence files developed for the in-house built CFD package are shown. As the turbulence model selected for the in-house built CFD package is k-epsilon realizable, there are two files associated with turbulence modelling. The first file (figure 5.7 (a)) is associated with turbulence kinetic energy (k), while the second file (figure 5.7 (b)) is associated with the turbulence dissipation (epsilon (e)), which determines the dissipation rate of the turbulence kinetic energy.

In figure 5.7 (a), the initial turbulence kinetic energy field is set as 0.1, while the values at the inlet and outlet faces are set lower at 0.01 and the values at the VAWT and domain faces are set even lower at 1e-20. The values are set as such in order for the turbulence kinetic energy residuals to converge faster (the values have been obtained experimentally). The wall function at the inlet and outlet faces has been selected as inletOutlet which provides specific inflow value in the case of a return flow. The wall function at the VAWT and the rest of the domain faces has been set as kqRWallFunction in order to emulate the wall function used by the commercial CFD solver, which is beneficial to rotating and high gradient flow problems.

In figure 5.7 (b), the initial turbulence dissipation field is set as 0.001, while the values at the inlet and outlet faces are set higher 0.01 and the values at the VAWT and domain faces are set lower at 1e-7. The values are set as such in order for the turbulence dissipation residuals to converge faster (the values have been obtained experimentally). The wall function at the inlet and outlet faces has been selected as inletOutlet which provides specific inflow value in the case of a return flow. The wall function at the VAWT and the rest of the domain faces has been set as epsilonWallFunction in order to emulate the wall function used by the commercial CFD solver, which is beneficial to rotating and high gradient flow problems.

For both turbulence kinetic energy (figure 5.7 (a)) and turbulence dissipation (figure 5.7 (b)) the type at the interface surfaces has been specified as CyclicAMI, which enforces a cyclic condition between the boundaries and the communication between them is performed using an arbitrary mesh interface (AMI).

```
FoamFile
{;
    format      ascii;
    class       volScalarField;
    location    "0";
    object      k;
}
// * * * * * * * * * * * * * * * * * * * * * * * * * * * * * * * * * * * * * * //
dimensions [ 0 2 -2 0 0 0 0 ];
internalField uniform 0.1;
boundaryField
{
    inlet
    {
        type inletOutlet;
        value uniform 0.1;
        inletValue uniform 0.01;
    }
    outlet
    {
        type inletOutlet;
        value uniform 0.1;
        inletValue uniform 0.01;
    }
```

```
    walls
    {
        type kqRWallFunction;
        value uniform 1e-20;
    }
    }
    Blades
    {
        type kqRWallFunction;
        value uniform 1e-20;
    }
    EndPlateBOTTOM
    {
        type kqRWallFunction;
        value uniform 1e-20;
    }
    EndPlateTOP
    {
        type kqRWallFunction;
        value uniform 1e-20;
    }
    Interface_surface_1
    {
        type cyclicAMI;
        value uniform 0;
    }
    Interface_surface_2
        type cyclicAMI;
        value uniform 0;
    }
}
// ********************************************************************* //
```

(a)

```
FoamFile
{
    format      ascii;
    class       volScalarField;
    location    "0";
    object      epsilon;
}
// * * * * * * * * * * * * * * * * * * * * * * * * * * * * * * * * * * * //
dimensions [ 0 2 -3 0 0 0 0 ];
internalField uniform 0.001;
boundaryField
{
    inlet
    {
        type inletOutlet;
        value uniform 0.01;
        inletValue uniform 0.01;
    }
    outlet
    {
        type inletOutlet;
        value uniform 0.01;
        inletValue uniform 0.01;
    }
    walls
```

Flow Diagnostics and Optimal Design of Vertical Axis Wind Turbines for Urban Environments
By Martin Zahariev, School of Computing and Engineering, University of Huddersfield, UK (2016)

94

```
    {
        type epsilonWallFunction;
        value uniform 1e-7;
    }
    Blades
    {
        type epsilonWallFunction;
        value uniform 1e-7;
    }
    EndPlateBOTTOM
    {
        type epsilonWallFunction;
        value uniform 1e-7;
    }
    EndPlateTOP
    {
        type epsilonWallFunction;
        value uniform 1e-7;
    }
    Interface_surface_1
    {
        type cyclicAMI;
        value uniform 0;
    }
    Interface_surface_2
    {
        type cyclicAMI;
        value uniform 0;
    }
}
// ************************************************************************* //
```

(b)

Figure 5.7: Turbulence files showing the initial field values and the individual faces types and values. (a) Turbulence kinetic energy file; (b) Turbulence dissipation file

In figure 5.8, the control file developed for the in-house CFD package has been shown, depicting the type of solver, the start time, the end time, the time step size, the write interval, the file format, the numerical precision of the file and the monitor setup. The control file governs the numerical analysis while the software is running. It is used to start the solver, record relevant data while the numerical analysis is running and when the solution is converged it stops the solver. The type of solver to be started, the start and end times and the time step size have been set so that the in-house built CFD package runs similar numerical analysis as the numerical analysis carried out using the commercial CFD solver. The write interval is used to set flow time at which to record the flow data and it has been set to record the data at pre-determined intervals, so that flow data is recorder at the right angular positions for comparisons purposes with the commercial CFD solver. The format of the files to be written and the time precision have been set to such values to ensure that the data is easy to read and accurate. As the main global parameter of the VAWT (obtained through the use of numerical analysis) is the torque, a monitor has been setup to record the forces and moments acting on the blades of the VAWT at each time step.

Flow Diagnostics and Optimal Design of Vertical Axis Wind Turbines for Urban Environments
By Martin Zahariev, School of Computing and Engineering, University of Huddersfield, UK (2016)

95

```
FoamFile
{
    format      ascii;
    class       dictionary;
    location    "system";
    object      controlDict;
}
// * * * * * * * * * * * * * * * * * * * * * * * * * * * * * * * * * * * * //
application pimpleDyMFoam;
startFrom startTime;
startTime 0;
stopAt endTime;
endTime 0.493678872;
deltaT 6.856651E-4;
writeControl runTime;
writeInterval 0.1;
purgeWrite 0;
writeFormat ascii;
writePrecision 10;
writeCompression uncompressed;
timeFormat general;
timePrecision 6;
runTimeModifiable true;
adjustTimeStep no;
maxCo 1.0;
maxDeltaT 1.0;

functions
(
    forces
    {
        type forces;
        functionObjectLibs ("libforces.so");
        log true;
        pName p;
        UName U;
        rhoName rhoInf;
        rhoInf 1.2;
        pRef 0;
        CofR (0 0 0);
        patches (Blades);
    }
);
// ********************************************************************* //
```

Figure 5.8: Control file showing the start time, end time, time step size, monitor setup, etc.

In figure 5.9, parts of the solver setup files, developed for the in-house built CFD package, are shown, as the complete files themselves are very lengthy and repetitive. The solver setup files govern the calculation schemes and are set at 2nd order accuracy corresponding to the schemes set for the commercial CFD solver. The solver setup files also govern the solver type and setting, the residuals controls and the relaxation factors, which have been shown in figure 5.9 (a) and (b). The solver type has been set as PIMPLE, which is a transient solver based on the SIMPLE algorithm (semi-implicit method for pressure-linked equations) in combination with the PISO algorithm (pressure-implicit split-operator). The residual controls for all of the residuals have been set to 0.0001 to ensure proper convergence. The relaxation factors for both fields and equations have been set to values similar to the ones used for the commercial CFD solver, in order to speed up the convergence process.

Flow Diagnostics and Optimal Design of Vertical Axis Wind Turbines for Urban Environments
By Martin Zahariev, School of Computing and Engineering, University of Huddersfield, UK (2016)

96

```
PIMPLE
{
        momentumPredictor yes;
        nOuterCorrectors 1;
        nCorrectors 2;
        nNonOrthogonalCorrectors 0;
        pRefCell 0;
        pRefValue 0;
        residualControl
        {
            U
            {
                relTol 0;
                tolerance 1.0E-4;
            }
            k
            {
                relTol 0;
                tolerance 1.0E-4;
            }
            epsilon
            {
                relTol 0;
                tolerance 1.0E-4;
            }
            omega
            {
                relTol 0;
                tolerance 0.0001;
            }
            nuTilda
            {
                relTol 0;
                tolerance 0.0001;
            }
            T
            {
                relTol 0;
                tolerance 0.0001;
            }

            p_rgh
            {
                relTol 0;
                tolerance 0.0001;
            }

            p
            {
                relTol 0;
                tolerance 1.0E-4;
            }

            "alpha.*"
            {
                relTol 0;
                tolerance 0.0001;
            }
        }
}
```

(a)

Flow Diagnostics and Optimal Design of Vertical Axis Wind Turbines for Urban Environments
By Martin Zahariev, School of Computing and Engineering, University of Huddersfield, UK (2016)

97

```
relaxationFactors
{
        fields
        {
            p 0.3;
            p_rgh 0.3;
            rho 0.5;
        }
        equations
        {
            epsilon 0.7;
            f 0.7;
            h 0.7;
            k 0.5;
            kl 0.7;
            kt 0.7;
            nuTilda 0.7;
            omega 0.5;
            q 0.5;
            R 0.5;
            T 0.5;
            U 0.7;
            v2 0.7;
            zeta 0.7;
            "alpha.*" 0.5;
            epsilonFinal 0.7;
            fFinal 0.7;
            hFinal 0.7;
            kFinal 0.5;
            klFinal 0.7;
            ktFinal 0.7;
            nuTildaFinal 0.7;
            omegaFinal 0.5;
            qFinal 0.5;
            RFinal 0.5;
            TFinal 0.5;
            UFinal 0.7;
            v2Final 0.5;
            zetaFinal 0.7;
            "alpha.*Final" 0.7;
        }
}
```

(b)

Figure 5.9: Parts of the solver setup files; (a) Showing the solver type, setting and residual controls; (b) Showing the relaxation factors of the fields and equations.

In figure 5.10, the mesh control file showing the application of the sliding mesh technique for the in-house built CFD package has been presented, as written in an open source CFD code. In figure 5.10, it can be seen that the type of body to be moved has been set as solid body, and then the cell zone of the rotor have been selected, so that the rotational domain is the one to move. It can also be seen that the type of motion has been set as rotating motion, as this is the exact type of motion of the VAWT in reality. It can also be seen in figure 5.10, how the origin and axis of rotation are set, and the angular acceleration is specified as 12.73 rad/s corresponding to TSR 0.7 for the helically twisted model with 0.5 revolutions of twist.

```
FoamFile
{
    format      ascii;
    class       dictionary;
    location    "constant";
    object      dynamicMeshDict;
}
// * * * * * * * * * * * * * * * * * * * * * * * * * * * * * * * * * * * * * //
dynamicFvMesh   solidBodyMotionFvMesh;

motionSolverLibs ( "libfvMotionSolvers.so" );

solidBodyMotionFvMeshCoeffs
{
    cellZone        Rotor;
    solidBodyMotionFunction  rotatingMotion;
    rotatingMotionCoeffs
    {
        origin          (0 0 0);
        axis            (0 0 1);
        omega           12.72727; // rad/s
    }
}
// ********************************************************************** //
```
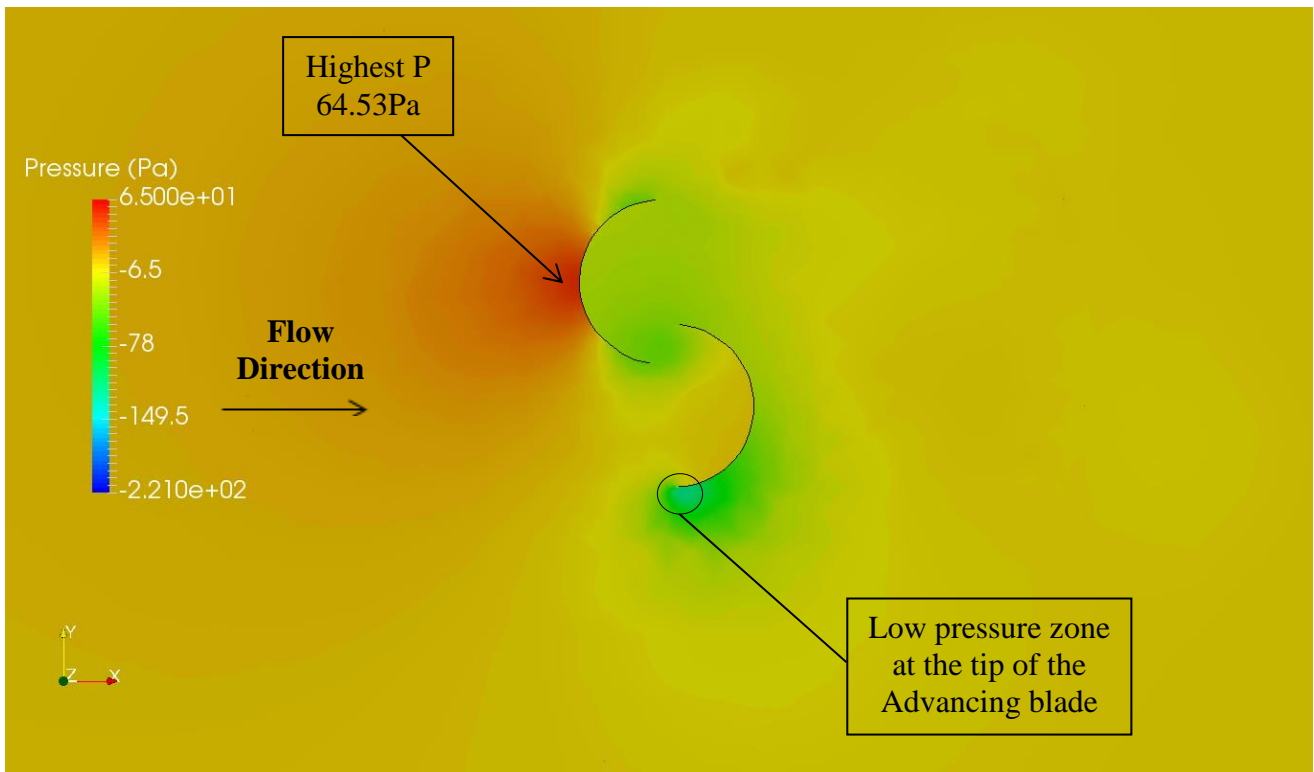
Figure 5.10: Mesh control file showing the application of the sliding mesh technique

5.2 Critical Flow Filed Analysis and Results Comparison

The detailed performance analysis of the helical VAWT with 0.5 revolutions of twist, using the in-house built CFD package, has been carried out at TSR 0.7 at which its coefficient of power is highest. The VAWT has also been numerically analysed with the in-house built CFD package at the full TSR range for comparison purposes of the global results. The qualitative analysis has been carried out at a cross sectional cut through the middle of the VAWT, where the scale and angular position of the VAWT have been kept constant for comparison purposes between the in-house built CFD package and the commercial CFD solver.

Figure 5.11 (a) depicts the variation of static gauge pressure in the vicinity of the helical VAWT, obtained using the in-house built CFD package. Figure 5.11 (b) depicts the variation of static gauge pressure in the vicinity of the helical VAWT, obtained using commercial CFD package. It can be seen in figure 5.11 (a) and (b) that for the in-house built CFD solver, the zone of low pressure at the tip of the advancing blade is lower than for the commercial CFD solver. It can also be seen in figure 5.11 that the maximum pressure value obtained using the in-house built CFD solver is 64.53Pa, while the one obtained using the commercial CFD solver is 65Pa, indicating that the results for maximum pressure are in a close agreement.

In general, the static gauge pressure variation plots are very similar between the two solvers and the maximum pressure zones sizes and values match closely. The only notable difference is the small zone of low pressure at the tip of the advancing blade, which is lower in value for the in-house built CFD package.

Flow Diagnostics and Optimal Design of Vertical Axis Wind Turbines for Urban Environments
By Martin Zahariev, School of Computing and Engineering, University of Huddersfield, UK (2016)

99

(a)
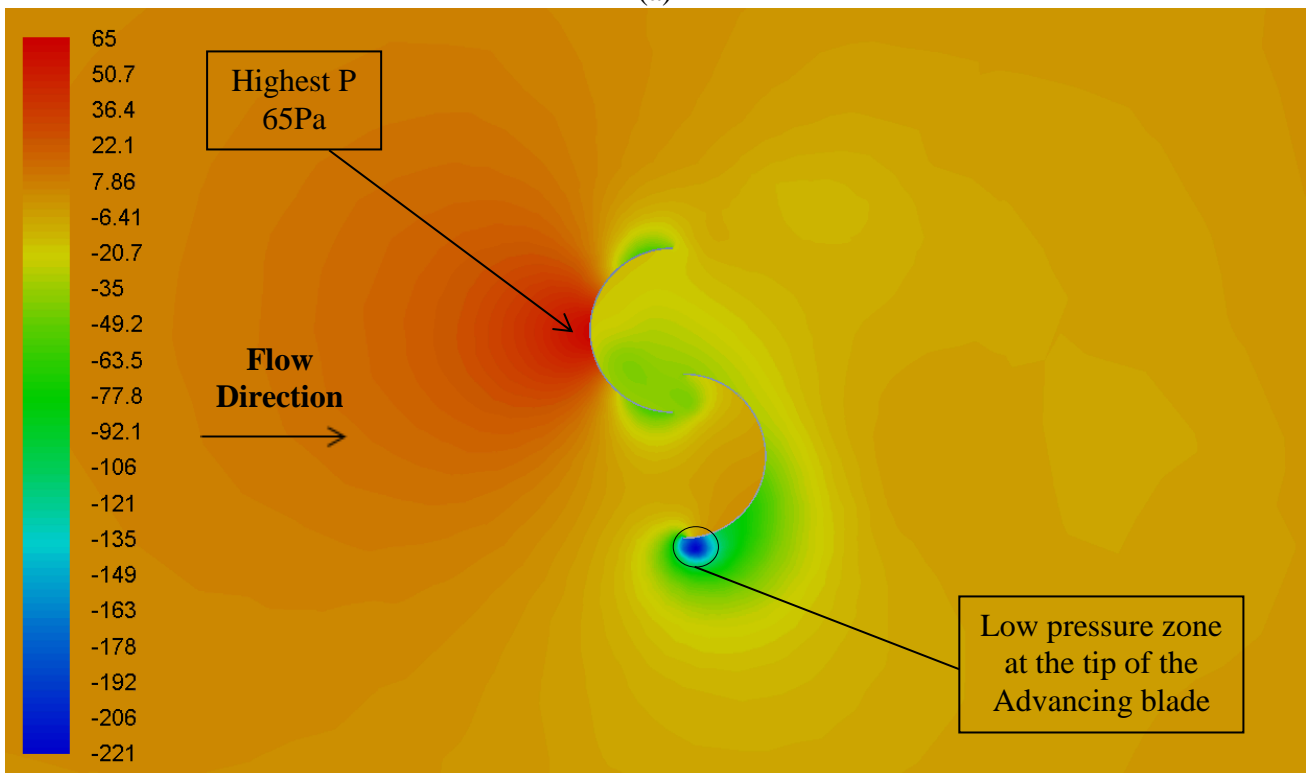
(b)

Figure 5.11: Static gauge pressure (Pa) variations in the vicinity of the helical VAWT with 0.5 revolutions of twist obtained using (a) In-house built CFD solver; (b) Commercial CFD solver

Flow Diagnostics and Optimal Design of Vertical Axis Wind Turbines for Urban Environments
By Martin Zahariev, School of Computing and Engineering, University of Huddersfield, UK (2016)

100

Figure 5.12 (a) depicts the variation in the flow velocity magnitude in the vicinity the helical VAWT, obtained using the in-house built CFD package. Figure 5.12 (b) depicts the variation in the flow velocity magnitude in the vicinity the helical VAWT, obtained using the commercial CFD solver. It can be seen in figure 5.12 (a) and (b) that the high velocity zone at the tip of the advancing blade is similar in size, but a little lower in value for the in-house built CFD package compared to the commercial CFD solver. It can also be observed that the maximum velocity obtained using the in-house built CFD package is 16.27m/s, while for the commercial CFD solver it is 16.4m/s, indicating that the results for maximum velocity are in close agreement. The downstream low velocity zone obtained using the in-house built CFD package is slightly smaller compared to the one of the commercial CFD solver, but its shape and value are similar.

In general, the flow velocity magnitude variation plots are similar between the two solvers, and the results for maximum velocity are in close agreement. The only notable differences in the results is the size of the downstream low velocity zone, which is slightly smaller for the in-house built CFD package, but the overall shape and values are similar.
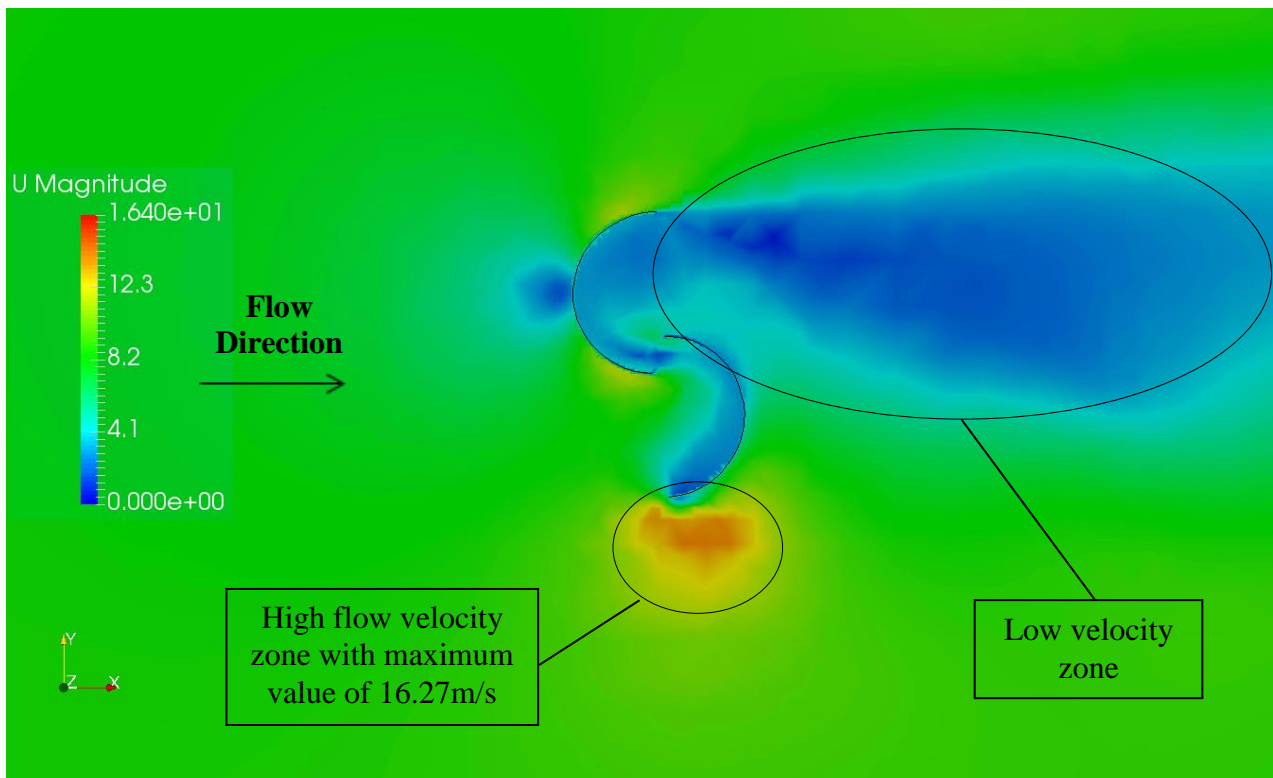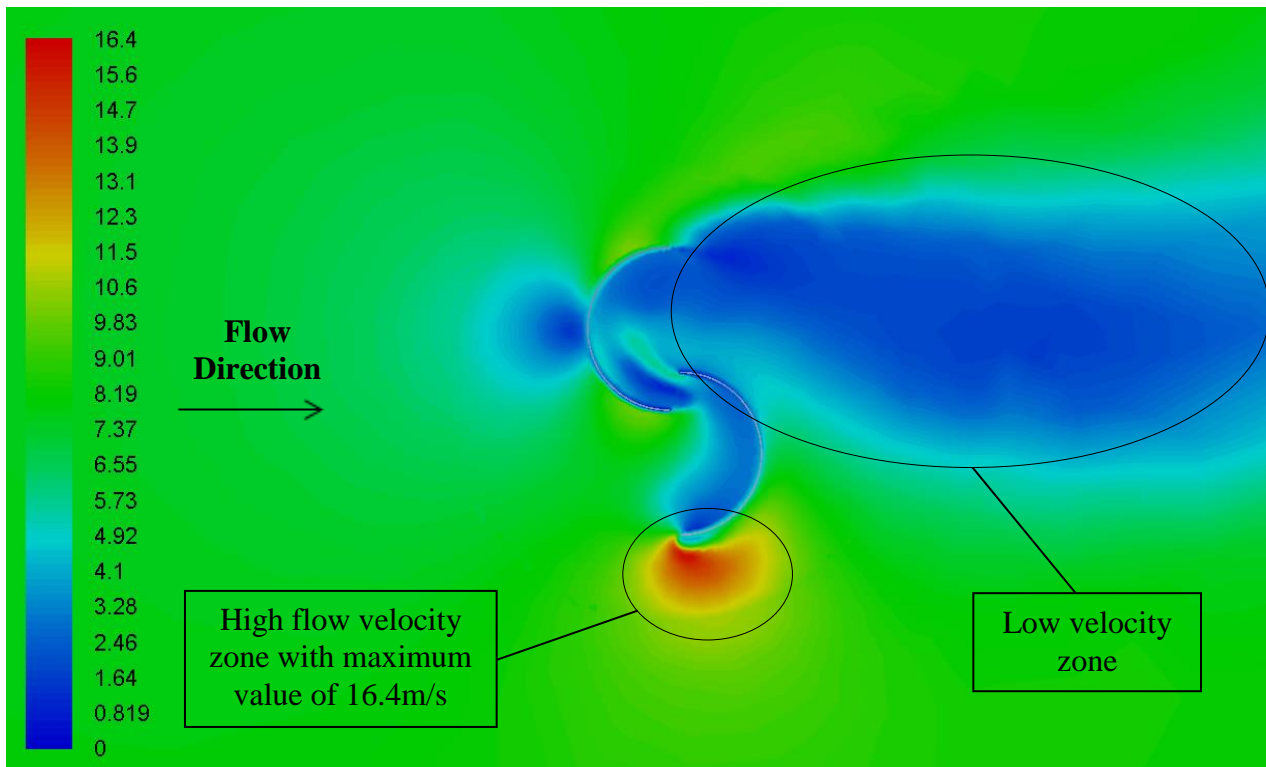

(a)

(b)

Figure 5.12: Velocity magnitude (m/s) variation in the vicinity of the helical VAWT with 0.5 revolutions of twist obtained using (a) In-house built CFD solver; (b) Commercial CFD solver

Once the detailed flow analysis of the local flow features in the vicinity of the helical VAWT has been carried out, using both the in-house built CFD packaged and the commercial CFD solver, the variations of the instantaneous coefficients of moment and power, generated in one complete revolution, have been depicted in figure 5.13. It can clearly be seen in figure 5.13 (a) and (b) that that cyclic variations produced by both, the commercial CFD solver and the in-house built CFD package, are similar. It can also be observed that the in-house built CFD package both under and over predicts the results at the positive and negative peaks.

In general, it can be summarized that the instantaneous coefficients of moment and power have very similar cyclic variations for both, the in-house built CFD package and the commercial CFD solver. It can also be summarized that the in-house built CFD package both over and under predicts the results at the peaks, with similar amount. Therefore, the average coefficients of moment and power have been found to be in a close agreement between the in-house CFD package and the commercial CFD solver.

Flow Diagnostics and Optimal Design of Vertical Axis Wind Turbines for Urban Environments
By Martin Zahariev, School of Computing and Engineering, University of Huddersfield, UK (2016)

102
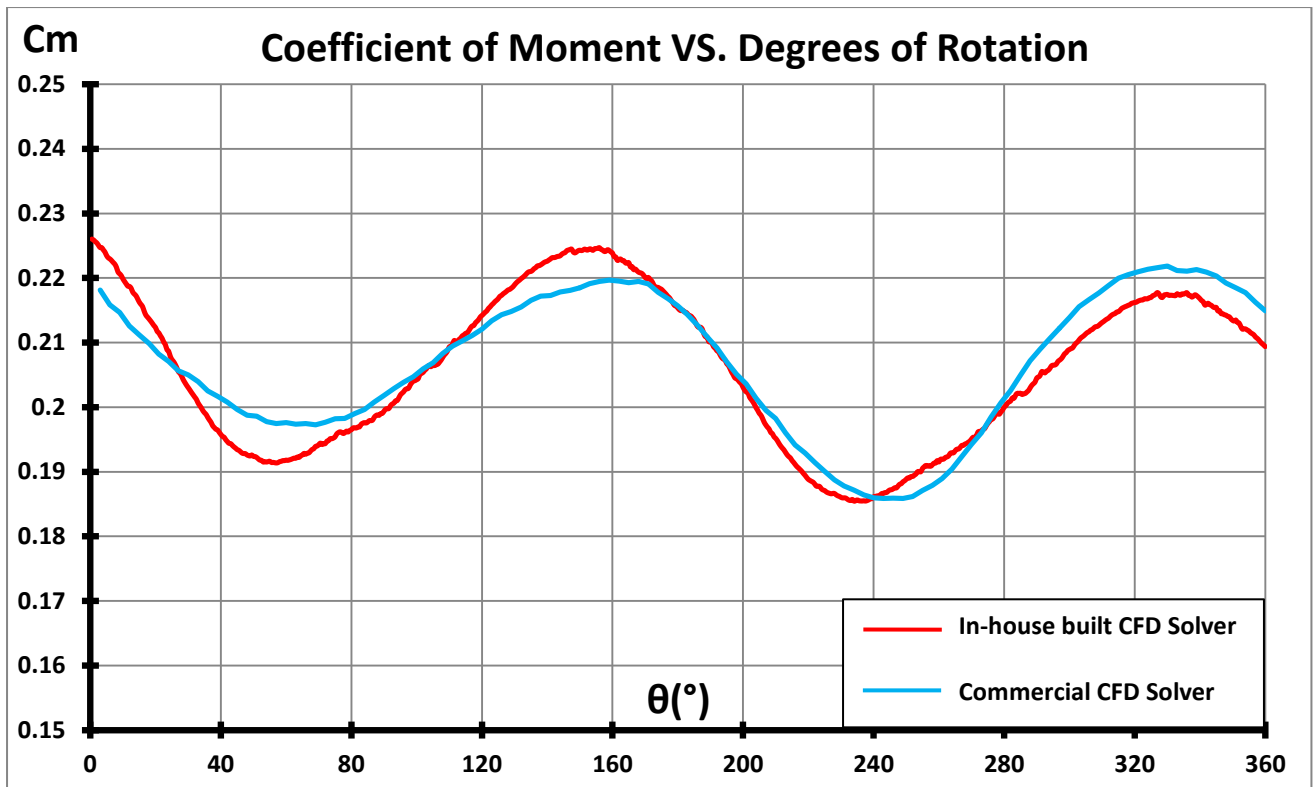
(a)
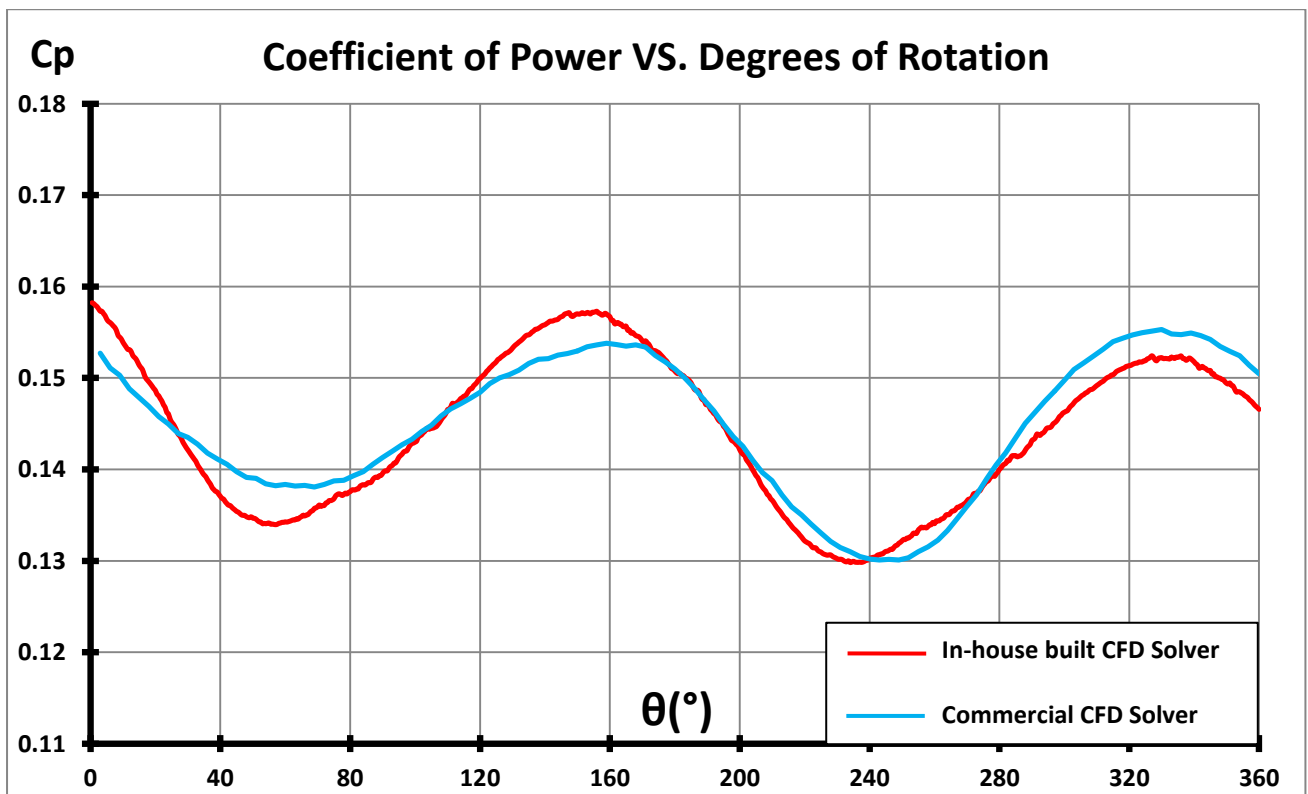
(b)

Figure 5.13: Variations of the instantaneous coefficients of (a) Moment (Cm) (b) Power (Cp), for both the in-house CFD package and the commercial CFD solver

Flow Diagnostics and Optimal Design of Vertical Axis Wind Turbines for Urban Environments
By Martin Zahariev, School of Computing and Engineering, University of Huddersfield, UK (2016)

103

The average coefficients of moment and power for the helical VAWT with 0.5 revolutions of twist, at each of the numerically examined TSR values, obtained using the in-house built CFD package, have been summarized in table 5.1 below.

Table 5.1: Average coefficients of moment and power at multiple TSR values

TSR	Coefficient of Moment	Coefficient of Power
0.5	0.2798	0.1399
0.6	0.2375	0.1425
0.7	0.2069	0.1448
0.8	0.1714	0.1371
0.9	0.1326	0.1193

In figure 5.14, the results for average coefficient of power at multiple TSR values obtained using both, the in-house built CFD package and the commercial CFD solver, have been compared with each other. It can clearly be seen in figure 5.14 that the differences between the commercial CFD solver and the in-house built CFD solver are very small at TSR values of 0.6 and 0.7, where the helical VAWT is in high efficiency region. At TSR 0.7 the in-house built CFD package predicts coefficient of power 0.1448, while the commercial CFD solver predicts 0.1456, showing that the results are almost identical. It can also be noticed that at lower TSR values (0.5) the in-house built CFD solver over predicts the results and at higher TSR values (0.8 and 0.9) the in-house built CFD solver under predicts the results. For example at TSR 0.5 the difference is visibly larger, where the in-house built CFD package predicts coefficient of power of 0.139, while the commercial CFD solver predicts coefficient of power of 0.136. Therefore, although the difference is larger at TSR 0.5 than at TSR 0.7, the results are still in close agreement as the difference is at the third decimal position.

In general, the predicted results using the in-house built CFD solver are almost identical with the results obtained using the commercial CFD solver at the TSR values at which the helical VAWT is most efficient (TSR 0.6 sand 0.7). At lower and higher TSR values than the optimal ones, there are discrepancies between the results obtained using the commercial and the in-house built CFD solvers, but the results are still in close agreement with each other and the differences are limited to the third decimal position.

Flow Diagnostics and Optimal Design of Vertical Axis Wind Turbines for Urban Environments
By Martin Zahariev, School of Computing and Engineering, University of Huddersfield, UK (2016)

104
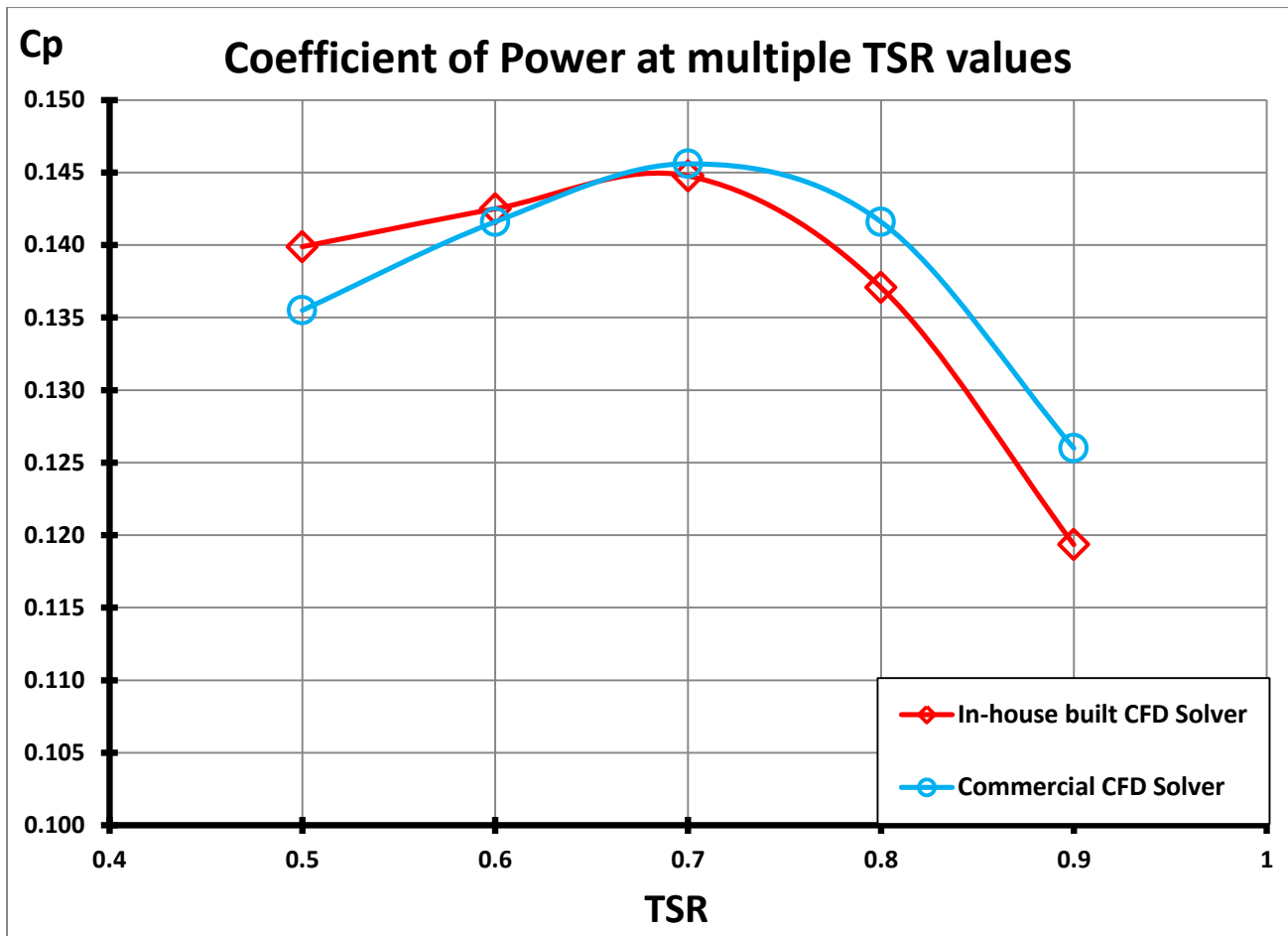
Figure 5.14: Average results for coefficient of power at multiple TSR values using both the in-house built CFD solver and the commercial CFD solver.

Once the qualitative and quantitative analysis has been carried out, and it has been established that the local flow field and the instantaneous and averaged global parameters are in close agreement between the in-house built CFD package and the commercial CFD solver, a further in-depth analysis of the local flow velocities has been carried out. The analysis has been made at five positions following the fluid flow through the VAWT. Two positions have been selected at the advancing blade, in order to see whether the in-house built CFD package accurately captures the effects associated with the fluid flow entering VAWT. One position has been selected at the overlap zone, in order to see if the in-house built CFD package accurately captures the effects associated with the disturbed flow in the overall region. And finally two positions have been selected at the returning blade, in order to see if the in-house built CFD package accurately captures the effects associated with the fluid flow leaving the VAWT. At the five selected positions, five lines have been plotted spanning the entire height of the VAWT, and then the flow velocity data has been extracted at numerous points across these lines. The location of the five positions can be seen in figure 5.15.

Flow Diagnostics and Optimal Design of Vertical Axis Wind Turbines for Urban Environments
By Martin Zahariev, School of Computing and Engineering, University of Huddersfield, UK (2016)

105

Figure 5.15: Five positions following the fluid flow through the VAWT
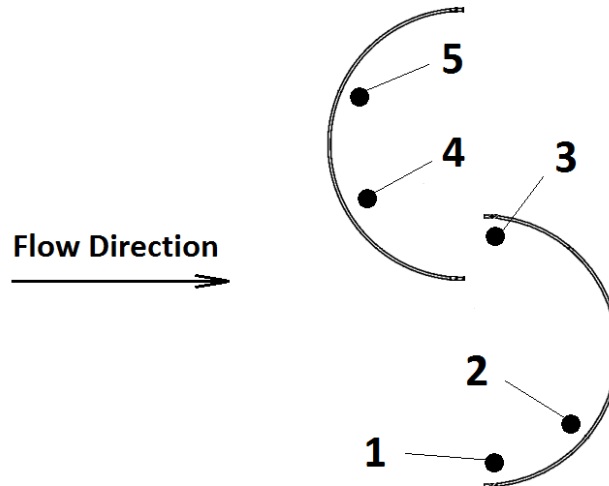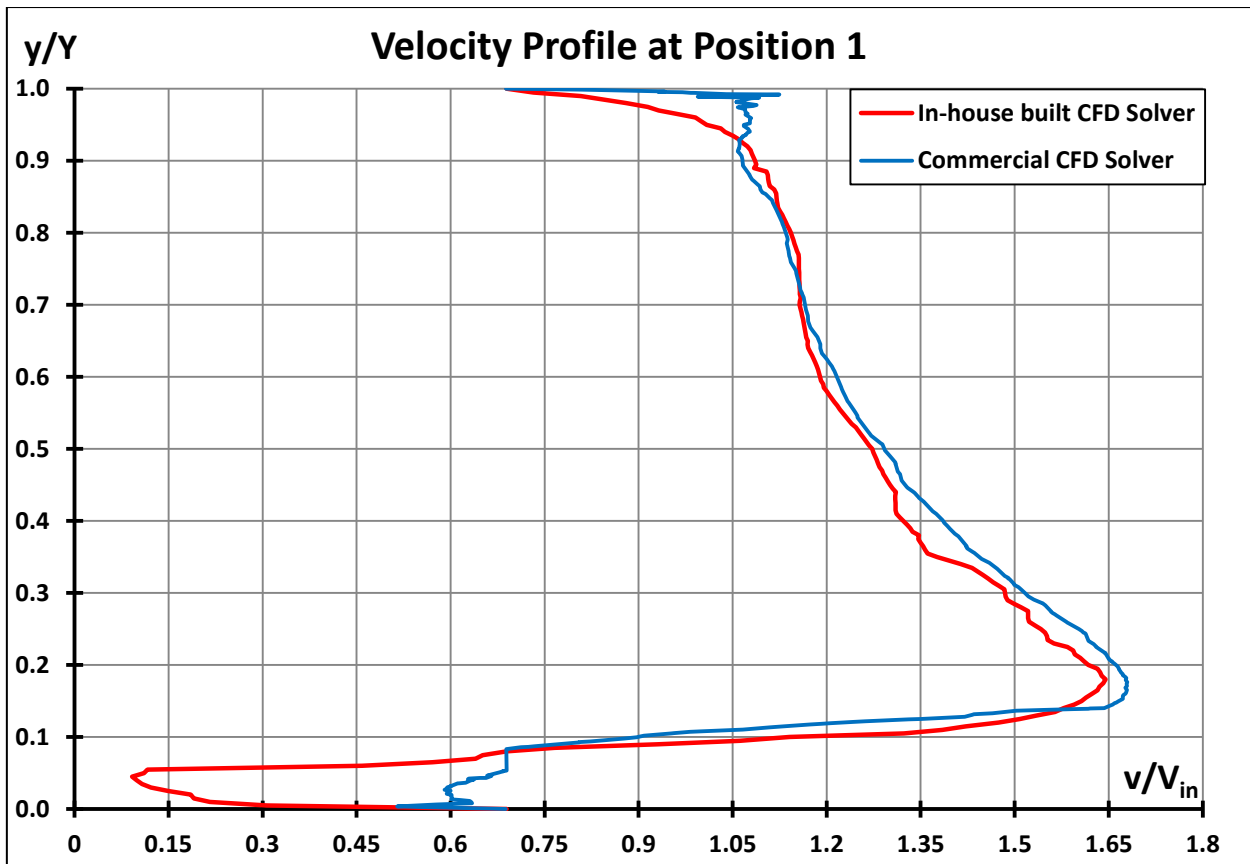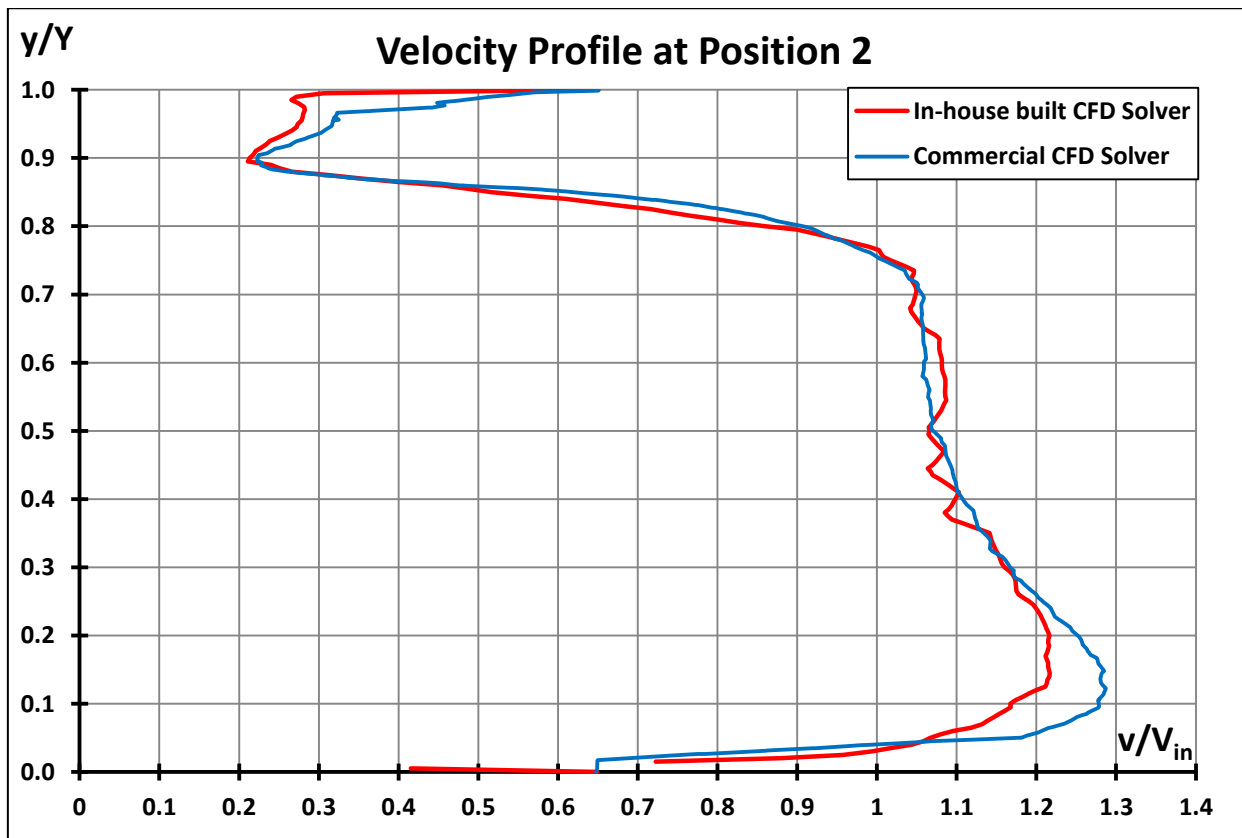
In figure 5.16, the local velocity data has been extracted at numerous points across the lines plotted at the five positions, in order to generate velocity profiles of high resolutions at each of the five positions. This analysis has been conducted by using both the in-house built CFD package and the commercial CFD solver and then the results have been compared in figure 5.16. In figure 5.16, y is the local vertical distance measured from the bottom of the VAWT, Y is the height of the VAWT, v is the local flow velocity and V_{in} is the inlet velocity.

In figure 5.16 (a) and (b), the local velocity data has been shown at positions 1 and 2, and it is clear that the results are almost identical between the in-house built CFD solver and the commercial CFD solver, indicating that the in-house built CFD package accurately captures the effects of the fluid flow entering the VAWT. In figure 5.16 (c), the local velocity data has been shown at position 3, where it is clear that the commercial CFD solver and the in-house built CFD solver are following similar patterns and both velocity profiles are highly irregular, indicating that both solvers are capturing the flow disturbance effects of the overlap zone. It can also be observed for position 3 that the results obtained using the in-house built CFD solver are higher at the top of the VAWT by around 1m/s, and lower at the bottom of the VAWT by the similar amount of 1m/s. It can be noticed in figure 5.16 (d) that the local velocity data at position 4 is exhibiting the same behaviour for both the in-house built CFD package and the commercial CFD solver. It can also be seen that for position 4, the results obtained using the in-house built CFD solver are a little lower at the top of the VAWT, while towards the middle and the bottom of the VAWT the results are almost identical between the two solvers. It can also be observed in figure 5.16 (e) that the local velocity data at position 5 is exhibiting almost identical behaviour for both the in-house built CFD package and the commercial CFD solver. It can also be noticed that the results obtained using the in-house built CFD solver are slightly more irregular at some places. This close agreement between the results at position 4 and 5 indicates that the in-house built CFD package accurately captures the effects associated with the flow leaving the VAWT.

In general, it can be summarized that the in-house built CFD package is predicting the local flow velocity across numerous points at the 5 positions with a high level of accuracy, and the results are in close agreement to the results obtained by using the commercial CFD package. It can also be summarized that the in-house built CFD package accurately captures the effects associate with the fluid flow entering the VAWT, the disturbances to the fluid flow at the overlap region and the effects of the fluid flow leaving the VAWT.

Flow Diagnostics and Optimal Design of Vertical Axis Wind Turbines for Urban Environments
By Martin Zahariev, School of Computing and Engineering, University of Huddersfield, UK (2016)

106

(a)

(b)

Flow Diagnostics and Optimal Design of Vertical Axis Wind Turbines for Urban Environments
By Martin Zahariev, School of Computing and Engineering, University of Huddersfield, UK (2016)

107

(c)

(d)

Flow Diagnostics and Optimal Design of Vertical Axis Wind Turbines for Urban Environments
By Martin Zahariev, School of Computing and Engineering, University of Huddersfield, UK (2016)

108

(e)

Figure 5.16: Local flow velocity profiles at position (a) 1 (b) 2 (c) 3 (d) 4 (e) 5

5.3   Summary of the work

An in-house CFD package for aerodynamic design analysis of the helically twisted VAWT with 0.5 revolutions of twist has been developed, based on already existing open source CFD code. The in-house built CFD package has been used to conduct critical flow field analysis of the helical VAWT and the predicted flow fields and performance parameters of the VAWT have been found to be in close agreement with the corresponding results obtained by using commercial CFD solver. Detail analysis has been carried out on the local flow fields, instantaneous coefficients of moment and power, the averaged coefficient of power at multiple TSRs (varying operational conditions) and at local positions where the local flow velocities have been obtained at numerous points. From all of the detailed analysis carried out in this chapter it has been determined that the in-house built CFD package predicts the local and global flow an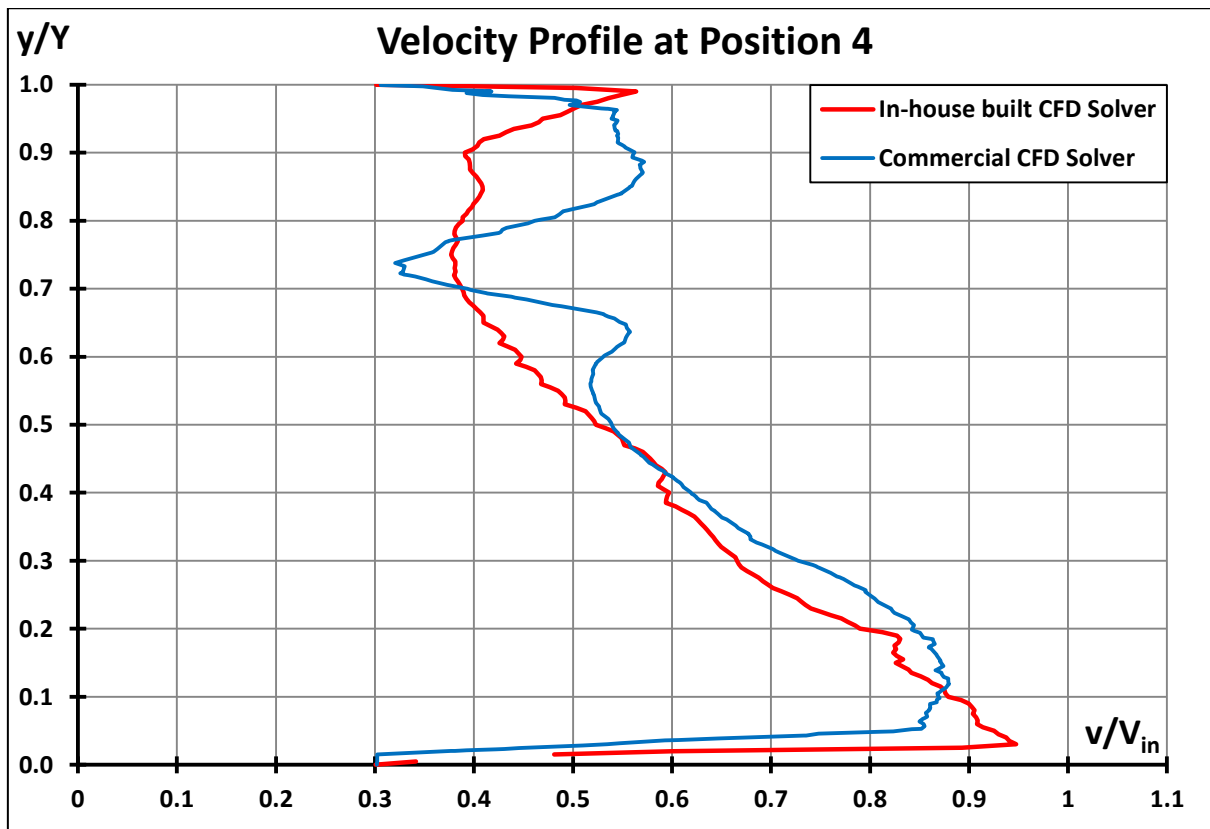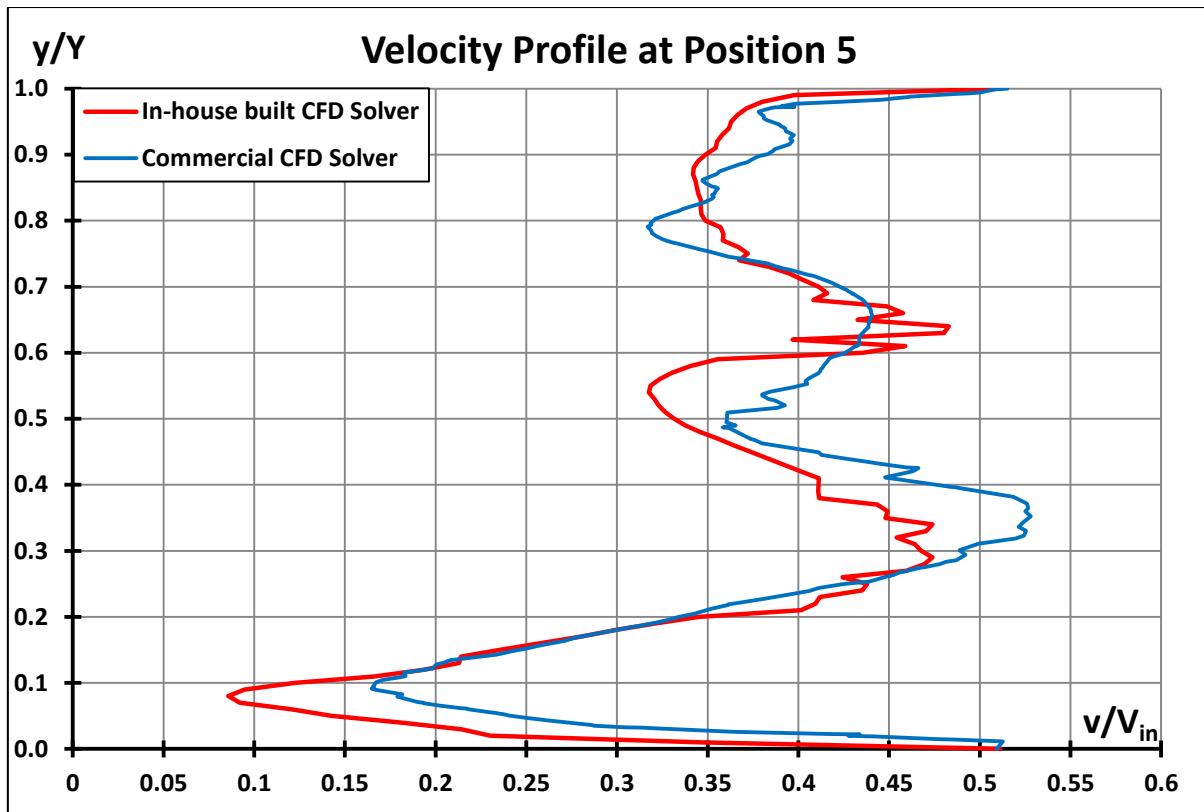d performance parameters of the helical VAWT to a high degree of accuracy and with a close agreement with the commercial CFD solver. Therefore, as the results obtained using the in-house built CFD package are accurate and in close agreement with the results of the commercial CFD solver, it can be concluded that the in-house built CFD package is a viable and cost effective alternative to the commercial CFD solvers for aerodynamic design analysis of VAWTs. As the in-house built CFD package is a viable and cost effective alternative to the commercial CFD solvers, it allows small-to-medium sized enterprises (SMEs) to benefit from the advancing CFD methods in their VAWT's related design and development work.

In the next chapter, the conclusion of the present research study has been presented and the major achievements of the research study and future recommendations have been discussed.

Flow Diagnostics and Optimal Design of Vertical Axis Wind Turbines for Urban Environments
By Martin Zahariev, School of Computing and Engineering, University of Huddersfield, UK (2016)

109

Chapter 6
Conclusions

From the results obtained in the previous chapters regarding the flow diagnostics and development of a design analysis package for drag based Vertical Axis Wind Turbines, detailed conclusions have been drawn in this chapter. The major achievements and contributions to the existing knowledge base are summarised, and wherever possible, referenced back to the initial aims of this study. Finally, the works carried out in this study are evaluated and requirements for future work in the area of drag based VAWTs for sustainable urban environment are defined.

6.1 Research Problem Outline

The need to harness wind energy in the urban environment is growing with the constant push towards renewable energy, driven by the EU and the UK governments. Drag based Vertical Axis Wind Turbines are a strong candidate for this purpose. However, these machines need to be designed optimally for widespread commercial recognition. In order to accomplish this, researchers have been trying to analyse the effects of various geometric parameters on the performance output of VAWTs. Flow diagnostics and shape optimisation of VAWTs have however been limited to either experimental or steady-state numerical methodologies. With the advent of powerful computing facilities and sophisticated software to analyse the flow fields, it has now become possible to computationally model a VAWT and analyse the flow in the vicinity of these machines under various operating conditions. This study also details the methodology to predict the complete performance spectrum of VAWTs with reasonable accuracy. Moreover, a design analysis CFD based package has been developed in the present study to analyse the performance of VAWTs under varying operating conditions. The developed package is both robust and inexpensive. It is expected that the developed package will help SMEs around the globe to develop technical and numerical expertise regarding flow diagnostics of VAWTs.

From a comprehensive review of the published literature, a number of limitations have been found out. In order to accurately predict the flow behaviour in VAWTs, a set of aims and objectives have been formulated which define the scope of this research study. A summary of the primary aims of the thesis is provided in the following sections of this chapter, along with the major achievements and contributions. For reference, the detailed objectives within each of these aims are provided in Chapter 2.

6.2 Research Aims and Major Achievements

In this section, the major achievements of the current research study have been referred back to the aims of the study, laid out in chapter 1.

Aim # 1: Flow diagnostics and optimisation of drag based concept VAWT designs for the complete performance spectrum

This research study offers a detailed numerical analysis of the flow fields and performance characteristics of a standard Savonius VAWT, at various operation conditions, allowing for deeper understanding of drag based VAWTs. The research study also provides detailed numerical analysis of innovative VAWT designs developed by incorporating advanced geometrical features to the standard Savonius VAWT design. These geometric features include internal guide vanes, tapered blades and helically twisted blades. The primary achievement from this particular facet of the research work is a deeper understanding of the effects of these features on the performance analysis of drag based VATWs, and the determination of the optimal VAWT design based on the combination of the features.

The second facet of aim 1 is the critical analysis of the complete performance spectrum of the optimal VAWT design obtained from the first facet of this aim. For this purpose, multiple complex numerical techniques have been used to mimic the start-up process of the VAWT and its acceleration towards steady operating point. The inherent complexity of this process makes this whole methodology quite innovative in terms of its usage.

Flow Diagnostics and Optimal Design of Vertical Axis Wind Turbines for Urban Environments
By Martin Zahariev, School of Computing and Engineering, University of Huddersfield, UK (2016)

111

Aim # 2: Development of an in-house built CFD package for aerodynamic design analysis of drag based VAWTs

In order to help SMEs to grow to their full potential, an attempt has been made towards the development of an inexpensive CFD based package for the design analysis of VAWTs, which can be easily integrated in SMEs. The developed package is based on already existing open source CFD solvers, however, these solvers are TUI based and hence, very complex to use. For engineers in SMEs, a robust and user-friendly package has been developed that is expected to enhance their technical and numerical skills. In order to prove the effectiveness of this package, an example has been analysed in detail. The example comprises of the optimal VAWT design analysed in the first aim of this study. Predictions from the developed package have been compared against a well-known and widely-used commercial CFD software. It has been shown that the developed package predicts the complex flow features in the vicinity of VAWTs with reasonable accuracy, in comparison with the commercial CFD solver.

6.3 Thesis Conclusion

In this section, the major conclusions are presented with respect to the research objectives of the current research study.

Objective 1: Detailed flow diagnostics of VAWTs with internal guide vanes.

Detailed flow analysis of drag based VAWTs with internal guide vanes have been carried out at various operating conditions and geometric configurations in the present study. The effects on the performance of the VAWT caused by the addition of internal guide vanes, with varying inclination angles and thicknesses, have been critically analysed. Both qualitative and quantitative analysis of the global and local parameters of the guide vanes models show that addition of internal guide vanes increases the time and distance it takes for the incident flow of air to pass through the VAWT. The reason for this is the inclined route air takes through the VAWT, caused by the inclination angel of the guide vanes. The amount of flow that takes place through the inclined route is determined by the thickness of the guide vanes. In general, it can be concluded that the addition of internal guide vanes has negative effects on VAWT's performance.

Objective 2: Detailed flow diagnostics of VAWTs with tapered blades.

Detailed flow analysis of drag based VAWTs with tapered blades has been carried out at various operating conditions and geometric configurations in the present study. The effects on the performance of the VAWT caused by tapering the blades in various ways (Delta-shaped, Rhomb-shaped and X-shaped) have been critically analysed. Both qualitative and quantitative analysis of the global and local parameters of the tapered blades models shows that 70% of the tapered VAWT operates at lower aspect ratio (lower efficiency), while the remaining 30% of the tapered VAWT operates at higher aspect ratio (higher efficiency). Once combined, it has been shown that the 30% higher efficiency area cannot offset the 70% area at lower efficiency, leading to the overall efficiency of the entire tapered VAWT to be lower. Hence, it can be concluded that tapering of blades has negative effect on VAWT's efficiency.

Flow Diagnostics and Optimal Design of Vertical Axis Wind Turbines for Urban Environments
By Martin Zahariev, School of Computing and Engineering, University of Huddersfield, UK (2016)
112

Objective 3: Detailed flow diagnostics of VAWTs with helically twisted blades.

Objective 4: Determination of the optimal design of VAWT.

Detailed flow analysis of drag based VAWTs with helically twisted blades has been carried out at various operating conditions and geometric configurations in the present study. The effects on the performance of the VAWT caused by addition of helical twist on the blades of the VAWT have been determined by numerically examining five models with different level of helical twist (0.25, 0.5, 1, 1.5 and 2 revolutions of twist). Both qualitative and quantitative analysis of the global and local parameters of the helically twisted models shows that only a moderate level of helical twist (0.25 and 0.5 revolutions of twist) is beneficial to the efficiency of the VAWT. Furthermore, introduction of helical twist reduces the torque variations of the VAWT significantly. It can be concluded that addition of moderate levels of helical twist to the blades of a standard drag based VAWT has positive effects on VAWT's efficiency, and reduces the torque variations significantly.

Objective 5: Detailed analysis of the optimal VAWT design to cover a wide range of operation i.e. from start-up to steady operation point.

Complete performance spectrum of the helically twisted VAWT with 0.5 revolutions of twist has been generated using dynamic mesh technique. The performance spectrum comprises of the start-up process of the VAWT, along with its acceleration towards the steady operating point. It has been found that VAWT's acceleration is very high at its start-up, which confirms the self-starting ability of the helical VAWT. The dynamic mesh technique has also being used to establish the instantaneous coefficient of power with respect to time, which provides data for the coefficient of power at different TSR values, making it possible to determine the TSR corresponding to maximum coefficient of power.

Objective 6: Development of an in-house built CFD package for aerodynamic design analysis of VAWTs.

An in-house built CFD package for aerodynamic design analysis of VAWTs has been developed, based on already existing open source CFD solvers. Detailed flow analysis of the helically twisted VAWT design has been carried out using the in-house built CFD package. The predicted flow fields and performance parameters of the VAWT have been found to be in close agreement with the one obtained through the use of commercial CFD solver. The detailed flow analysis carried out in this section encompassed critical analysis of the local flow fields, the instantaneous coefficients of moment and power, and the average coefficient of power at multiple TSRs. From all of the detailed analysis carried out in this section, it has been determined that the in-house built CFD package predicts the local and global performance parameters of the VAWT with reasonable accuracy. Hence, the developed package can be integrated in SMEs to help develop their business.

6.4 Recommendation for Future Work

In light of the concluding remarks provided in the previous section, a vast potential for further research in this particular area has been unlocked. The main areas identified for further work are described below which are associated to further performance-related analysis, design and optimization of VAWTs.

Recommendation # 1

A further research into drag based VAWTs' individual geometric features has to be carried out. Moreover, a detailed analysis on the effects of combinations of these advanced geometric features has to be carried out. Such research studies can benefit greatly from the use CFD techniques to minimize cost, and develop models combining multiple numerical modelling features.

Recommendation # 2

A further research into the dynamic mesh techniques, such as the six degree of freedom model used in this work is required, as the potential in the area is great and can even eliminate the requirement for prototypes once the computational power reaches the required levels. Enhancement of the dynamic mesh technique is recommended, to allow for load control of the solid body and friction forces to be added, which will increase the overall accuracy further, and will produce numerical environment which resembles the reality much closer.

Recommendation #3

A further research into the development of in-house built CFD package for aerodynamic design analysis of VAWTs is required. A simple GUI can be added, allowing multiple geometrical changes to be made faster, and the operational environment to be changed with ease. Research into the development of in-house packages for VAWT's geometry creation and meshing is required, which will results in an even lower cost package that can generate geometries and meshes to a high standard. In general, a comprehensive and complete in-house built CFD package for aerodynamic design analysis of VAWTs is required that allows changes to be made quickly and with relative ease.

Flow Diagnostics and Optimal Design of Vertical Axis Wind Turbines for Urban Environments
By Martin Zahariev, School of Computing and Engineering, University of Huddersfield, UK (2016)

114

References

[1]   Bratley, J. (2013, June 19). Wind Energy Definition.
        Retrieved January 6, 2016, from website: http://www.clean-energy-ideas.com
        URL:http://www.clean-energy-ideas.com/energy/energy-dictionary/wind-energy-definition

[2]   Gipe, P. (2004). Wind Power: Renewable Energy for Home, Farm, and Business, 2nd
        Edition. Retrieved on 12th of December 2015. White River Junction, Vermont, VT 05001,
        POB: 428: Chelsea Green Publishing Company.

[3]   Nixon, N. (2008, October 17). Timeline: The history of wind power
        Retrieved on 5th of January 2015, from website: http://www.theguardian.com
        URL: http://www.theguardian.com/environment/2008/oct/17/wind-power-renewable-energy

[4]   Croll, K. (2012, March). Papers of James Blyth.
        Retrieved February 20, 2015, from website: http://www.strath.ac.uk
        URL: http://www.strath.ac.uk/archives/iotm/march2012/

[5]   Hutchens, L. (2012, November 2). Eggbeater VAWT Design More Powerful and Efficient.
        Retrieved February 20, 2015, from website: http://www.greenoptimistic.com
        URL:http://www.greenoptimistic.com/eggbeater-vawt-design-powerful-efficient-
        20121102/#.VOY6-SwRS9c

[6]   Scheurich, F. (2011). Modelling the Aerodynamics of Vertical-Axis Wind Turbines.
        Glasgow: University of Glasgow.

[7]   windturbine-performance. (2014). Analysing performance of Darrieus rotor
        Retrieved March 14, 2015, from website: http://www.windturbine-performance.com
        URL: http://www.windturbine-performance.com/www/darrieus.htm

[8]   Barnard, M. (2014, April 7). Vertical Axis Wind Turbines: Great In 1890, Also-rans In 2014.
        Retrieved January 6, 2015, from website: http://cleantechnica.com
        URL: http://cleantechnica.com/2014/04/07/vertical-axis-wind-turbines-great-1890-also-rans-
        2014/.

[9]   Bullis, K. (2013, April 8). Will Vertical Turbines Make More of the Wind?
        Retrieved November 9, 2014, from website: http://www.technologyreview.com
        URL: http://www.technologyreview.com/news/513266/will-vertical-turbines-make-more-of-
        the-wind/

[10]   Villarreal, C. (2008). Optimization of the efficiency of a Savonius wind turbine for urban
        media using a genetic algorithm.
        Monterrey: Monterrey Institute of Technology and Higher Education.

[11]   Tala, H., Patel, H., Sapra, R., & Gharte, J. (October 2014). Simulations of Small Scale
        Straight Blade Savonius Wind Turbine Using Latest CAE Techniques to get Optimum Power
        Output. International Journal of Advance Foundation and Research in Science & Engineering
        (IJAFRSE), 37-50.

Flow Diagnostics and Optimal Design of Vertical Axis Wind Turbines for Urban Environments
By Martin Zahariev, School of Computing and Engineering, University of Huddersfield, UK (2016)

115

[12]   Alexander, A., & Holownia, B. (1978). Wind Tunnel Test of a Savonius Rotor. Journal of Industrial Aerodynamics, 343-353.

[13]   Albani, A., & Ibrahim, M. Z. (2013). Preliminary Development of Prototype of Savonius Wind Turbine for Application in Low Wind Speed in Kuala Terengganu. Malaysia. International Journal of Scientific & Technology Research, Volume 2, Issue 3, March 2013, pg: 102-108.

[14]   Sutherland, H. J., Berg, D. E., & Ashwill, T. D. (2012). A Retrospective of VAWT Technology. Albuquerque, New Mexico 87185 and Livermore, California 94550: Sandia National Laboratories.

[15]   Ragheb, M., Ragheb A. M. (2011, July 5). Wind Turbines Theory, Betz Equation and Optimal Rotor Tip Speed Ratio. Retrieved January 7, 2015, From website: http://www.intechopen.com URL: http://www.intechopen.com/books/fundamental-and-advanced-topics-in-wind-power/wind-turbines-theory-the-betz-equation-and-optimal-rotor-tip-speed-ratio

[16]   Martino, J. (2014, April 2). Advancements in Wind Turbine Technology: Improving Efficiency and Reducing Cost. Retrieved November 9, 2014, from website: http://www.renewableenergyworld.com URL: http://www.renewableenergyworld.com/rea/news/article/2014/04/advancements-in-wind-turbine-technology-improving-efficiency-and-reducing-cost.

[17]   Rolland, S., & Auzane, B. (2012). The Potential of Small and Medium Wind Energy in Developing Countries. Brussels: Alliance for Rural Electrification.

[18]   RenewableUK. (2013). Small and Medium Wind UK Market Report. London: RenewableUK.

[19]   Local Government Association. (2012, May 1). How much do wind turbines cost and where I can get funding? Retrieved November 13, 2014, from: http://www.local.gov.uk URL: http://www.local.gov.uk/home/-/journal_content/56/10180/3510194/ARTICLE

[20]   Altaeros Energies. (2014). BAT: The Buoyant Airborne Turbine. Retrieved September 1, 2015, from website: http://www.altaerosenergies.com URL: http://www.altaerosenergies.com/bat.html

[21]   Ragheb, M. (2014, February 28). Modern Wind Generators Champaign, IL, United States: University of Illinois.

[22]   Patel, S. (2011, January 4). Changing Winds: The Evolving Wind Turbine. Retrieved November 13, 2015, from website: http://www.powermag.com URL: http://www.powermag.com/changing-winds-the-evolving-wind-turbine/?pagenum=2

[23]   Ferris, D. (2010, May 23). What Wind Turbine 2.0 Will Look Like Retrieved September 2, 2015, from website: http://theferrisfiles.com URL: http://theferrisfiles.com/2010/05/what-wind-turbine-2-0-will-look-like/

Flow Diagnostics and Optimal Design of Vertical Axis Wind Turbines for Urban Environments
By Martin Zahariev, School of Computing and Engineering, University of Huddersfield, UK (2016)

116

[24]   Jha, A. (2010, February 22). Turbine design breathes new life into hopes for UK's renewable targets. Retrieved March 29, 2015, from website: http://www.theguardian.com
URL: http://www.theguardian.com/environment/2010/feb/22/aerogenerator-wind-turbine

[25]   Wind Power Monthly. (2010, October 27). Close up - The Aerogenerator X a new take on vertical-axis. Retrieved September 6, 2015, from http://www.windpowermonthly.com
URL:http://www.windpowermonthly.com/article/1037466/close---aerogenerator-x-new-vertical-axis

[26]   Dr. Zha, G. (2015). A Novel Concept of a Pre-Swirled Augmented Vertical Axis Wind Turbine (PA-VAWT). Boca Raton, Florida, USA: Wind Power Systems Internal Report - 2015-0001 Proprietary Material.

[27]   Turbina Energy Ag. (2014). Expert opinion on bird- and bat conservation.
Untere Mauerstr. 6-8 • 37671 Höxter: Bioplan GbR.

[28]   Ragheb, M. (2014, July 19). Vertical Axis Wind Turbines.
Retrieved March 20, 2015, from website: http://mragheb.com
URL:http://mragheb.com/NPRE%20475%20Wind%20Power%20Systems/Vertical%20Axis%20Wind%20Turbines.pdf

[29]   Sloan, J. (2012, January 10). Off-grid turbine: Helix in the wind.
Retrieved September 9, 2015, from website: http://www.compositesworld.com
URL: http://www.compositesworld.com/articles/off-grid-turbine-helix-in-the-wind

[30]   Ashfor, M. (2008, January 18). Harnessing Wind Power in the City.
Retrieved September 8, 2015, from website: http://scienceline.org
URL: http://scienceline.org/2008/01/tech-ashford-turbines/

[31]   Helix Wind Corp. (2015). S594 Wind Turbine.
Retrieved September 9, 2015, from website: http://www.helixwind.com
URL: http://www.helixwind.com/en/S594.php

[32]   Bonanomi, A. (2014, January 27). The long-lasting wind mini-turbine.
Retrieved September 10, 2015, from website: http://www.powertransmissionworld.com
URL: http://www.powertransmissionworld.com/the-long-lasting-wind-mini-turbine/

[33]   Bach, V. G. (1931). Untersuchungen uber Savonius-Rotoren und verwandte Strömungsmaschinen. Berlin: Mitteilung aus dem Institut für Technische Strömungsforschung an der Technischen Hochschule.

[34]   Smulders, P. T. (1976). Physical Aspects of Windmill Design.
Eindhoven, Netherlands: Department of Physics, Eindhoven University of Technology.

[35]   Shankar, P. N. (1979). Development of vertical axis wind turbine.
Proceedings of the Indian Academy Of Science, 49-66.

[36]   Crook, W., Puust, T., Robinson, M., & Vencel, L. (1980). Feasibility Study on A Low Power Vertical Axis Wind-Powered Generator. Salisbury: Defence Research Centre Salisbury.

Flow Diagnostics and Optimal Design of Vertical Axis Wind Turbines for Urban Environments
By Martin Zahariev, School of Computing and Engineering, University of Huddersfield, UK (2016)

117

[37] Ogawa, T., & Yoshida, H. (1986). The Effects of a Deflecting Plate and Rotor End Plates on Performances of Savonius-Type Wind Turbine.
Bulletin of Japan Society of Mechanical Engineers, 2115-2121

[38] Fernando, M. S. (1987). On The Performance and Wake Aerodynamics of the Savonius Wind Turbine. British Columbia: University of British Columbia.

[39] Aldoss, T., & Kotb, M. (1991). Aerodynamic Loads on a Stationary Savonius Rotor.
The Japan Society of Mechanical Engineers International Journal, 52-55.

[40] Fujisawa, N., & Gotoh, F. (1992). Visualization study of the flow in and around a Savonius rotor. Experiments in Fluids, 407-412.

[41] Fujisawa, N. (1995). Velocity measurements and numerical calculations of flow fields in and around Savonius rotors.
Journal of Wind Engineering and Industrial Aerodynamics, 39-50.

[42] Dua, Z., & Selig, M. (2000). The effect of rotation on the boundary layer of a wind turbine blade. Renewable Energy, 167-181.

[43] Ackermann, T., & Soder, L. (2000). Wind energy technology and current status: a review. Renewable and Sustainable Energy Reviews, 315-374.

[44] Gupta, R., Das, R., & Sharma, K. (2006). Experimental Study of a Savonius- Darrieus Wind Machine. Proceedings of the International Conference on Renewable Energy for Developing Countries (pp. 1-11). Washington, D.C: National Institute of Technology, Silchar, Assam India.

[45] Nakajima, M., Iio, S., & Ikeda, T. (2008). Performance of Double-step Savonius Rotor for Environmentally Friendly Hydraulic Turbine.
Journal of Fluid Science and Technology, 410-419.

[46] Yaakob, O. B., Tawi, K., & Suprayogi Sunanto, D. (2009). Computer Simulation Studies on the Effect Overlap Ratio for Savonius Type Vertical Axis Marine Current Turbine. International Journal of Engineering, 79-87.

[47] Alam, M. J., & Iqbal, M. (2010). A Low Cut-In Speed Marine Current Turbine.
Journal of Ocean Technology, 49-61.

[48] Mahmouda, N., El-Haroun, A., Wahba, E., & Nasef, M. (2012). An experimental study on improvement of Savonius rotor performance . Alexandria Engineering Journal, 19-25.

[49] Morshed, K. N. (2010). Experimental and Numerical Investigations on Aerodynamic Characteristics of Savonius Wind Turbine with Various Overlap Ratios.
Electronic Theses & Dissertations, Paper 773

[50] Mohamed, M., Janiga, G., Pap, E., & Thévenin, D. (2011). Optimal blade shape of a modified Savonius turbine using an obstacle shielding the returning blade.
Energy Conversion and Management Journal, 236-242.

Flow Diagnostics and Optimal Design of Vertical Axis Wind Turbines for Urban Environments
By Martin Zahariev, School of Computing and Engineering, University of Huddersfield, UK (2016)

118

[51]   Mohamed, M. H. (2011). Design Optimization of Savonius and Wells Turbines. Magdeburg: University of Magdeburg.

[52]   Dobrev, I., & Massouh, F. (2011). CFD and PIV investigation of unsteady flow through Savonius wind turbine. Energy Procedia, 711-720.

[53]   Patel, C., Patel, V., Prabhu, S., & Eldho, T. (2013). Investigation of Overlap Ratio for Savonius Type Vertical Axis Hydro Turbine.
International Journal of Soft Computing and Engineering, 379-383.

[54]   Ahmed, W., Zahed, M. J., Rahman, M. A., & Mamun, M. (2014). Numerical Study of Two and Three Bladed Savonius Wind Turbine. 2nd International Conference on Green Energy and Technology (pp. 36-40). Dhaka: University of Dhaka.

[55]   Al-Faruk, A., & Sharifian, A. (2014). Influence of Blade Overlap and Blade Angle on the Aerodynamic Coefficients in Vertical Axis Swirling type Savonius Wind Turbine.
19th Australasian Fluid Mechanics Conference (pp. 1-4). Melbourne: Australasian Fluid Mechanics Society.

[56]   ANSYS Inc. (2006, December). Modeling Turbulent Flows.
Retrieved March 4, 2015, from website: http://www.engr.uconn.edu
URL:http://www.engr.uconn.edu/~barbertj/CFD%20Training/Fluent/5%20Modeling%20of%20Turbulent%20Flows.pdf

[57]   ANSYS Inc. (2011, May 14). Turbulence Summary.
Retrieved February 12, 2015, from website: http://www.ansys.com
URL:http://www.ansys.com/staticassets/ANSYS/Conference/Confidence/San%20Jose/Downloads/turbulence-summary-4.pdf

[58]   Park, K. (2013) Optimal Design of a Micro Vertical Axis Wind Turbine for Sustainable Urban Environment, Ph.D. Thesis, University of Huddersfield, U.K.

[59]   Park, K. Asim, T. Mishra, R. (2012) Computational Fluid Dynamics based Fault Simulations of a Vertical Axis Wind Turbines, Journal of Physics: Conference Series, 364, 012138

[60]   Shahzad, A. Asim, T. Mishra, R. Paris, A. (2013) Performance of a vertical axis wind turbine under accelerating and decelerating flows, Procedia CIRP, 11, 311-316

[61]   Colley, G. and Mishra, R. (2011) Computational flow field analysis of a vertical Axis Wind Turbine. In international conference on Renewable Energies and Power Quality, Las Palmas, Gran Canaria

[62]   McTavish, S., Feszty, D. & Sankar, T. (2010) The Design and Development of a Novel Vertical Axis Wind Turbine Using Computational Fluid Dynamics
European Wind Energy Conference (Pages 1-10), Warsaw, Poland Publisher: European Wind Energy Association.

Flow Diagnostics and Optimal Design of Vertical Axis Wind Turbines for Urban Environments
By Martin Zahariev, School of Computing and Engineering, University of Huddersfield, UK (2016)
119